Investigation of Thermally Stimulated Luminescence Characteristics of Synthetic and Natural Quartz

Ph.D Thesis
in
Physics Engineering
University of Gaziantep

Supervisor
Assoc.Prof. Dr. A. Necmeddin YAZICI

by

Hüseyin TOKTAMIŞ

January 2008

GAZİANTEP UNIVERSITY
GRADUATE SCHOOL OF
NATURAL & APPLIED SCIENCES
Department of Engineering Physics

Name of the thesis: Investigation of Thermally Stimulated Luminescence Characteristics of   Synthetic and Natural Quartz

Name of the student: Hüseyin TOKTAMIŞ
Exam date: 18.01.2008

Approval of the Graduate School of Natural and Applied Sciences

Prof. Dr. Sadettin ÖZYAZICI
Director

I certify that this thesis satisfies all the requirements as a thesis for the degree of Master of Science/Doctor of Philosophy.

Prof. Dr. Zihni ÖZTÜRK
Head of Department

This is to certify that we have read this thesis and that in our opinion it is fully adequate, in scope and quality, as a thesis for the degree of Master of Science/Doctor of Philosophy.

Assoc.Prof. Dr. A. Necmeddin YAZICI
Supervisor

Examining Committee Members   signature

Prof. Dr. Zehra YEĞİNGİL   _____

Prof. Dr. Ömer Faruk BAKKALOĞLU   _____

Prof. Dr. Melda ÇARPINLIOĞLU   _____

Prof. Dr. Zihni ÖZTÜRK   _____

Assoc. Prof. Dr. A. Necmeddin YAZICI   _____

To my father, who have never grudged his financial support during my education life.

ABSTRACT

INVESTIGATION OF THERMALLY STIMULATED LUMINESCENCE CHARACTERISTICS OF SYNTHETIC AND NATURAL QUARTZ

TOKTAMIŞ, Hüseyin
Ph.D. in Physics Eng.
Supervisor: Assoc.Prof. Dr. A. Necmeddin YAZICI
January 2008,   124 pages

Quartz is one of the most important synthetic and natural crystals used in thermally stimulated luminescence studies, shortly named thermoluminescence (TL), and TL age estimation of historical samples which include the quartz minerals. Natural quartz minerals are highly found in the crust of the earth, the historical vestiges and meteors. It exhibits a number of TL peaks when quartz is heated from room temperature to 500°C. In this work, thermally stimulated luminescence characteristics of synthetic quartz which is purchased from Aldrich Company and natural quartz extracted from ceramics of Kubad Abad palace, Beyşehir, Konya, Turkey were carried out for different aims. The first aim was to see the stabilities of TL peak intensities and kinetic parameters of synthetic and natural quartz at different annealing temperatures. The second aim was to investigate the effects of thermal treatments on the TL intensity and kinetic parameters of natural quartz. The thermoluminescence dose responses of synthetic and natural quartz after different annealing protocols and the effects of heating rates on the thermoluminescence characteristics of synthetic and natural quartz constitute the third and fourth aim of this thesis, respectively.

Key Words: quartz, annnealing, thermoluminescence, heating rate, dose response.

ÖZ

SENTETİK VE DOĞAL KUVARS'IN ISISAL OLARAK UYARILMIŞ IŞILDAMA KARAKTERİSTİKLERİNİN ARAŞTIRILMASI

TOKTAMIŞ, Hüseyin
Doktora Tezi, Fizik Müh. Bölümü
Tez Yöneticisi: Doç. Dr. A. Necmeddin YAZICI
Ocak 2008, 124 sayfa

Kuvars, kısaca termoluminesans (TL) olarak adlandırılan ısısal olarak uyarılmış ışıldama çalışmalarında ve kuvars mineraller içeren tarihi eserlerin yaş tayinlerinde kullanılan çok önemli sentetik ve doğal kristallerden biridir. Kuvars yerkürenin kabuğunda, tarihi kalıntılarda ve meteorlarda bolca bulunur ve oda sıcaklığından $500^{o}C$ sıcaklığa kadar ısıtıldığında TL tepeleri açığa çıkar. Bu tez çalışmasında, Aldrich firmasından satın alınan sentetik ve Türkiye'nin Konya ilinin Beyşehir ilçesinde bulunan Kubad Abad sarayının seramiklerinden çıkartılan doğal kuvars'ın termolüminesans (TL) karakteristikleri farklı amaçlar için çalışıldı. Bunlardan birincisi, farklı tavlama sıcaklıklarında sentetik ve doğal kuvars'ın kinetik parametrelerinin ve TL tepe şiddetlerinin kararlıklarını görmek için yapılmıştır. İkinci amaç ise ısısal denemelerin doğal kuvarsın kinetik parametreleri ve TL tepe şiddetleri üzerindeki etkilerinin incelenmesidir. Farklı tavlama işlemlerinden sonra sentetik ve doğal kuvars'ın termolüminesans (TL) doz tepkileri ve ısıtma oranının sentetik ve doğal kuvars'ın termolüminesans karakteristikleri üzerine etkileri sırasıyla üçüncü ve dördüncü amacı oluşturur.

Anahtar Kelimeler: kuvars, tavlama, termolüminesans, ısıtma oranı, doz tepkisi.

ACKNOWLEDGEMENT

CONTENTS

LIST OF FIGURES

LIST OF TABLES

CHAPTER 1

INTRODUCTION

Thermoluminescence (TL) is the physical phenomenon of an insulator or semiconductor which can be observed when the solid is thermally stimulated. At above 200 ^{o}C temperature a solid emits (infra) red radiation of which the intensity increases with increasing temperature. This is thermal or black body radiation. TL, however, is the thermally stimulated emission of light following the previous absorption of energy from radiation [1]. From this description the three essential ingredients necessary for the production of TL can be deduced. Firstly, the material must be an insulator or a semiconductor—metals do not exhibit luminescent properties. Secondly, the material must have at some time absorbed energy during exposure to ionising radiation. Thirdly, the luminescence emission is triggered by heating the material [2]. A thermoluminescent material is thus a material that during exposure to ionising radiation absorbs some energy, which is stored. The stored energy is released in the form of visible light when the material is heated. Note that TL does not refer to thermal *excitation*, but to *stimulation* of luminescence in a sample which was excited in a different way. This means that a TL material cannot emit light again by simply cooling the sample and reheating it another time. It should first be re-exposed to ionising radiation before it produces light again. The storage capacity of a TL material makes it in principle suitable for dosimetric applications.

Since the early 1950s, the TL has been one of the important techniques for the measuring nuclear radiation doses [3]. Not only to measure radiation dose, but also it was subsequently applied to archaeological dating in the early 1960s [4-6] and to geological dating in the beginning of the 1980s [7]. Many scientists have carried out different thermoluminescence materials to obtain best dosimeter. Dosimeters are used in commercial areas, hospitals, nuclear power plants and research laboratories. In regular dosimetric applications, one can choose an appropriate material with reproducible results in repeated measurements, linear dose dependence for the kind of radiation in question as well as dose-rate independence and long time stability. However, this situation is significantly more complicated in retrospective dosimetry

such as in accident dosimetry where the exposure to radiation is to be determined by using existing materials such as porcelain [8].

A good thermoluminescence dosimeter (TLD) candidate has to need reproducibility, stability, linearity and dose-rate dependence. The reproducibility is an obvious requirement. However, a sensitization effect has been found in some material e.g. quartz [9]. This is an increase of sensitivity as a result of irradiation followed by an annealing above $500\,^{\circ}\mathrm{C}$. The stability is a desirable feature that the sample in hand is irradiated; the potential TL signal should be stable prior to the beginning of the heating. Linearity of the TL signal with dose is very desirable. However, superlinearity has been found in many materials, even in the very well recognized dosimetric material LiF [10]. This has been explained by different models based on the competition of the radiative transitions with transitions into non-radiative centers either during the excitation or during the heating (or both). At high doses, sublinear dose dependence always occurs, when the TL intensity goes toward saturation.

Quartz used in this thesis as the sample is the retrospective dosimetry. Synthetic and natural quartz are the two sorts of the quartz. Natural quartz are extracted from porcelains, tiles and sediments in the ancient vestiges and also found in rocks come from meteors and due to the volcanic eruption.

This Ph.D thesis was done to investigate the thermoluminescence properties of the synthetic quartz which was purchased from the Aldrich Company and natural quartz mineral, which was extracted from the tiles of Kubad Abad palace. It was build up as the summer residence of Seljuk Sultan Alaeddin Keykubad (1220-1236) and lies on the south-west shores of Lake Beysehir, west of Konya in Turkey.

The thesis consists of six chapters. In chapter 2, a brief literature survey about luminescence and thermoluminescence was given. Also, some important models, mathematical expressions about TL phenomenon and TL methods to find the kinetic parameters of used samples were given in this chapter.

Chapter 3 has more specific literature survey than chapter 2. It includes knowledges about quartz, and its thermoluminescence properties. In this chapter, the structures of quartz and the variations of them at different specific temperatures were mentioned. And, we also gave literature survey about pre-treatment effects on the TL properties of quartz before irradiation. Some of these pre-treatment effects are thermal annealing, dose response, predose and heating rate.

The necessary explanations about the experimental equipments, samples and procedures were given in chapter 4. The used equipments were classified into two parts: before and after irradiations. Furthermore, experimental procedures were given in detail along this chapter.

All the experimental results were given in chapter 5. In the first part of this chapter, the results of variation of kinetic parameters and intensities of TL peaks of annealed synthetic quartz at 500 ^{o}C and 600 ^{o}C were given. The results of effects of thermal treatment on the TL intensity and kinetic parameters of natural quartz, results of thermoluminescence dose response of synthetic and natural quartz and results of heating rate effects on the thermoluminescence of synthetic and natural quartz were given in the next parts of this chapter. Finally, we have discussed and concluded all experimental results with support of published studies in chapter 6.

CHAPTER 2

THEORY OF THERMOLUMINESCENCE

2.1 Luminescence

Luminescence is a light phenomenon which is observed when an irradiated insulator or wide band-gap semiconductor is stimulated by an excitation energy. This excitation energy classifies the luminescence. For example, heat for thermoluminescence, light for optically stimulated luminescence, electron beam for cathadoluminescence, mechanical energy for triboluminescence, electrical energy for electroluminescence, biochemical energy for bioluminescence and sound waves for sonoluminescence can be given for excitation energy.

The description of wide band gap materials is based on a band model that corcerns absorption and storage of ionizing radiation energy and release of the stored energy as the emission of photon by thermally or optically stimulation. In the band model, absorbtion of radiation energy means creation of electron-hole pairs. The property of storing energy is due to the presence of crystal defects such as vacancies and impurities. The defects are able to capture the electrons and holes generated in the irradiation process.

A crystal defect is classified as a trap center if the defect is able to capture a charge carrier and reemit it back to the band it comes from. A crystal defect where carriers of opposite sign can be captured, resulting in an electron-hole recombination, is classified as a recombination center. For the trap center we assume that only transition between the center and the conduction band and valence band are possible. For recombination centers, we assume that only recombination of conduction electron and a valence hole is possible. Finally, an electron-hole pair is assumed initially to consist of a conduction electron and a valence hole. Exchange of charge carriers between the crystal defects are assumed to take place through the conduction and valence band [11,12].

4

Figure 2.1 shows the typical transitions used in simulations presented in the dissertation. During the ionizing irradiation of the crystal, electron –hole pairs are generated by excitation of electron from the valence band to the conduction band. The excited electrons are freely moving in the crystal until they are captured by an electron trap center T_1 and T_2, or by a recombination center R. A hole generated in the valence band is captured into either a hole trap center T^h or the recombination center R. Recombinations are assumed to be accompanied by emission of photons, i.e. luminescence. However, nonradiadive recombinations are also possible.
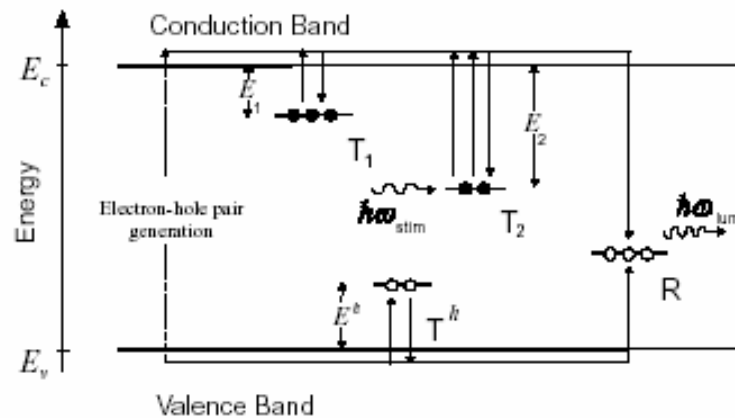
Figure 2.1 Basic concepts of irradiation, thermally and optically process between trap centers and recombination centers in a simple phenomenological band model. The transitions define whether a defect is a trap center T or a recombination center R. A recombination of an electron into a R center is assumed to be followed by photon emission[15]

By heating the crystal, captured electrons and holes can be freed thermally into the conduction or valence band and then make a transition to the radiative recombination center R. This process is termed thermally stimulated luminescence (TL). Alternatively, external light exposure of the crystal can release captured electrons from a trap center to the conduction band from where they can recombine into the recombination center R. This phenomenon is termed optically stimulated luminescence (OSL).

The optically or thermally freed charge carriers in the conduction/valance band can be measured as electrical current when a voltage source is applied across the crystal. These measurements are termed thermally and optically stimulated conductivity (TSC, OSC), respectively.

2.2 Thermally Stimulated Luminescence (TL)

Thermally stimulated luminesence, usually termed thermoluminescence (TL), has been used extensively to measure nuclear radiation doses since the early 1950s [3], following the commercial availability of sufficiently sensitive and reliable photomultiplier (PM) tubes. TL was subsequently applied to archaeological dating in the early 1960s [4, 5, 6] and to geological dating in the beginning of the 1980s [7]. Techniques and methods used in thermoluminescence dating are reviewed by Aitken [5]. TL is usually observed by heating a sample at a constant rate to the finite temperature (e.g. 500 oC) and recording the luminescence emitted as function of temperature. The TL signal is characterised by a so-called "glow curve", with distinct peaks occurring at different temperatures, which relate to the electron traps present in the sample. Defects in the lattice structure are responsible for these traps.

A typical defect may be created by the dislocation of a negative ion, providing a negative ion vacancy that acts as an electron trap. Once trapped, an electron will eventually be evicted by thermal vibrations of the lattice. As the temperature is raised these vibrations get stronger, and the probability of eviction increases so rapidly that within a narrow temperature range trapped electrons are quickly liberated. Some electrons then give rise to radiative recombinations with trapped "holes", resulting in emission of light (TL). A typical TL glow curve obtained from sedimentary feldspar is shown in Fig. 2.2. The temperature peaks corresponding to different electron trap depths are clearly seen.

Although a TL glow curve may look like a smooth continuum, it is composed of a number of overlapping peaks derived from the thermal release of electrons from traps of different stabilities. The lifetime of electrons in deep traps is longer than that of electrons in shallow traps. Normally, traps giving rise to glow peaks lower than $200\,^{o}C$ are not useful for dosimetry as electrons can be drained from these traps over a prolonged time even at environmental temperatures. Stable glow peaks suitable for dosimetry usually occur at $300\,^{o}C$ or higher. However, anomalous (i.e. unexpected) fading of high temperature glow peaks at room temperature has been observed in some feldspars. This is explained as a quantum mechanical tunnelling effect [13]. Another complication in TL measurements is thermal quenching. Some high temperature peaks in quartz and feldspars are subject to thermal quenching pro

processes, i.e. the increased probability of non-radiative recombination at higher temperatures [14].
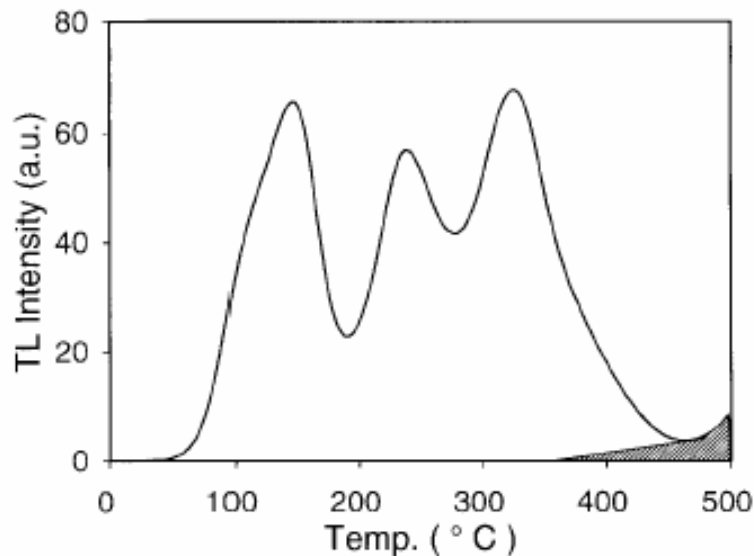
Figure 2.2 Typical TL glow curve from a sedimentary K-feldspar sample given a beta dose of 8 Gy in addition to the natural dose (approximately 200 Gy). The $150^{o}C$ peak evident in this figure has been created by the recent beta dose; it is not usually evident in the natural signal as it has normally decayed away. The shaded area is the lack body radiation observed when the sample is heated a second time with no additional irradiation [15]

2.3 Models in Thermoluminescence

The aim of a mathematical analysis concerning the thermoluminescent emission of light is to achieve a satisfactory knowledge of the phenomena related to it. From a theoretical point of view, TL is directly connected to the band structure of solids and particularly to the effects of impurities and lattice irregularities. These can be described as centers that may occur when ions of either signs move away from their original sites, thus leaving vacancy states, able to interact with free charge carriers and to trap them; alternatively, ions can diffuse in interstitial positions and break locally the ideal lattice geometry; finally, impurity ions can perturb the lattice order, because of their sizes and valences, generally different from their neighbor ones. Moreover, these extrinsic defects can interact with the intrinsic ones, and eventually either of them can aggregate in more complex configurations. From an atomic standpoint a defect can be described by means of the sign and number of

7

charge carriers it may interact with, and the eventual existence of excited states; to such a description, a characteristic energy for each center corresponds: this may be defined as the amount of energy able, when supplied, to set the trapped charges free, thus destroying the center and restoring a situation of local order. It is feasible therefore to describe the band structure in term of valence and conduction bands, parted from each other by a forbidden gap in which the defects are represented as sites localized at different depths, below the conduction band, where free charge carriers of either sign may be trapped. Therefore, the mapping of the forbidden gap reveals quite a complex configuration, and the experimental TL emission study can provide a satisfactory tool to get detailed information on its most meaningful parameters. These are, for each site, the characteristic energy (E), a frequency factor (s), connected to the transition frequency, and a kinetic order (b) synthesizing the quality of the involved phenomena.

The kinetic order ranges between 1 and 2. The former value corresponds to a situation where a charge (electron) is supplied energy to raise in the conduction band and, consequently, to fall to a center where it undergoes recombination with hole; the latter one stands for a situation where this phenomenon has the same probability of retrapping. Intermediate cases are likely to occur as well as contributions from non radiative events ($b = 0$). The mathematical models based upon these definitions are consisting of convenient differential equations systems, yielding for each case, the evolution of charged carriers populations, the analytical forms of which are to be checked by means of suitable experimental data. It is therefore evident how the involved parameters are to be conveniently adjusted until a fair agreement between theory and practice is attained. The most promising tool is the observation and the recording of TL emission, under several experimental conditions, as a function of temperature which the TL sample is heated to, or of heating up time. For a constant heating rate, these two observations are equivalent. The plot shape depends on the physical and chemical properties of the material and on the kind of the treatment it is submitted to. However it is always a single- or multi-peak structure, as may be expected from the general equations, and a correspondence can be pointed out between a peak and an electron trap level. This is explained by considering how, at a certain temperature, the amount of thermal energy supplied reaches, for a given level, the threshold necessary to raise the relative trapped charges in the conduction band from where they can give rise to radiative recombination events. For this purpose,

8

other centers, able to trap positive charge carriers, are involved, and they are likely to be connected to the quality of the emitted light. The analytical form for a single peak, which the overall curve is a superposition of, can fully described by means of some geometrical parameters as the peak position, its left and right widths, the ratio between them, the overall width, the height. This last one is dependent on the heating rate and increases, for given experimental conditions, with the increasing of it. These geometrical parameters can be shown to correspond to the main physical ones: the mathematical expressions can be evaluated by a convenient analytical manipulation of the involved equations. It is also to be remarked that the experimental uncertainties, obtained by means of the glow-curve plot, allow for an estimate of the physical errors related to them, and their evaluations can point out a well defined method as the fittest one.

2.3.1 Randall-Wilkins model (First-order kinetics)

In 1945, Randall and Wilkins [16] extensively used a mathematical representation for each peak in a glow curve, starting from studies on phosphorescence. Their mathematical treatment was based on the energy band model and yields the well-known first order expression. The following figure, Fig. 2.3, shows the simple model used for the theoretical treatment.
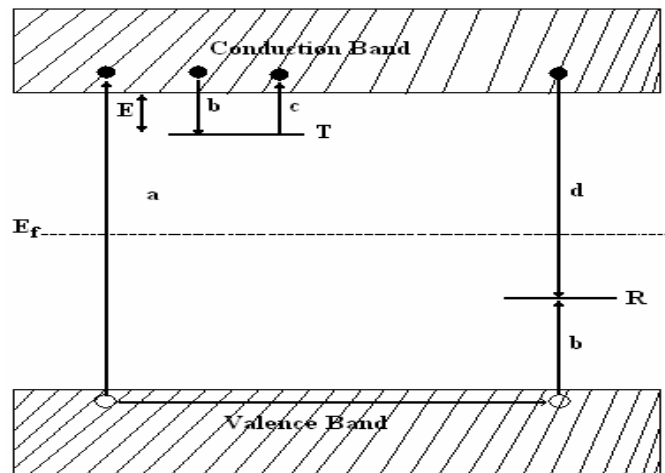
Figure 2.3 Energy band model showing the electronic transitions in a TL material according to Randall-Wilkins model (simple two-level model) (a) generation of electrons and holes; (b) electron and hole trapping; (c) electron release due to thermal stimulation; (d) recombination. ($\bullet$) shows electrons, ($\circ$) shows holes. Level T is an electron trap, level R is a recombination centre, E_f is Fermi level

Between the delocalized bands, conduction band (CB), and valence band (VB), two localized levels (metastable states) are considered, one acting as a trap, T, and the other acting as a recombination center, R. The distance between the trap T and the bottom of the CB is called activation energy or trap depth: E. This energy is the energy required to liberate a charge, i.e., an electron, which is trapped in T. The probability p, per unit of time, that a trapped electron will escape from the trap, or the probability rate of escape per second, is given by the Arrhenius equation, having considered that the electrons in the trap have a Maxwellian distribution of thermal energies

$$p = s \exp\left\{-\frac{E}{kT}\right\} \tag{2.1}$$

where E is the trap depth (eV), k the Boltzmann's constant, T the absolute temperature (K), s the frequency factor (sec^{-1}), depending on the frequency of the number of hits of an electron in the trap, seen as a potential well. The life time, τ, of the charge carrier in the metastable state at temperature T, is given by

$$\tau = p^{-1} \tag{2.2}$$

If n is the number of trapped electrons in T, and if the temperature is kept constant, then n decreases with time t according to the following expression:

$$\frac{dn}{dt} = -np \tag{2.3}$$

Integrating this equation

$$\int_{n_o}^{n} \frac{dn}{n} = -\int_{t_o}^{t} p.dt \tag{2.4}$$

one obtains

$$n = n_o . \exp\left[-s \exp\left\{-\frac{E}{kT}\right\}.t\right] \tag{2.5}$$

where n_0 is the number of trapped electrons at the initial time $t_0 = 0$. Assuming now the following assumptions:

- irradiation of the thermoluminescent material at a low enough temperature so that no electrons are released from the trap,
- the life time of the electrons in the conduction band is short,
- all the released charges from trap recombine in luminescent center,

10

- the luminescence efficiency of the recombination centers is temperature independent,

- the concentrations of traps and recombination centers are temperature independent,

- no electrons released from the trap is retrapped

According to the previous assumptions, the intensity ($I(t)$) of TL in photons per second at any time t during heating is proportional to the rate of recombination of holes and electrons at R. If m (m^{-3}) is the concentration of holes trapped at R the TL intensity can be written as

$$I(t) = -\frac{dm}{dt} \qquad (2.6)$$

Here it is assumed that each recombination produces a photon and that all produced photons are detected. The rate of recombination will be proportional to the concentration of free electrons in the conduction band n_c and the concentration of holes m,

$$I(t) = -\frac{dm}{dt} = n_c m A \qquad (2.7a)$$

with the constant A the recombination probability expressed in units of volume per unit time which is assumed to be independent of the temperature.

The rate of change of the concentration of trapped electrons n is equal to the rate of thermal release minus the rate of retrapping,

$$-\frac{dn}{dt} = np - n_c(N-n)A_r \qquad (2.7b)$$

with N the concentration of electron traps and A_r the probability of retrapping (m^3/s). Likewise, the rate concentration of free electrons is equal to the rate of thermal release minus the rate of retrapping and the rate of recombination,

$$\frac{dn_c}{dt} = np - n_c(N-n)A_r - n_c m A \qquad (2.7c)$$

Eqs.(2.7a)-(2.7c) described the charge carrier traffic in the case of release of a trapped electron from a single-electron trap and recombination in a single centre. For TL produced by the release of holes the rate equations are similar to Eqs.(2.7a)-(2.7c). These equations form the basis of many analyses of TL phenomena. There is

11

no general analytical solution. To develop an analytical expression some simplifying assumptions must be made. An important assumption is at any time

$$\left|\frac{dn_c}{dt}\right| << \left|\frac{dn}{dt}\right|, \qquad \left|\frac{dn_c}{dt}\right| << \left|\frac{dm}{dt}\right| \qquad (2.8)$$

This assumption is called by Chen and McKeever [17] the quasiequilibrium assumption since it requires that the free electron concentration in the conduction band is quasistationary. The trapped electrons and holes are produced in pairs during the irradiation. Charge neutrality dictates therefore

$$n_c + n = m \qquad (2.9)$$

which for $n_c{\approx}0$ means that $n{\approx}m$ and

$$I(t) = -\frac{dm}{dt} \approx -\frac{dn}{dt} \qquad (2.10)$$

Since $dn_c/dt{\approx}0$ one gets from (2.7a) and (2.7b):

$$I(t) = \frac{mAns\exp\left\{-\dfrac{E}{kT}\right\}}{(N-n)A_r + mA} \qquad (2.11)$$

Even Eq.(2.11) cannot be solved analytically without additional simplifying assumptions. Randall and Wilkins [16, 17] assumed negligible retrapping during the heating stage, i.e. they assumed $mA>>(N-n)A_r$. Under this assumption Eq.(2.11) can be written

$$I(t) = -\frac{dn}{dt} = n.p = sn\exp\left\{-\frac{E}{kT}\right\} \qquad (2.12)$$

Eq.(2.12) represents an exponential decay of phosphorescence.
Using Equation (2.5) in Equation (2.12) one obtains:

$$I(t) = n_o.s.\exp\left(-\frac{E}{kT}\right)\exp\left[-s.t.\exp\left\{-\frac{E}{kT}\right\}\right] \qquad (2.13)$$

Usually the temperature is raised as a linear function of time according to

$$T(t) = T_o + \beta t \qquad (2.14)$$

with β the constant heating rate and T_0 the temperature at $t=0$. With using eq.(2.14), heating rate can be written as $\beta=dT/dt$ and introducing it into equation (2.4)

$$\int_{n_o}^{n}\frac{dn}{n} = -\left(\frac{s}{\beta}\right)\int_{T_o}^{T}\exp\left(-\frac{E}{k.T'}\right)dT' \qquad (2.15)$$

And the number of trapped electrons (n) in term of β

$$n = n_o . \exp\left[-\left(\frac{s}{\beta}\right) \int_{T_o}^{T} \exp\left(-\frac{E}{k.T^{\iota}}\right) dT^{\iota} \right]$$ (2.16)

Then, using eq. (2.12), the intensity as function of temperature

$$I(T) = -\frac{1}{\beta}\frac{dn}{dt} = n_o \frac{s}{\beta} \exp\left\{ -\frac{E}{kT} \right\} \exp\left\{ -\frac{s}{\beta} \int_{T_o}^{T} \exp\left\{ -\frac{E}{kT^{\iota}} \right\} dT^{\iota} \right\}$$ (2.16)

This expression can be evaluated by mean of numerical integration, and it yields a bell-shaped curve, as in Fig. 2.4, with a maximum intensity at a characteristic temperature T_m.
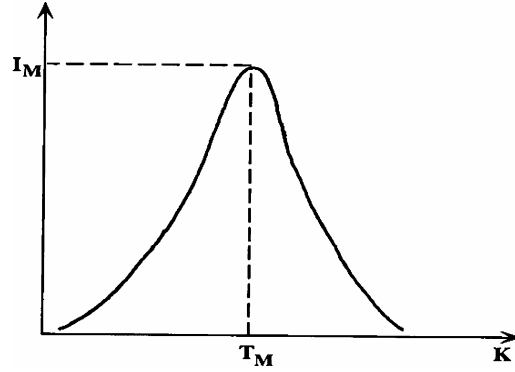
Figure 2.4 A bell shaped glow curve as a result of Randall-Wilkins model

Some observation can be done on Equation (2.16):
- $I(T)$ depends on three parameters E, s and b,
- E has values around $20kT$ in the range of occurance of TL peaks,
- $\exp(- E/kT)$ is of the order of 10^{-7},
- when T is slightly greater than of T_0, the argument of the second exponential function is about equal to unity and decreases with increasing temperature. $I(T)$ is then dominated by the first exponential and increases very fast as the temperature increases. At a certain temperature, T_m, the behaviour of the two exponential functions cancel: at this temperature the maximum temperature occurs,
- above T_m, the decrease of the second exponential is much more rapid than the increase of the first exponential and $I(T)$ decreases until the traps are totally emptied.

13

An important relationship, the so called condition at the maximum, is obtained by equation (2.16) by setting its first derivative equal to zero at $T = T_m$, i.e.,

$$-\frac{dn}{dt} = 0 \text{ at } T = T_m \qquad (2.17)$$

Using equation (2.16) it is derived

$$\left[\frac{d(\ln I)}{dT}\right]_{T=T_m} = \frac{E}{kT_m^{\ 2}} - \frac{s}{\beta}\exp(-\frac{E}{kT_m}) = 0 \qquad (2.18)$$

And the following expression is obtained

$$\frac{\beta E}{kT^2_{\ m}} = s\exp(-\frac{E}{kT_m}) \qquad (2.19)$$

From equation (2.19), the frequency factor is easly determined as

$$s = \frac{\beta E}{kT^2_{\ m}}\exp\left(\frac{E}{kT_m}\right)\left(\sec^{-1}\right) \qquad (2.20)$$

From equation (2.19), Furetta et al. [18] have mentioned some interesting remarks :

- for a constant heating rate T_m shifts toward higher temperatures as E increases or s decreases;
- for a given trap (E and s are constant values) T_m shifts to higher temperatures as heating rate increases;
- T_m is independent of n_0.

2.3.2 Garlick-Gibson model (Second-order kinetics)

In 1948, Garlick and Gibson [19], in their studies on phosphorescence, considered the case when a free charge carrier has probability of either being trapped or recombining within a recombination center. The term second order kinetics is used to describe a situation in which retrapping is present. They assumed that the escaping electron from the trap has equal probability of either being retrapped or of recombining with hole in a recombiantion centre.

Garlick and Gibson considered the possibility that retrapping dominates, i.e. $mA \ll (N-n)A_r$. Further they assume that the trap is far from saturation, i.e. $N \gg n$ and $n=m$. With these assumptions, Eqn.(2.11) becomes

$$I(t) = -\frac{dn}{dt} = s\frac{A}{NA_r}n^2\exp\left\{-\frac{E}{kT}\right\} \qquad (2.21)$$

It is seen that now dn/dt is proportional to n^2 which means a second-order reaction. With the additional assumption of equal probabilities of recombination and retrapping, $A=A_r$, integration of Eq.(2.21) gives

$$I(T) = \frac{n_0^2}{N}\frac{s}{\beta}\exp\left\{-\frac{E}{kT}\right\}\left[1+\frac{n_0 s}{N\beta}\int_{T_0}^{T}\exp\left\{-\frac{E}{kT'}\right\}dT'\right]^{-2} \tag{2.22}$$

This is the Garlick–Gibson TL equation for second-order kinetics. The main feature of this curve is that it is nearly symmetric, with the high temperature half of the curve slightly broader than the low temperature half. This can be understood from the consideration of the fact that in a second-order reaction significant concentrations of released electrons are retrapped before they recombine, in this way giving rise to a delay in the luminescence emission and spreading out of the emission over a wider temperature range.

2.3.3 May- Partridge model (General-order kinetics)

The first- and second-order forms of the TL equation have been derived with the use of specific, simplifying assumptions. However, when these simplifying assumptions do not hold, the TL peak will fit neither first- nor the second-order kinetics. May and Partridge [20] used for this case an empirical expression for general-order TL kinetics, namely:

$$I(t) = -\frac{dn}{dt} = n^b s'\exp\left\{-\frac{E}{kT}\right\} \tag{2.23}$$

where s' has the dimension of $m^{3(b-1)}$ s^{-1} and b is defined as the general-order parameter and is not necessarily 1 or 2. Integration of Eq.(2.23) for $b\neq 1$ yields

$$I(T) = \frac{s''}{\beta}n_0\exp\left\{-\frac{E}{kT}\right\}\left[1+(b-1)\frac{s''}{\beta}\int_{T_0}^{T}\exp\left\{-\frac{E}{kT'}\right\}dT'\right]^{-b/(b-1)} \tag{2.24}$$

where now $s''=s'n_0^{b-1}$ with unit s^{-1}. Eq.(2.24) includes the second-order case ($b=2$) and reduces to Eq.(2.16) when $b\rightarrow 1$. It should be noted that according to Eq.(2.23) the dimension of s' should be $m^{3(b-1)}$ s^{-1} that means that the dimension changes with the order b which makes it difficult to interpret physically. Still, the general-order case is

15

useful since intermediate cases can be dealt with and it smoothly goes to first- and second-orders when $b \rightarrow 1$ and $b \rightarrow 2$, respectively (see Fig.2.5).
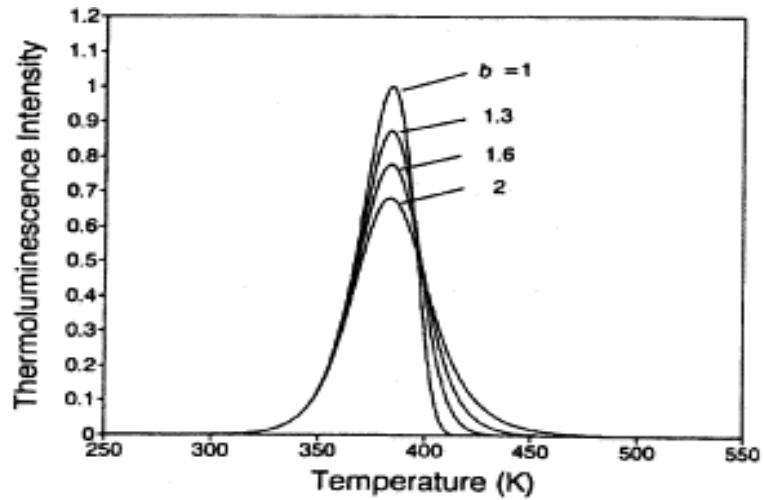
Figure 2.5 Comparison of first-order (b=1), second-order (b=2) and intermediate-order (b=1.3 and 1.6) TL peaks, with E=1 eV, s=1×10^{12} s^{-1}, n_0=N=1 m^{-3} and β=1 K/s (from [21])

2.3.4 Advanced models

The one trap–one centre model shows all the characteristics of the phenomenon TL and explains the behaviour of the glow peak shape under variation of the dose and heating rate. However, there is no existing TL material known that accurately is described by the simple model. This does not mean that the simple model has no meaning. On the contrary, it can help us in the interpretation of many features which can be considered as variations of the one trap–one centre model. There is no room to discuss all the advanced (more realistic) models in detail. The reader is referred to the text book of Chen and McKeever [17] for a deeper and quantitative treatment. Here, only some models are very briefly mentioned in order to get some idea about the complexity of the phenomenon in a real TL material.

In general, a real TL material will show more than one single electron trap. Not all the traps will be active in the temperature range in which the specimen is heated. A thermally disconnected trap is one which can be filled with electrons during irradiation but which has a trap depth which is much greater than the active trap such that when the specimen is heated only electrons trapped in the active trap

(AT) and the shallow trap (ST) (see Fig.2.6(a)) are freed. Electrons trapped in the deeper levels are unaffected and thus this deep electron trap (indicated in Fig.2.6(a) with DET) is said to be thermally disconnected. But its existence has a bearing on the trapping filling and eventually on the shape of the glow peak [22].

It was assumed that the trapped electrons are released during heating while the trapped holes are stable in the recombination centre. A description in which the holes are released and recombine at a centre where the electrons are stable during heating is mathematically identical. However, the situation will change if both electrons and holes are released from their traps at the same time at the same temperature interval and the holes are being thermally released from the same centres are acting as recombination sites for the thermally released electrons and vice versa (see Fig.2.6(b)). In this case Eq.(2.10) is no longer valid. New differential equations should be drafted. Analysis of this complicated kinetic model reveals a TL glow curve which retains the simple Randall–Wilkins (Eq.(2.16)) or Garlick–Gibson (Eq.(2.22)) shape, depending upon the chosen values of the parameters. However, the E and s values used in Eq.(2.16) and Eq.(2.22) in order to obtain a fit on this complicated kinetic model need further interpretation.

Another process which might happen is a recombination without a transition of the electron into the conduction band (Fig.2.6(c)) Here the electron is thermally stimulated into an excited state from which a transition into the recombination centre is allowed. This means that the trap has to be in the proximity of a centre.
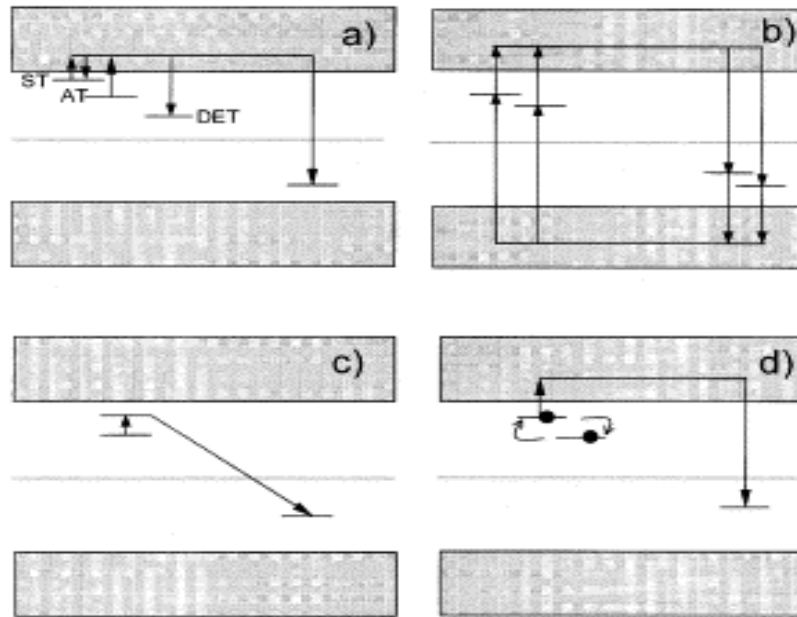
Figure 2.6 Advanced models describing the thermally stimulated release of trapped charged carriers including: (a) a shallow trap (ST), a deep electron trap (DET), and a active trap (AT); (b) two active traps and two recombination centres; (c) localised transitions; (d) defect interaction (trapping centre interacts with another defect).

The transition probability may strongly depend on the distance between the two centres. Under certain assumptions an expression for the TL intensity can be derived [22] which has the same form as Eq.(2.16) but with *s* replaced by a quantity related to the probability for recombination. This means that these localised transitions are governed by first-order kinetics.

Finally, Fig.2.6(d) mentions the possibility that the defect which has trapped the electron is not stable but is involved in a reaction with another defect. The result may be that at low temperature the trap depth is changing while the trapped electron concentration is stable. At higher temperatures, electrons are involved in two processes: the escape to the conduction band and the defect reaction. Piters and Bos [23] used defect reactions incorporated into the rate equations and glow curves simulated. It appears that the simulated glow curves can be very well fitted by Eq.(2.16) It is clear that (again) the fitting parameters do not have the simple meaning of trap depth and escape frequency.

2.4 Trapping Parameter Determination Methods

The determination of trapping parameters from thermoluminescence glow curves has been a subject of interest for half a century. There are various methods for evaluating the trapping parameters from the glow curves [16, 17, 22, 24, 25].

When one glow peak is highly isolated from the others, the experimental methods such as initial rise, variable heating rates, isothermally decay, and peak shape methods are suitable methods to determine these parameters. However in most materials, the glow curve consists of several peaks. In case of overlapping peaks, there are essentially two ways to obtain these parameters, the first one is the partial thermal cleaning method and the second one is the computer glow curve deconvolution program. In most cases, the partial thermal cleaning method can not be used to completely isolate the peak of interest without any perturbation on it. Therefore, the computer glow curve deconvolution program has become very popular method to evaluate trapping parameters from TL glow curves in recent years [26].

2.4.1 Peak shape method

Evaluation of E from the shape of the peak utilising parameters such as T_m, full width at half-maximum $\omega = T_2 - T_1$, half width on the high temperature side of the maximum $\delta = T_2 - T_m$, half width on the low-temperature side of the maximum $\tau = T_m - T_1$, and $\mu_g = \delta/\omega$ called the shape parameter.

The order of kinetics b can be estimated by means of shape parameters. Chen [24] found that μ_g is not sensitive to changes in E and s, but it changes with the order of kinetics b. It has been shown that the ranges of μ_g varies from 0.42 for b=1 to 0.52 for b=2 in case of linear heating.

The first peak shape method was developed by Grossweiner [25]; later Chen [24] modified Halperin and Braner's equations [27] for calculating E values;

$$E_\tau = \left[1.51 + 3(\mu_g - 0.42)\right]\frac{kT_m^2}{\tau} - \left[1.58 + 4.2(\mu_g - 0.42)\right]2kT_m$$

$$E_\delta = \left[0.976 + 7.3(\mu_g - 0.42)\right]\frac{kT_m^2}{\delta} \tag{2.25}$$

$$E_\omega = \left[2.52 + 10.2(\mu_g - 0.42)\right]\frac{kT_m^2}{\omega} - 2kT_m$$

After determination of the activation energy and the order of kinetics, using the following expressions the frequency factor s, it must be noted that this parameter called as pre-exponential factor in the general order kinetic, can be estimated for first order in eq. (2.20) and general order in eq. (2.26) kinetics respectively.

$$s = \frac{\beta E}{kT_m^2} \left[\exp(-\frac{E}{kT_m})(1 + (b-1)\frac{2kT_m}{E}) \right]^{\frac{b}{b-1}}$$

(2.26)

2.4.2 Isothermal decay method

The isothermal decay is a quite different method of analysis of the trapping parameters in which the TL sample temperature is kept constant and the light emission can be recorded as a function of time. Generally, in the isothermal decay method, the following equation is solved for constant T for the first order kinetics

$$I(T) = -c\frac{dn}{dt} = c\frac{n_0}{\tau}\exp(-\frac{t}{\tau})$$

(2.27)

where n_0 is the initial value of n and $\tau = s^{-1}\exp(\frac{E}{kT})$. The above equation shows that at a constant temperature T, the light emission will decay exponentially with time t and a plot of $ln(I)$ against t will give a straight line with a slope $m = s\exp(-\frac{E}{kT})$. In order to find E and s, the experiments are carried out at two different constant temperatures T_1 and T_2, resulting in two different slopes m_1 and m_2. Thus the activation energy can be determined by using the following equation

$$E = \frac{k}{(\frac{1}{T_2} - \frac{1}{T_1})}\ln(\frac{m_1}{m_2})$$

(2.28)

The isothermal decay method is not applicable to higher order kinetics. In 1979; a method has been proposed by Kathuria and Sunta [28] to calculate the order of kinetics from the isothermal decay of thermoluminescence. According to this method; if the decaying intensity from the sample is held at a constant temperature, the plot of $I^{(\frac{1}{b}-1)}$ versus t gives a straight line, when the proper value of b is chosen. Therefore, various b values are tried and the correct one is that giving a straight line.

2.4.3 CGCD method

Computer Glow Curve Deconvolution (CGCD) is one of the most important method to determine trapping parameters from TL glow curves. This method has the advantage over experimental methods in that they can be used in largely overlapping-peak glow curves without resorting to heat treatment

In this study, a CGCD program was used to analyse the glow curve of quartz. The program was developed at the Reactor Institute at Delft, The Netherlands [29]. This program is capable of simultaneously deconvoluting as many as nine glow peaks from glow curve. Two different models were used in the computer program. In the first model, the glow curve is approximated from first order TL kinetic by the expression,

$$I(T) = n_0 s \ \exp(-\frac{E}{kT})\exp\left[(-\frac{s}{\beta}\frac{kT^2}{E}\exp(-\frac{E}{kT}) * (0.9920 - 1.620\frac{kT}{E_a})\right] \tag{2.29}$$

In the second model the glow curve is approximated with general order TL kinetics by using the expression,

$$I(T) = n_0 s \ \exp(-\frac{E}{kT})\left[1 + (-\frac{(b-1)s}{\beta}\frac{kT^2}{E}\exp(-\frac{E}{kT}) * (0.9920 - 1.620\frac{kT}{E_a})\right]^{\frac{b}{b-1}} \tag{2.30}$$

where n_0 (m^{-3}) is the concentration of trapped electrons at t=0, s (s^{-1}) is the frequency factor for first-order and the pre-exponential factor for the general-order, E (eV) the activation energy, T (K) the absolute temperature, k (eVK^{-1}) Boltzmann's constant, β (^{0}Cs^{-1}) heating rate and b the kinetic order.

The summation of overall peaks and background contribution can lead to composite glow curve formula as shown below

$$I(T) = \sum_{i=1}^{n} I_i(T) + a + b\exp(T) \tag{2.31}$$

where $I(T)$ is the fitted total glow curve, a allows for the electronic noise contribution to the planchet and dosimeters infrared contribution to the background.

Starting from the above equation (2.31), the least square minimisation procedure and also FOM (Figure of Merit) was used to judge the fitting results as to whether they are good or not. i.e.

21

$$FOM = \sum_{i=1}^{n} \frac{\left| N_i(T) - I(T) \right|}{A} = \sum_{i=1}^{n} \frac{\left| \Delta N_i \right|}{A} \qquad (2.32)$$

where $N_i(T)$ is the i-th experimental points (total n=200 data points), $I(T)$ is the i-th fitted points, and A is the integrated area of the fitted glow curve.

From many experiences [30-31], it can be said that if the values of the FOM are between 0.0% and 2.5% the fit is good, 2.5 % and 3.5% the fit is fair, and > 3.5% it is bad fit.

To have a graphic representation of the agreement between the experimental and fitted glow curves, the computer program also plots the function,

$$X(T) = \frac{N_i(T) - I_i(T)}{\sqrt{I_i(T)}} \qquad (2.33)$$

which is a normal variable with an expected value 0 and σ=1 where $\sigma^2(T)=I_i(T)$.

2.4.4 Initial rise method

The simplest, and most generally applicable method for evaluating the activation energy E of a single TL peak is the initial rise method. The basic premise upon this method which is based is that at the low temperature end of the peak, all the relevant occupancies of the states, the trap, the recombination center and, in some cases, other interactive states can be considered as being approximately constant.

The rise of the measured intensity as a function of temperature in this region is, therefore, very close to exponential, thus

$$I(T) = C \exp(-E / kT) \qquad (2.34)$$

where the constant C includes all the dependencies on the other parameters and occupancies, E is the activation energy (eV), k is the Boltzmann`s constant (eV/K^{-1}) and T is the temperature (K).

Plotting ln(I) against $1/T$ a linear plot is obtained with slope equal to $-E/k$. Hence it is possible to evaluate E without any knowledge of the frequency factor s by means of equation

$$E = -kd(\ln(I)) / d(1/T) \qquad (2.35)$$

Once the value of E was determined, the frequency factor (s) was obtained from the equation

$$\frac{\beta E}{kT_m} = s \exp(-\frac{E}{kT})$$

(2.36)

where T_m is the temperature at the maximum intensity. This method can only be used when the glow peak is well defined and clearly seperated from the other peaks.

2.4.5 Heating rate method

Another important method is various heating rates for the determination of activation energies. If a sample is heated at two different linear heating rates β_1 and β_2 the peak temperatures will be different. Equation (2.36) can therefore, be written for each heating rate and dividing the equation for β_1 (and T_{m1}) by the equation for β_2 (and T_{m2}) and rearranging, one gets an explicit equation for the calculation of E

$$E = k \frac{T_{m1}T_{m2}}{T_{m1} - T_{m2}} \ln[(\frac{\beta_1}{\beta_2})(\frac{T_{m2}}{T_{m1}})^2]$$

(2.37)

The major advantage of the heating rate method is that it only requires data to be taken at a peak maximum (T_m, I_m) which, in case of a large peak surrounded by smaller satellites, can be reasonably accurately determined from the glow curve. Furthermore the calculation of E is not affected by problems due to thermal quenching, as with the initial rise method.

When various heating rates for the first-order kinetics are used, the following expression is obtained:

$$\ln(\frac{T_m^2}{\beta}) = (\frac{E}{k})(\frac{1}{Tm}) + cons\tan t$$

(2.38)

23

A plot of ln (T_m^2/β) versus $(1/T_m)$ should yield a straight line with a slope E/k, then E is found. Additionally, extrapolating to $1/T_m = 0$, a value for $ln(sk/E)$ is obtained from which s can be calculated by inserting the value of E/k found from the slope. This method of various heating rates are applicable for general-order kinetics which includes the second-order case. For the general order case, one can plot $ln\left[I_m^{b-1}(T_m^2/\beta)^b\right]$ versus $1/T_m$, whose slope is equal to E/k.

CHAPTER 3

THERMOLUMINESCENCE IN QUARTZ

Quartz, SiO_2, is the most abundant mineral in the crust of the Earth [32]. It is a non-toxic, inert material and its addition to food would not cause toxicological implications as with most of the standard dosimeter types [33]. Moreover, quartz is inherent to common dust which is often found concomitant to agricultural procedure. Natural quartz can be found in archaeological artifacts, geological materials (rocks and sediments) etc., furthermore, it is present in extraterrestrial material as meteorites and rocks of the Moon and Mars [34-35]. The physical properties of natural quartz can be applied in many fields, from research areas as dating and radiation dosimetry to commercial areas.

Quartz is a silicate commonly found in geological formations and in archaeological vestiges. As mentioned in Chapter 1, its thermoluminescence (TL) has been used in geological and archaeological dating [36]. Quartz is also an important material from a technological point of view. It is a possible source of silicon, a very good insulator and is also used in optical devices [37]. Furthermore, it has been employed as a substrate for different applications in material engineering, biological and chemical devices. The TL emission of quartz has been the subject of investigations carried out by a number of workers. Most of these relate to the applications in archaeological dating since quartz is a very important component of the raw material used in ancient pottery.

Quartz exhibits a number of TL peaks when irradiated grains are heated from room temperature to 500°C. Peaks at about 100°C, 180°C, 220°C, 260°C, 305°C, 350°C and 450°C were identified by Franklin et al. [38]. According to these authors, peaks at 260°C, 350°C and 450°C appear to emit at 470 nm while a second set that includes the peak at 305°C and the others at lower temperatures, all emit at or below

435 nm. Two peaks at about 325°C and 375°C were observed for sand-sized grains extracted from pottery by Fleming [39]. The peak at 375°C was preferred for dating while the peak at 325°C appeared not to give reliable dose response. The 100°C TL peak can be found in various laboratory-irradiated samples of synthetic and natural quartz. This peak appears to emit at 380 nm and the luminescence center associated to that emission has been identited by Yang and McKeever [40] with the $[H_3O_4]^o$ hole centers.

3.1 Quartz (SiO$_2$) Structure

Quartz and its polymorphs, tridymite and cristobalite, occur naturally in the temperature ranges smaller than 870°C, between 870 and 1470°C and bigger than 1470°C, respectively. Both tridymite and cristobalite are metastable at ambient temperatures and both occur as natural minerals. All three minerals have α and β modifications- α quartz being stable below 573°C and β quartz being stable between 573°C and 870°C. The α-β transition is a displacive phase change, involving small adjustments in atomic positions without bond rearrangement, and is reversible. The α form is rhombohedral and the β form has a hexagonal structure. In both forms, the oxygen atoms are tetrahedrally shared between those of silicon. Two of the Si-O bonds in α quartz make an angle of 66° with the optic axis whilst the two others make an angle of 44°. Therefore, oxygens occur in two equivalent pairs.

The nature of the Si-O bond in SiO$_2$ is described as being ~40% ionic and ~60% covalent [41-42]. The covalent component gives the material a rigid structure such that macroscopic diffusion of lattice atoms is prevented. Dislocations and defects exist in the structure of quartz, but have complex structures and are rather poorly defined. Misplaced lattice atoms tend to be located near impurities. The mixed ionic and covalent nature of SiO$_2$ lattice has resulted in two basic mechanisms for damage by radiation-namely, Si-O bond rupture (requiring only ionising radiation) and direct "knock-on" collisions resulting in vacancy and interstitial creation. This second mechanism requires energetic nuclear particle. Particle radiation can induce large scale damage in quartz by lattice atom displacement and alter the material's character. Extensive literature exists on the topic of permanent damage effects in quartz and major studies [43-44] can be given for SiO$_2$ structure.

Both ionising and elastic collision processes [45-46] cause the luminescence phenomena in quartz.

3.2 Defects in Quartz

Natural quartz contains various minor and trace of impurities, especially aluminium, germanium, titanium and the alkali metals lithium, sodium and potasium. Aluminium, germanium and titanium are not only present as trace impurities, but may also require ionic charge compensation by monovalent cations. The presence of hydrogen in the quartz crystal may result in $[H_3O_4]^0$ centres as hole traps. The 380 nm TL emission at 110°C is produced by recombination of electrons with these holes. The Si in the $[SiO_4]^0$ tetrahedrons of the quartz crystal may be substituted by Al^{+3} and a monovalent cation (H^+, Li^+, Na^+) to give an $[AlO_4/M^+]^0$ centre. The cations are located interstitially in the SiO_2 lattice. The main centres known in quartz are aluminum, titanium, germanium, $E^{'}$ and oxygen centres.

3.2.1 $E^{'}$ centre

This is one of the most studied centres in quartz and associated with oxygen vacancies. The $E^{'}$ centres have been found in all forms of SiO_2 and well characterized in α-quartz and silica glass [44]. The intensity of the $E^{'}$ centre of quartz extracted from quaternary sediments often decreases after gamma ray irradiations, in regard to that of natural samples. This indicates that the $E^{'}$ centre is already saturated in these non-irradiated samples [47]. Figel et al. [48] and Ruffa [49] idendified $E_1^{'}$ centre as an oxygen vacancy with an unpaired electron located on one of two non equivalent Si atoms shown in figure 3.1.

The $E_2^{'}$ centre consists of an oxygen vacancy with an associated proton. Electron spin resonance (ESR) and optical absorption data indicate a relationship between absorbtion bands at 215nm (5.8eV) and at 235nm (5.3 eV) with ESR signals from the $E_1^{'}$ and $E_2^{'}$ centres respectively. An intense absorption band is also observed at 7.6 eV and has been associated with trapped holes at oxygen interstitials. Thus, the 7.6 eV and $E^{'}$ centres are viewed as complements of each other. Apart from vacancy and interstitial centres, broken slicon and oxygen bonds are important defects in quartz (SiO_2). Non-bridging oxygen in quartz causes to oxygen dangling bonds,

which are potential hole traps, and empty Si orbitals which may localise electrons in a manner similar to the $E^{'}$ centres. The broken oxygen bonds can be easily created by ionising radiation.
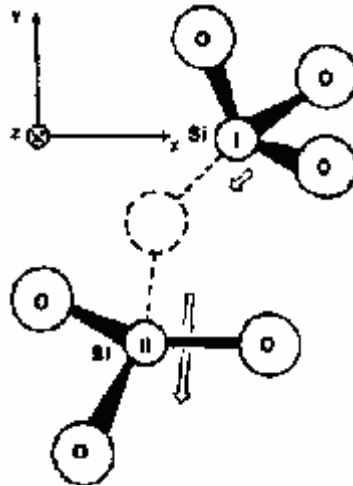
Figure 3.1 Model for the E_1 centre in α-quartz, consisting of an oxygen vacancy (dotted circle) with an unpaired electron located at the Si (I) site. The arrows indicate the asymetric relaxation of the Si atoms from their normal lattice positions [50]

Greaves [51] and Lucovsky [52, 53] explain many of the electronic properties of the slica on the basis of electron traps and hole traps produced during bond rupture [54].

3.2.2 Introduction of impurities

The introduction of impurities into the SiO_2 lattice gives rise to several new optical absorption bands. Monovalent alkali ions (such as Na^+, Li^+, K^+) can act as network modifiers by inducing non-bridging oxygen without the action of radiation. A concise review of the literature concerning Al defects in α -quartz is given by Weil [55].

Al^{+3} due to its nearly similar atomic size easily substitutes for Si^{+4} in lattice and is the most pervasive impurity in quartz. Thus, an aluminum ion would need an additional positive charge to compensate for the charge of replaced silicon. This charge compensation is provided by monovalent alkalis such as Li^+ or Na^+ ions or

the protons H^+ located interstitially near aluminum atoms or holes trapped at oxygen sites. Due to strong Coulombic force of attraction between the interstitial ions (or the holes) with the aluminum and because of their high mobility, the charge compensators are usually located adjacent to the substitutional aluminum ions. Such a situation gives rise to various aluminum-associated centers e.g. Al-OH⁻, Al-Li⁺, Al-Na⁺, or Al-H⁺ shown in figure 3.2. In addition, several unidentified H⁻ containing growth-defects also occur in quartz. During irradiation of quartz, protons from these defects move to aluminum sites for charge compensation of the electron excess defect. These defect centers can be monitored by a variety of experimental techniques such as ESR in case of Al-H⁺ centers, near infrared absorption in the case of Al-OH centers, acoustic loss in the case of Al-Na⁺ and also Al-OH⁻ centers. Substitutional aluminum and the unidentified hydrogen-containing (OH⁻) growth-defect centers are probably the most important point defect centers in quartz from the point of view of resonator performance. There is however, no satisfactory picture yet forthcoming for the growth-defects. The experiments have shown [56] that these defects tend to trap alkalis as well during growth. The hydrogen content in quartz is generally found to be in excess of the amount required to satisfy the charge imbalance at aluminum sites.
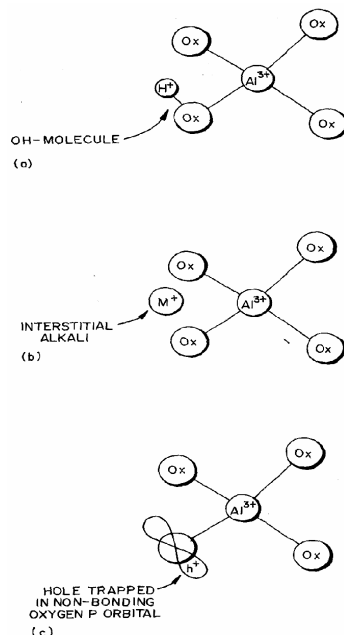
Figure 3.2 Schematic representation of Al-related defects in quartz crystals

Germanium, like Si, is tetravalent and enters the SiO_2 lattice substitutionally for Si. Its higher affinity makes it a strong electron trap. Diffusion of the alkali ions to the Ge sites, at temperature >200K, in order to stabilise the electron was suggested by Mackey [57]. In Ge-free specimens, hole trapping at Al still takes place, which requires that other sites must act as complementary electron traps.

3.3 Thermoluminescence (TL) in Quartz

Electrons and holes, the primary products of ionizing radiation, are highly mobile in crystalline quartz. They are partly converted to excitons and partly localized at traps which existed prior to irradiation. Excitons are self-trapped and are annihilated either by the radiative or nonradiative recombination. Radiative recombination of excitons gives rise to luminescence at 450 nm (~2.8 eV) under ionizing radiation at low temperatures [58–60]. A fraction of the trapped electrons and holes recombine with their counterparts during irradiation via either radiative or non-radiative processes. Radiative recombination will give luminescence characteristic of the recombination center. Those electrons and holes remaining after irradiation will be trapped separately, and will store the energy of the radiation. They can be the basis of a luminescence dosimetry, such as TL and OSL.

The TL of quartz irradiated at room temperature consists of three major peaks at 110, 325, and 370°C. Although the peak temperature will depend on the heating rate, these are called as conventional peak temperatures. The 110°C peak, called the predose peak, has a short half-life (146 min has been quoted [61]; even shorter lifetimes may result when other decay channels are available) at room temperature and so can only be observed for a short time after a laboratory radiation. It appears after short laboratory irradiation following an historical dose and subsequent thermal activation, in which case its intensity is related to the historical dose. The 325 °C peak can be bleached by visible light and is called the rapidly bleached peak and the 370 °C peak is more stable against optical bleaching [62]. Both of these peaks can be used for dating in a range from a few ten years to 1 million year [63, 64].

Luminescence emitted by ionizing radiation at room temperature of quartz consists of blue (~450nm) and red (~650nm) bands [65]. The blue luminescence band is usually very broad and is known to comprise several bands of different origins: 380, 420, and 450 nm. Luminescence under ionizing radiation at liquid

nitrogen temperature is much stronger and consists of peaks at 450, 425, and 380 nm, which are quenched for irradiation in the temperature ranges 120–160, 170–210, and 220–300 K, respectively [66]. The 450 nm band observed at liquid nitrogen temperature has been ascribed to the recombination of self-trapped excitons [58]. The origin of the 425 nm band, of which the intensity is not affected by H sweeping, is not yet clear. It might be due to the recombination of defect-perturbed self-trapped excitons. According to Alanso et al., [66] the intensity of the 380 nm band is proportional to the concentration of Al-impurities. They showed also that H sweeping eliminates the 380 nm band, and consequently the band was assigned to the electron–hole recombination at the $[AlO_4/M^+]^0$. On the other hand, Halperin and Sucov [67] showed that the luminescence under x-ray irradiation at liquid nitrogen temperature was enhanced for samples preirradiated above 150 K, where dissociation of $[AlO_4/M^+]^0$ took place and ascribed the luminescence band to arise from the electron–hole recombination at $[AlO_4]^-$. The same assignment has been made for the emission band at 380 nm observed in TL peaks. Itoh et al. [68] emphasized that the assignment of the 380 nm luminescence band to the electron–hole recombination at $[AlO_4]^-$ has been supported most conclusively by spectroscopic experiments. The 420 and 650 nm bands are considered to be related to defects produced by irradiation [69], whether by charge-state change or damage processes associated with electronic excitation. The 450 nm band observed at room temperature might be ascribed to the recombination of the self-trapped excitons, but is more probably due to defect-perturbed self-trapped excitons.

The TL spectrum for each peak provides important information for understanding the nature of the recombination centers. The 110 °C peak consists of luminescence bands at 380 and 420 nm, depending on sample history. The 325 and 375 °C peaks consist of bands at 380, 420, and 475 nm (blue), respectively [38]. The 420 nm band has not been observed to predose. Both the 325 and 375 °C peaks also include a band at 690 nm (red) [70]. Franklin *et al.* [38] showed that the blue TL emission spectra in the intermediate temperature between 95 and 325 °C changes from 376 to 430 nm gradually as the temperature increases. They suggest that the change in the peak is a temperature shift, and that the luminescence originates from a single defect species. This is unlikely since the temperature shift, which is observed between room temperature and 325 °C, is about a factor of 100 larger than expected either from thermal expansion or from the normal shifts associated with force-

constant changes. The intensity ratio of the blue to red luminescence varies depending on samples and on the annealing condition, although no systematic relationship has been found. Franklin *et al.* [71] suggest that the blue and red luminescence arises from different grains.

Itoh et al. [68] considered that some of these TL luminescence bands arise from defects existing prior to irradiation. The 380 nm band emitted under ionizing radiation appears to be the same as the 380 nm band emitted in 110 °C TL. Martini *et al.* [72] measured the intensity of the 110 °C TL peak, which gives rise to the 380 nm emission, for samples annealed at various temperatures before irradiation. They showed an enhancement after annealing above 1400 °C, where the $[AlO_4/M^+]^0$ centers dissociate.

3.3.1 The main trap centers (TL peaks) in quartz

A system simulated by Bailey [73], shown in figure 3.3, contains what is regarded as being the major elements of the electronic system of natural (sedimentary) quartz. Evidence for the centres included in the model comes from a number of sources. Strong empirical evidence exists for centres not included in the present model (electron traps that give rise to TL peaks below 0 °C for example; Malik et al. [74], Alexander et al. [75]), however.

Figure 3.3 shows the illustrated model [73], where all allowed charge transitions are indicated by arrows. This gives details of the trapping centres present in the model along with brief notes as to the intended correspondence to quartz.
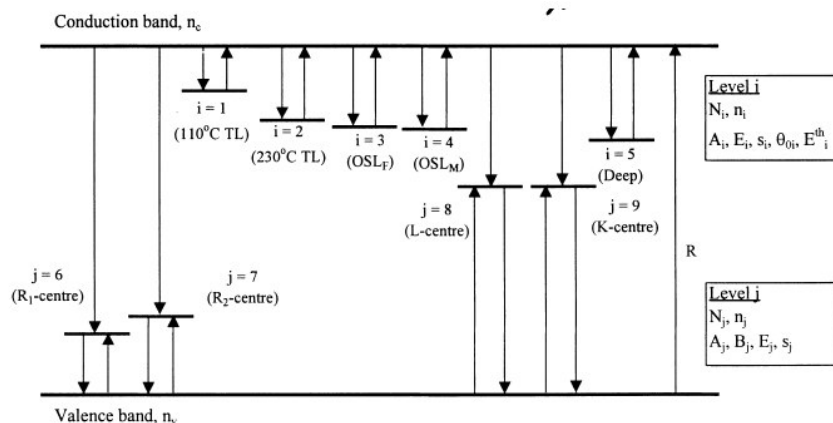
Figure 3.3 A model simulated by Bailey [73] includes electron and hole trap centers

3.3.1.1 The electron trapping centers

Level 1 '110 °C TL Peak': Level 1 is a relatively shallow electron trapping centre, giving a TL peak at about 100 °C. The corresponding TL signal observed empirically in measurements of quartz (the *110* °C TL peak) has been described in many publications (see, for example, Zimmerman [9]; Yang and McKeever [40]; Alexander et al. [73]) and is found in sedimentary quartz samples. The precise position of the peak varies between samples and is generally within the range 90-120 °C. However, for simplicity, as is commonly the practice, the peak, in this range will be referred to as the 110 °C TL peak. Some debate exists over the existence of photo-stimulation out of the trap responsible for the 110 °C TL peak, and in the present model Level 1 is assigned an optical eviction rate in accordance with the findings of Bailey [73].

Level 2 '230 °C TL Peak': Level 2 is a `medium stability' electron trapping centre, yielding a simulated TL peak at about 230 °C. A number of peaks can be observed in natural sedimentary quartz within the temperature range 100-300 °C (see Aitken [36]). These are, in most cases, of significantly lesser magnitude than those at 110 °C and 330 °C and play only a minor role in the charge trafficking of the majority of samples. Although this is the general rule, there are samples for which the charge released from such `medium-stability' traps is not insignificant (see Rhodes and Bailey [76]). Level 2 is included in the present model therefore, as a generic `medium stability' TL peak.

Levels 3 and 4 'fast and medium OSL components (330 °C TL Peak)': Levels 3 and 4 yield TL peaks at 330 °C and both give rise to photo-stimulated luminescence signals. These levels represent the fast and medium OSL components, respectively (Bailey et al.[77], Bailey [78]). The terms `fast' and `medium' refer to the relative depletion rates of these signals under photo-stimulation.

***Level 5 'Deep (`thermally disconnected') electron centre':*** An extremely thermally stable `deep' trap is also included in the this model, Level 5. Although direct empirical evidence for such traps is not easy to obtain, theoretical studies (e.g., Dussel and Bube [79], Kelly [80]) suggest that a deep `thermally disconnected' electron trap is necessary in such models. Sunta et al. [81], using their `interactive

trap system' model, suggest that deep (thermally disconnected) traps are an essential part of luminescence systems in order to produce consistent explanations of a wide variety of phenomena (including, for example, TL peak shapes, supralinear growth and pre-dose sensitisation). It is also likely from a physical point of view that there are a variety of electron trapping centres with a thermal stability significantly greater than that of Levels 3 and 4.

3.3.1.2 The hole trapping centers

The Bailey's model [73] has four hole trapping centres and recombination of electrons from the conduction band is allowed at each of these levels.

Levels 6 and 7 'thermally unstable non-radiative recombination centres': These levels are similar in many respects to the `Reservoir centre' (`R-centre') postulated by Zimmerman [9] and play an important role in the `dose quenching' and subsequent `thermal activation' characteristics of quartz.

Level 8 'thermally stable radiative recombination centre': Recombination of electrons with trapped holes at Level 8 produces luminescence in the this model and this level is termed the `luminescence centre' (`L-centre'). Recombination at Level 8 in the model is equivalent to recombination of electrons at the hole centre responsible for the OSL and TL emissions at 380 nm (see, for example, Franklin et al.[38]; Huntley et al. [82]; note that Scholefield et al. [83] and Franklin et al. [38] show the peak emission wavelength in this region to be temperature dependent, moving to lower emission energies at higher temperatures.). Yang and McKeever [40] attribute the 380 nm 110 °C TL emission to recombination of electrons at $(H_3O_4)°$ hole centres. Zimmerman [9] assigned an optical depth of approximately 5 eV to the luminescence centre (`L-centre') responsible for this emission (this being the photon energy required for ionisation of electrons from the valence band to this centre). It is assumed that the centre studied by Zimmerman [9] and that designated to the $(H_3O_4)°$ hole centre by Yang and McKeever [40] are the same. The work of Franklin et al. [38] suggests that this centre also gives rise to the 380 nm quartz OSL emission. Further evidence is available which suggests that both the 110 °C TL and main OSL signals are at least partially due to recombination at the L-centre: Huntley et al. [84] found the wavelength band of the quartz OSL emission that thermally sensitises to be the same as that of the 110 °C TL emission; Aitken and Smith [85],

Stokes [86] and also Wintle and Murray [87] found that thermal sensitisation occurred in parallel between the 110 °C TL peak and the main OSL signal (the fast and medium components described by Bailey et al.[77]).

Level 9 'thermally stable `non-radiative' recombination centre': Level 9 represents all recombination centres other than the R-centres (Levels 6 and 7) that are either non-radiative or emit photons at energies outside the UV detection window. As with deep (thermally disconnected) electron traps, direct evidence for the existence of non-radiative `killer' centres is also difficult to acquire. Emission bands (of the 110 °C TL peak), distinct from the main 380 nm band, have been identified by a number of authors. Yang and McKeever [40] report a band centred on 460 nm, assigned to the $(AlO_4)°$ centre. There is evidence of this emission (at ~2.7 eV) also in the OSL emission spectra presented by Huntley et al. [84]. The emission at ~460 nm, and another at ~420 nm (as described by Bailif. [88]) are of significantly lesser magnitude than that at 380 nm and, for simplicity, specific representations of the centres responsible for these signals have not been included in this model.

3.4 Effects of Pre-treatments upon the TL from Quartz

The various pretreatments upon the TL from quartz give rise to change in TL sensitivity of quartz. Thermal treatment (annealing), pre-dose effect and heating-rate effect are three significant examples of mentioned pretreatments.

3.4.1 Thermal treatment (Annealing)

There is a change of TL sensitivity (intensity) when quartz sample is annealed. Usually, the change is an increase. The enhancement of TL sensitivity of 110 °C peak of quartz was described or addressed to be the result of an increase in the number of activated luminescence centers [9]. More practitioners found a large sensitivity enhancement of the 110°C TL peak after high temperature annealing [40, 89-90]. The enhanced sensitivity after high temperature annealing was suggested to be not a pre-dose effect [40]. This suggestion was confirmed by a clear enhancement of phototransferred thermoluminescence (PTTL) sensitivity in a sediment (natural) quartz sample after high temperature annealing [91]. The observation of TL

sensitivity as a function of annealing even resulted in an attempt to estimate the firing temperature of a potsherd [92-93].

The TL sensitivity change of other low temperature TL peaks in quartz was not intensively studied as 100 °C TL peak or PTTL. Only few observations of effects of annealing on high temperature TL peaks were reported. For 300 and 350 °C TL peak in quartz extracted from a well-fired sherd, the sensitivity change is strongly dependent on the temperature treatment [94]. In a German quartz sample, compared with 400 °C annealing, 700 °C annealing enhanced the 360 °C TL sensitivity by a factor of 10, a rapid increase was found for annealing temperatures above 570 °C, in which the enhancement effect was related to alteration in recombination centers [95]. Many protocols were proposed to correct the measured signals concerning the sensitivity changes caused by heating [96]. The correction requires a comprehensive understanding of the sensitivity changes.

Due to the study of Han et al. [98], an annealing at temperature lower than 140 °C has negligible effects on their sensitivities. For high temperature TL sensitivities, the annealing at a temperature of about 200 up to 800 ^{o}C can cause an obvious decrease. A level of about 20% of its natural value was observed for the most effective annealing. Annealing at temperatures lower than 200 °C did not change the sensitivities and annealing at temperatures higher than 800 °C could result in an enhancement. Results of annealing on low temperature TL sensitivities do not support the suggestion that the firing temperature of a potsherd can be determined by TL studies of the quartz [92-93], because the TL sensitivities of TL peaks at 110 and 230 °C were not only dependent on the maximum temperature to which the granitic quartz had been fired, but also on the annealing time. The firing temperature can only be estimated if the pottery was manufactured in a same way, i.e., the same firing time. At least, it is true for the pottery that is mainly manufactured with granitic quartz, or for the case that the annealing has the same effects on both granitic quartz and sedimentary quartz. There is no effect on the TL sensitivity if the annealing temperature is low enough, lower than 140 °C for the low temperature TL sensitivities and lower than 200 °C for the high temperature TL sensitivities. This suggests that a TL measurement involving heating treatment at these temperatures needs no correction of TL sensitivity change. The experiment of cycle measurement revealed that the high temperature TL sensitivity could increase

with the measurement time. This observation is different from that after annealing for a long time. This enhancement is explained as a result of some effect similar to pre-dose effect. The number of trapped electrons (holes) induced by a test dose is thought to be proportional to the number of emptied traps. If the TL intensity is also proportional to the number of trapped electrons [36], then there should be a proportional relation between the numbers of TL traps and the TL intensity. Hence, the TL sensitivity in the above results can be replaced with the trap population.TL traps are associated with a form of crystal defects, such as 110 °C TL traps were related to point defects in quartz [97]. Their behaviours under ionizing radiation were studied and a trap model was proposed [98]. Low temperature TL traps were called thermally sensitive traps, and radiation had negligible effects on the population of low temperature TL traps.

High temperature TL traps were called radiation sensitive traps, and their population could increase with the received radiation dose. It is assumed that annealing can create new thermally sensitive traps, resulting in an increase of their population. If the annealing temperature is in the range of 200-800 °C, radiation sensitive traps can be destroyed, resulting in a decrease of their population. Because of these characteristics, TL traps can be a potential geochronometer with a high upper dating limit because they are more stable than the trapped electrons (holes). Radiation sensitive traps are stable when the temperature is lower than 200 °C. Higher temperatures can reduce their population, especially 300-700 °C. It is believed that their population could reach a minimum level in quartz when crystallized. Although the change of TL sensitivity after annealing is explained to be caused by trap creation and destruction, trap transformation from TL irrelevant type to TL relevant type is another possible mechanism [99].

In many TL dating methods thermal treatment is a necessary step, so it is very important to understand the influence of these thermal treatments on the TL properties of the crystal [100]. An increase in sensitivity is often observed, and can be related to the absorbed radiation dose prior to thermal treatment although sensitization by heat treatment alone has been reported from crystalline quartz [40]. Zimmerman [9] explained the sensitization using a phenomenological model that involves an increase in the radiative recombination probability at the luminescence sites. This enhancement is induced by the pre-dose and the thermal treatment. They

proposed a model based on competition traps, where the deeper trap is partially removed during the thermal treatment. As was expected, the annealing increases the sensitivity of the samples, especially around the 110 °C TL peak. The sensitivity of the quartz samples at 900 °C is increased by more than 3 orders of magnitude [101]. A strong sensitization of the TL emission of quartz that appears to be due only to the effect of the thermal treatment [101]. $[H_3O_4]^o$ hole center which involves the replacement of a host Si by three protons plus captures a hole [40, 102] . Therefore, the increase of the sensitivity as a function of thermal treatment is directly related to the creation of $[H_3O_4]^o$ centers that act as luminescence centers.

Zimmerman Model:

The annealing effect on TL sensitivity of quartz can be explained with Zimmerman model. Fig.3.4. shows the schematic diagram of multiple levels of R traps applied on the basis of the model of Zimmerman [9].
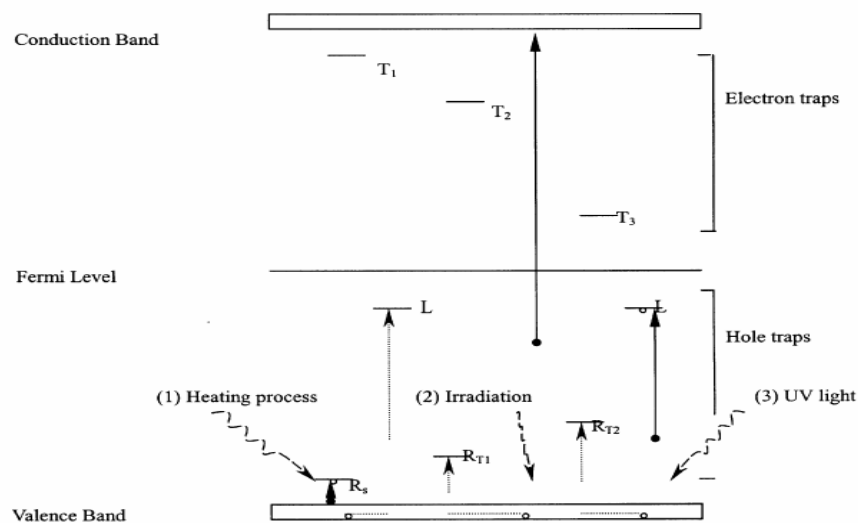
Figure 3.4 Schematic diagram of multiple levels of R traps applied on the basis of the model of Zimmerman [9]. (●) represents an electron; (o) represents a hole

Annealing can change the relative concentration between the L and R hole centers. When quartz is annealed between 160 and 300 °C, holes are thermally released from R_s-centers. The holes in the deeper (more stable) RT-centers are unaffected. This gives rise to increases in both the OSL and TL sensitivities. When

the thermal energy increases by annealing from about 300 to 600 °C, holes from R_s and R_T centers are transferred to L centers and the OSL and TL sensitivities both increase significantly. Because R_s is less stable than the R_T center holes, holes from R_s centers will be transferred at relatively lower temperature than holes from R_T centers.

3.4.2 Dose response and pre-dose effect

The TL dose response of quartz and its well-known change of sensitivity upon thermal and radiation treatments have been studied in both natural and synthetic samples [102]. Chen et al. [89] found that the "110 °C" TL peak of unfired synthetic quartz exhibits a highly superlinear growth with absorbed dose. Specifically, they found that the maximum TL intensity I_{max} follows a dose dependence of the form:

$$I_{max} = aD^k \tag{3.1}$$

Here, D represents the absorbed dose; a and k are constants. By plotting Eq. (3.1) on a log–log scale, a linear graph is obtained with slope k. The value of k is a direct measure of the degree of superlinearity [17], and it is called as the "superlinearity slope k". It is noted that k is assumed constant within a certain dose range. It is also noted that superlinear growth of I_{max} is known to occur only for low doses. Chen et al. [89] found that this superlinearity is removed by firing the samples above 300 °C. The work [89] was limited to the "110 °C" TL peak and to doses under 10 Gy. These authors explained both the superlinearity and the well-known change in the TL sensitivity of synthetic quartz by using the recombination during heating model. According to this model, firing the quartz samples at high temperatures removes the competitors and results in a reduction of the superlinearity. Chen et al. [89] suggested that the role of the competitors may be filled by electron traps known as E_1 centers.

Charitidis et al. [103] studied the dependence of the TL dose response on the pre-dose delivered to the sample. By carefully controlling the pre-dose conditions, these authors showed that a high pre-dose effectively removes the superlinearity effect. Recently, Charitidis et al. [104] extended the experimental work of Chen et al. [89] by measuring the sensitivity and TL dose response of several glow-peaks in

synthetic quartz as a function of the annealing temperature. Their measurements extended the range of annealing to temperatures between 300 °C and 900 °C. These authors obtained complete TL dose response curves between 0.1 and 170 Gy at each annealing temperature. Chen et al. [89] and Charitidis et al. [104] found that the superlinearity slope k of the "110 °C" TL peak is strongly reduced as the firing temperature increases. Furthermore, it was found that each TL dose-response curve consists of two dose regions, which on a log–log scale appear linear with different slopes k, indicating two different degrees of superlinearity. For doses less than 11 Gy, the superlinearity slope k drops continuously from a value of 2 at room temperature to a value of 1 for an annealing temperature of 700 °C, and then slowly increases to a value of 1.2 at a temperature of 900 °C. For doses between 20 and 100 Gy, the superlinearity slope k exhibited a very different behavior, by remaining constant at a value of 2.5 from room temperature up to annealing temperatures of 500 °C, and then decreases continuously to a value of 0.6 at an annealing temperature of 900 °C.

Chen and Leung [105] developed a mathematical model based on two electron and two hole trapping states. The model is a modification of the Zimmerman theory that explained first the predose effect [9, 106]. Chen and Leung [105] simulated the sequence of experimental actions taken during the pre-dose dating technique, by solving the differential equations for each stage in the experiment. Pagonis et al. [107] showed that the model of Chen and Leung [105] can also be used to describe the behavior of the superlinearity of the "110 °C" TL peak as a function of the annealing temperature, as well as a function of the predose amount. It is found that the model accurately reproduces several features observed experimentally by Charitidis et al. [104].

Modified Zimmerman Model:

Zimmerman [9, 106] first proposed a predose model consisting of one electron trapping state T, a luminescence center L and a hole reservoir. R. Chen [108] proposed a modification of the Zimmerman model by adding an extra electron level S which competes for electrons during the heating stage. By using physical arguments concerning the observed experimental behavior of quartz samples, Chen

and Leung [105] were able to arrive at a "good" set of parameters for the modified Zimmerman model, which explains successfully the following experimental results:

- Linear dependence of the TL signal on the test dose.
- Exponential approach of the sensitivity to saturation with repeated additive doses.
- Quenching by high dose exposure, UV reversal and the distinction between reservoir and center saturations. Further work using this model is necessary in order to obtain a quantitative description of these phenomena in agreement with experimental data available in the literature.
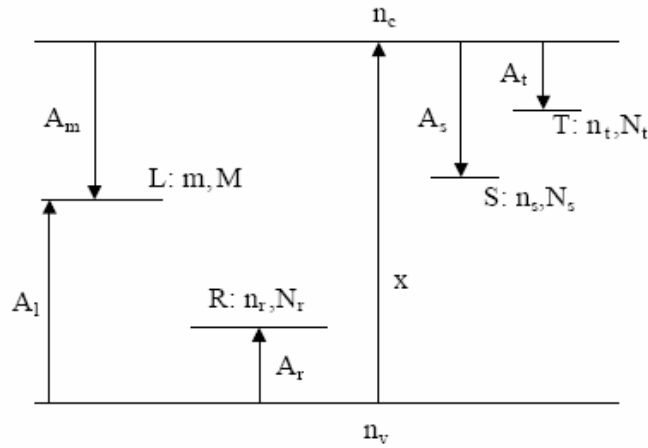
Figure 3.5 The energy scheme used in modified Zimmerman predose model [105]

Fig. 3.5 shows the energy scheme used by Chen and Leung [105]. It consists of two trapping states T and S and the hole reservoir R, with total concentrations N_t ; N_s and N_r (in cm^{-3}) and with instantaneous occupancies denoted by n_t ; n_s and n_r (in cm^{-3}) correspondingly. The activation energy for the main traps T is E_t (in eV) and the frequency factor is s_t (s^{-1}), while the competitor traps S are considered to be thermally disconnected. The activation energy for the hole reservoir R is E_r (in eV) and the frequency factor is s_r (s^{-1}). The retrapping probability coefficients for R, T and S are denoted by A_r; A_t and A_s (in cm^3 s−1), and n_c and n_v (cm^{-3}) represent the concentrations of electrons and holes in the conduction and valence band, respectively. The rate of production of electron–hole pairs x (in cm^{-3} s^{-1}) is proportional to the dose rate. The quantity $D = xt$ represents the total concentration of

pairs produced, and is proportional to the dose (where t is the irradiation time in sec and D is in cm^{-3}). M and m denote, respectively, the concentration and occupancy of the hole centers (cm^{-3}) and A_m; A_l (cm^3 s^{-1}) are, respectively, the recombination probability coefficients of electrons and holes into the recombination center L.

3.4.3 Heating rate effect

In the thermoluminescence (TL), the glow curve is affected by some experimental parameters. Heating rate is one of the most important experimental variables, which changes the glow curve shape [109]. In addition to the conventionally used heating rate in TL readers, very high ones had been reportedly achieved by laser heating [110]. In the TL dosimetry, the absorbed dose and TL intensity are affected by changes in heating rate [111-112]. Many investigations have been carried out by scientists in order to understand that how the TL glow curve changes under the different heating rate [112-115]. Taylor and Lilley [112] pointed out that changes in intensity, caused by the change of heating rate, may have a bearing on the determination of the trapping parameters E (trap depth) and s (frequency factor). As a result of many studies, a decrease in TL intensity was observed with increasing heating rate [115]. This phenomenon has been explained to be due to thermal quenching, whose efficiency increases as temperature increases. Thermal quenching of the luminescence is the phenomenon in which the luminescence efficiency decreases as the temperature increases.

In order to account for thermal quenching, the luminescence efficiency expression in equation (3.2) can be used [115]

$$\eta = [1 + c \exp(-W/kT)]^{-1} \qquad (3.2)$$

where W is the activation energy of luminescence efficiency due to the thermal quenching, k is the boltzman constant and Naperian logarithm of the integrated TL intensity can be written as

$$\ln(\text{integrated TL}) = (W/k)T_m^{-1} + F \qquad (3.3)$$

where F is constant with heating rate. Hence the slope of the plot of *ln (integrated TL)* against *$1/T_m$* gives *W/k*. In this formula, *T_m* is the maximum peak temperature. The temperature of a TL peak shifts to higher values as the heating rate increases. Thus, at low heating rates the TL peak may appear in a range where thermal

quenching is minimal, whereas at higher heating rates the peak temperature may be such that thermal quenching is strong [116]. Also, Berkane-Krachai et al. [117] have studied that heating rate effect on TL response and showed that the TL response decreases when heating rate increases and this reduction of TL sensitivity is well described using a Mott-Seitz theory. Hornyak et al. [118] have investigated about this subject and implied that the peak temperature shifted about 42 $^{\circ}$C from the lowest heating rate to highest heating rate. They observed gradual decrease in TL intensity with increase heating rate. This decrease from 0.5 to 4 $^{\circ}$C/s of about 8% may well be due to thermal quenching.

During experiment, the measured temperature may be different from the sample temperature caused by a small temperature lag due to the thermal contact of the heater and the sample. Therefore, there is a linear ramp in the sample with a temperature lag and so that the T_m read from glow curve will be systematically lower than its actual value. Consequently, the sample thickness has an important influence on temperature gradient and temperature lag especially at higher heating rates [119].

CHAPTER 4

EXPERIMENTAL EQUIPMENTS AND PROCEDURES

4.1 Equipments in Laboratory

The thermoluminescence laboratory has two main rooms. In the first room, there are a furnace, a sieve, a digital balance, and etc. They were used to prepare the samples to the experimental applications. The irradiation and reading process were carried out in the other room called as darkroom. Radiation source and TL reader are present in this room.

Figure 4.1 Thermoluminescence laboratory

4.1.1 Radiation source and irradiator

The samples were irradiated at room temperature immediately after quenching by a ^{90}Sr-^{90}Y β (beta)-source. The activity of this source is about 100 mCi. It was calibrated by manufacturer on March, 10, 1994. The recommended working life-time is about 15

years. Stronium-90 emits high energy beta particles from their daughter products (^{90}Sr β-0.546 MeV together with ^{90}Y β-2.27 MeV). Beta radiation is absorbed by air, so its intensity declines with distance much more rapidly than inverse square law calculations would indicate. The typical strength of a 100 mCi Sr-90-^{90}Y β-source installed in a 9010 Optical Dating System is 1.42 Gy/minute=0.0238 Gy/sec for fine grains on aluminium, or 1.5 Gy/min=0.025 Gy/sec for 100 mg quartz on stainless still. The irradiation equipment is an additional part of the 9010 Optical Dating System which is purchased from Little More Scientific Engineering, UK [120]. The irradiation source equipment is interfaced to a PC computer using a serial RS-232 port.
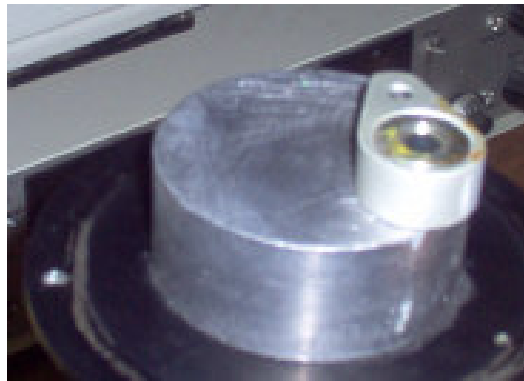
Figure 4.2 ^{90}Sr-^{90}Y β-source

Feature of the 9010 Optical Dating System:

- Precision on paleodose determination typically 3-5%, often better (90-125 micrometer quartz).
- System design removes the need to handle sample discs after they are first placed in the tray.
- 64 disc positions enable large numbers of dose points to be well defined.
- Temperature control of samples during illumination
- Reproducible and precise sample positioning

High speed of operation. A short exposure (≤ 1 second) to all 64 samples takes only ten minutes

Figure 4.3 9010 Optical Dating System (irradiator)

4.1.2 TLD reader and analyzer

The glow curve measurements for quartz crystals were made using a Harshaw TLD System 3500 Manual TL Reader [121]. It economically provides high reliability. The technical architecture of the system includes both the Reader and a personal computer connected through a standard RS-232 serial communication port to control the 3500 Reader.

Figure 4.4 Harshaw TLD System 3500 Manual TL Reader

The basic block diagram of reader is shown in figure 4.5. All functions are divided between the reader and the specialized WinRems software that runs on the PC. All data storage, instrument control, and operator inputs are performed on the PC. Signal acquisition and conditioning are performed in the reader. In this way, each glow curve can be analyzed using a best-fit computer program based on a Marquardt algorithm minimisation procedure, associated to first-order and general-order kinetic expressions. The program resolves the individual peaks present in the curve, giving the best values for the different peak parameters. The instrument includes a sample change drawer for inserting and removing the TLD elements. The reader uses contact heating with a closed loop feedback system that produces adjustable linearly ramped temperatures from 1 ^{o}C to 50 ^{o}C per second accurate to within ± 1 ^{o}C to 600 ^{o}C in the standard reader.
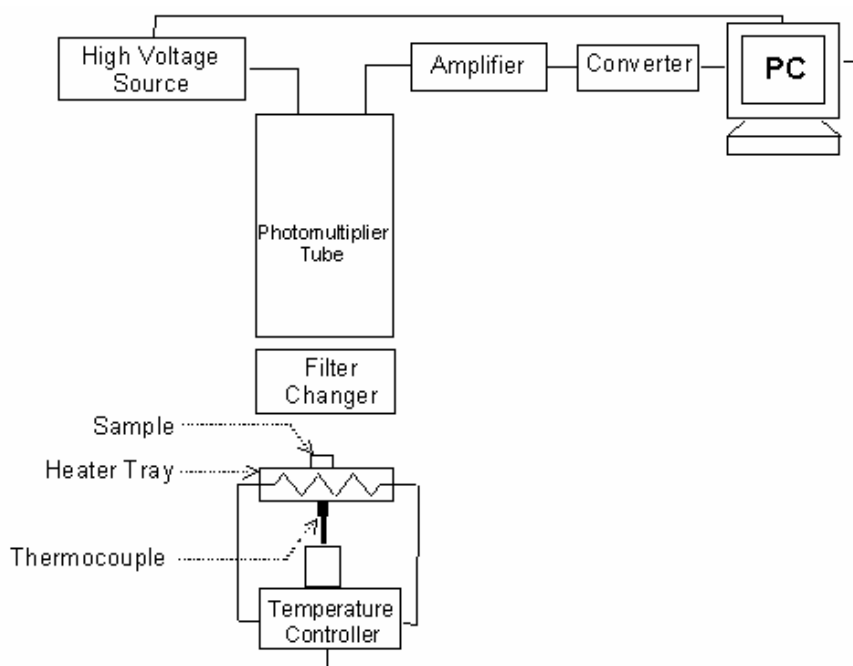
Figure 4.5 The basic block diagram of TL reader.

4.1.3 Equipments used before irradiation process

In the given work, a microprocessor controlled electrical oven, a digital balance and sieves were also used to anneal the samples at different temperatures to estimate the weight of the used samples and to sieve crushed samples for desired dimensions,

respectively. The dimensions of particle vary from 50 µm to 2 mm. The temperature range of oven changes from RT up to 1200 °C and its sensitivity was estimated ± 1 °C. In addition, some chemicals were used to clean samples.

Figure 4.6 Some of the used equipments: oven, chemicals, sieves and digital balance.

4.2 Used Samples

In all experiments, two kinds of sample have been used for this thesis
- Synthetic quartz
- Natural quartz

4.2.1 Synthetic quartz

The acid purified synthetic quartz (APSQ) samples used in this study were in the form of powder produced by Fluka Company. The extended specifications of this sample are given in Table 4.1. It is white quartz and packed in Switzerland with 323564/1-896 analysis number.

Table 4.1 Extended Specifications of acid purified synthetic quartz (APSQ)

Loss on ignition	≤0.1%, 900 °C
particle size	40-100 mesh
Chloride (Cl)	≤50 mg/kg
Ca	≤50 mg/kg
Cd	≤50 mg/kg
Co	≤50 mg/kg
Cu	≤50 mg/kg
Fe	≤100 mg/kg
K	≤500 mg/kg
	≤100 mg/kg
Ni	≤50 mg/kg
Pb	≤50 mg/kg
Zn	≤50 mg/kg

4.2.2 Natural quartz

The natural quartz were in the form of powder and extracted from the tiles of Kubad Abad palace. It has been deduced that the production of tiles of Kubad Abad Palace was made from the clay materials in the same region [124]. The Kubadabad Palace, established as the summer residence of Seljuk Sultan Alaeddin Keykubad (1220-1236), lies on the south-west shores of Lake Beysehir, west of Konya [123-124]. It was first discovered in 1949 by Zeki Oral, and subsequently excavated in the 1960s by K.Otto-Dorn and more recently by a team of archaeologist from Ankara University under the direction of Prof. Rüçhan Arik. The palace is one of a suite of buildings that make up the royal vacation town of Kubadabad, formerly only known from the descriptions of the contemporary historian Ibn Bibi.

The pure natural quartz was obtained by quartz inclusion technique, which was developed by Fleming [39]. It has been applied to extract the quartz samples from the tiles. A layer (2-3 mm) of the outer surface of tile samples was removed by filing. The rest of fragment was firstly pulverised and then the obtained powder sample was sieved between 40-150 μm. The obtained powder sample was washed in 10% HCl acid to dissolve carbonates. In additional treatment, sample was stayed in diluted HF (1M) to eliminate remaining clay materials. Finally, the quartz minerals in a powder form have been obtained after the collection of iron elements from powder sample by using a magnet. In addition, the results of XRF analysis of tile

powder and quartz extracted were indicated in Table 4.2 [124]. This mineralogical analysis was made in the university of Fribourg at the geology department of Geosciences in Switzerland with x-ray fluorescence spectrometer, its name is Philips PW2400.

Table.4.2 Results of XRF analysis for tile powder and quartz extracted

	SiO_2 (%)	TiO_2 (%)	Al_2O_3 (%)	Fe_2O_3 (%)	MnO (%)	MgO (%)	CaO (%)	Na_2O (%)	K_2O (%)	P_2O_5 (%)
Tile powder	89.08	0.24	6.01	0.53	0.02	0.53	1.18	1.28	0.82	0.13
Quartz extracted	99.68	0.13	0.05	0.01	0.00	0.04	0.03	0.00	0.03	0.01
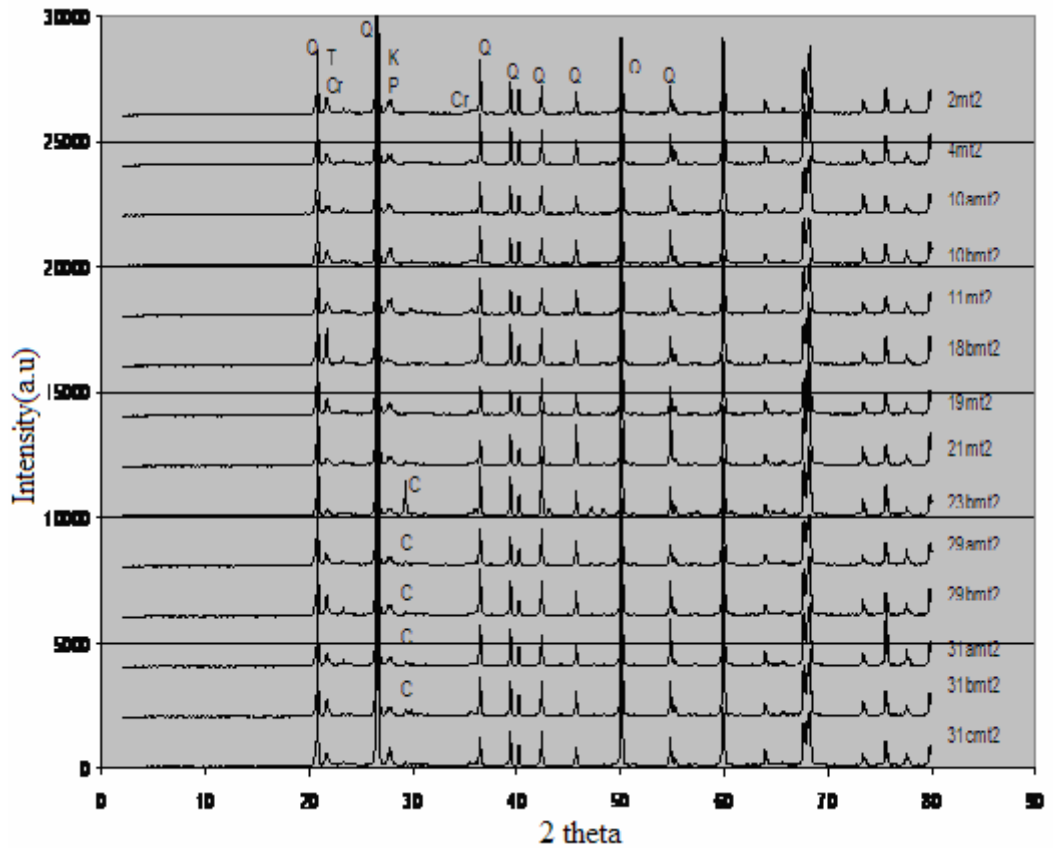
Figure 4.7 Results of XRD analysis for tile powder and quartz extracted

50

Figure 4.8 Synthetic and natural quartz samples used in this thesis

4.3 Experimental Procedures

This thesis includes four main works:

- Investigation of variation of kinetic parameters and intensity of TL peaks of annealed synthetic quartz at 500 $^{\circ}$C and 600 $^{\circ}$C

- Effects of thermal treatment on the TL intensity and kinetic parameters of natural quartz

- Thermoluminescence dose response of synthetic and natural quartz

- Heating rate effects on the thermoluminescence of synthetic and natural quartz

4.3.1 Investigation of variation of kinetic parameters and intensity of TL peaks of annealed synthetic quartz at 500 °C and 600 °C

We prepared twenty two synthetic powder quartz samples and each of them had 30 mg weight. Two of them were used for cycle of measurement and others were for annealing time. Aluminum vessels were used to put the powder synthetic quartz. After all samples were annealed, they were irradiated about 15 minutes (≈13.5 Gy) at RT with β-rays from a calibrated ^{90}Sr-^{90}Y source. The time duration between irradiation and TL reading was always kept constant at about 1 minute. The samples were read out in the dark room with a Harshaw QS 3500 manual type reader that was interfaced to a PC where the TL signals were studied and analyzed.

Glow curves were obtained using a platinum planchet at a linear heating rate of 1 ^{o}C/s. In a contact heating, the temperature control is achieved with the temperature of the heating element (planchet) and therefore a thermal lag exists between samples and heater at the high heating rates (>2 ^{o}C/s). A standard clean glass filter was always installed in the reader between sample and photomultiplier tube. This filter allows the light whose wavelength between ≈250 nm and ≈1000 nm to pass through it and there upon eliminates unwanted infrared lights that are emitted from heater.

The reader is controlled via WinREMS™, Bicron's Windows-based dosimetry management system. The flexible design of the controlling software enables the user to set up a file to automatically record dosimeter ID and patient information or to manually enter each dosimeter ID. This same software provides all calibration and quality control functions, as well as storing, reporting, and exporting all dosimetry data. Exported glow curves were analyzed with using a Computer Glow Curve Deconvolution (CGCD) method to get kinetics parameters of all peaks.

In the cycle of experiment, one of the two samples was annealed at 500 °C for 1 hour before irradiation process and then it was cooled to RT for irradiation. After the irradiation process, its glow curve was recorded by the TL reader. To see the effect of annealing on the TL intensity, this process was repeated ten times using the same sample. The similar experimental procedure was also performed at 600 °C to discriminate the effect of annealing at different temperatures.

In addition, to observe the effect of annealing on the TL intensity, the annealing procedures at 500 °C and 600 °C were also performed as a function of time using different sample in each experiment. The following annealing durations 30, 45, 60, ... and 1500 minutes were chosen for these experiments.

4.3.2 Effects of thermal treatment on the TL intensity and kinetic parameters of natural quartz

In this study, the experiments were classified into three groups according to desired aims:

Cycle of measurement experiments

In this part, it was tried to find the most suitable annealing temperature for the used samples. Two samples were used for this part. The aluminum discs were again used to put powder quartz samples and each one was exactly weighted 30 mg. Firstly, the samples were annealed at 500 and 600 $^{\circ}$C for 1 hr. After the samples were annealed, they were irradiated by beta irradiator ^{90}Sr-^{90}Y source for 30 minutes (~27 Gy) at room temperature in the darkroom. The irradiated samples were read out by Harshaw TLD System 3500 Manual TL Reader. Finally, the obtained glow curves were analyzed in computer using CGCD method. This procedure was repeated eight times using the same sample.

Annealing time experiments

In the second part of experiments, the experimental study was made to see the effect of the annealing time on the TL intensity and kinetic parameters of natural quartz samples. Nine samples were used for eight different annealing times and one unanneal process in this part and each one was weighted 5 mg. All samples were annealed at 600 °C except for one sample, irradiated by beta irradiator ^{90}Sr-^{90}Y source for 30 minutes (~27 Gy), read out by TLD system and then analyzed in computer by CGCD program.

Annealing temperature experiments

The last part of this study was the annealing of samples at different temperatures to see the variation of TL intensity and kinetic parameters of natural quartz. In this case, fifteen samples were used for fifteen different annealing temperatures. All samples were annealed 1 hour, irradiated by beta irradiator ^{90}Sr-^{90}Y source for 1 hour (~54 Gy), read out by TLD system and then analyzed in computer by CGCD program. Each sample had 5 mg weight.

4.3.3 Thermoluminescence dose response of synthetic and natural quartz

This study was based on the investigation of dose responses of natural quartz and synthetic quartz. In this study, the dose responses of synthetic and natural quartz were carried out by four main parts.

Different samples (unused) without heat treatment

This part was carried out to see effects of applied dose on the thermoluminescence peak intensities, shape of glow curves and region areas with using region of interest method in synthetic and natural quartz samples.

In this part fifteen powder synthetic and fifteen powder natural quartz samples were used and each one was 30 mg for synthetic quartz and 5 mg for natural quartz. Firstly, they were irradiated by beta irradiator ^{90}Sr-^{90}Y source for 1, 5, 15, 30 s, 1, 5, 15, 30 m, 1, 2, 4, 8, 16 h, 1 and 2 days at room temperature in darkroom. In other words, these values vary between 0,015 and 2600 Gy. Secondly, the irradiated samples were read out by Harshaw TLD System 3500 Manual TL Reader. Finally, the obtained glow curves were analyzed in region of interest method by using WinRems program.

Same sample (reused) without heat treatment

In the second part, the above procedure was repeated using same (reused) synthetic and natural quartz sample to see differences on the dose response of different (unused) and same (reused) samples.

Different samples (unused) with heat treatment

The main aim of third part is to see the effects of the heat treatment on the dose response of synthetic and natural quartz samples. In this part fifteen synthetic and fifteen natural quartz samples were used. Before irradiation of the samples, all of them were annealed in the oven at 600 ^{o}C for 1hour.

Same samples (reused) with heat treatment

This part has the same procedure with the third part but there was only one difference that the same sample was used in this part for all different doses.

4.3.4 Heating rate effects on the thermoluminescence of synthetic and natural quartz

In this study, the effect of heating rate (β) on the glow curves of the natural and the synthetic quartz was also studied. The samples were weighted 5 mg for natural quartz and 20 mg for synthetic quartz. For each measurement, the natural and synthetic quartz samples were irradiated about 54 Gy and 27 Gy, respectively. These dose levels were chosen to see all glow peaks in the glow curves of both samples. All the recorded glow curves were analyzed with using a Computer Glow Curve Deconvolution (CGCD) method to get kinetics parameters of all peaks. Annealing process was made in a microprocessor controlled furnace whose range varies from room temperature to 1200 $^{\circ}$C. Heating rate was carried out for 1, 2, 4, 8 and 16 $^{\circ}$C/sec.

The effects of heating rate of both natural and synthetic quartz samples were carried out with and without annealing processes. In the annealing process, all samples were annealed at 600 $^{\circ}$C for 1 hour.

CHAPTER 5

EXPERIMENTAL RESULTS

The experimental results were examined under four main folders:

- The investigation of kinetic parameters and intensities of TL peaks of synthetic quartz as a function of annealing temperature at 500 $^{\circ}$C and 600 $^{\circ}$C
- The effects of thermal treatments on the TL intensity and kinetic parameters of natural quartz
- The thermoluminescence dose responses of synthetic and natural quartz after different annealing protocols
- The effects of heating rates on the thermoluminescence of synthetic and natural quartz

5.1 The Investigation of Intensities of TL peaks of Synthetic Quartz as a Function of Annealing Temperature at 500 and 600°C

In this part; we have investigated the influence of thermal treatments on the kinetic parameters (trap depth and frequency factor) and intensities of TL peaks of synthetic quartz at 500 $^{\circ}$C and 600 $^{\circ}$C. In this case, the variation of kinetic parameters and the intensities of TL peaks were firstly followed with cycle of measurement and then as a function of annealing time.

A typical analyzed glow curve of used synthetic quartz measured at a heating rate of 1°C/s after the application of heat treatment at 600 $^{\circ}$C for 1 hour is shown in figure 5.1 where both the experimental points and fitted glow peaks are presented. It was observed that the glow curve structure of this sample is well described by a linear combination of at least five first-order glow peaks between RT and 400 $^{\circ}$C.
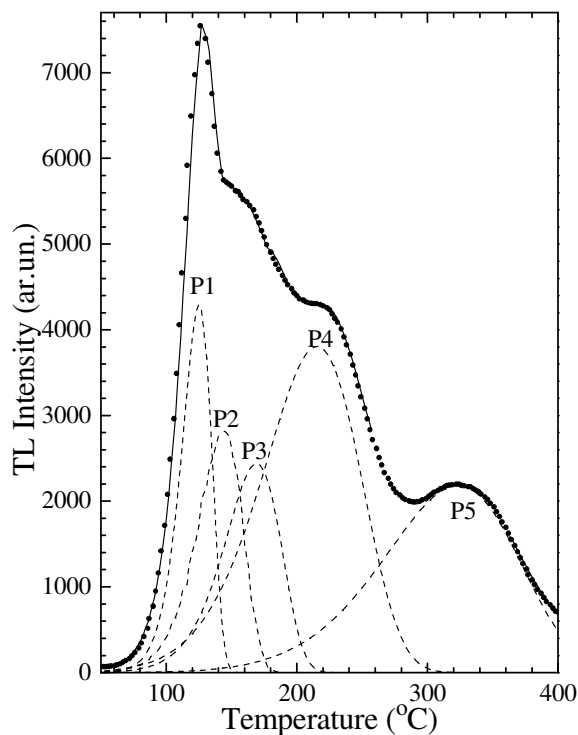
Figure 5.1 A typical analysed glow curve of annealed quartz at 600 ^{o}C for 1 h measured after ≈30 Gy irradiation at RT. The glow curve was measured by heating the sample to 400˚C at a heating rate of 1˚C s^{-1}. In the figure, solid circles represent the experimental points

5.1.1 Cycle of measurement

If the sensitivity of a sample or at least its dosimetric peak does not change after several cycles of exposures and readouts, it can be considered as a good phosphor. Thus, the studied material was also tested for its reproducibility. The reference samples were exposed to beta-ray for 30 min after annealing procedure at 500 ^{o}C and 600 ^{o}C for 1 h and then their glow curves were recorded between RT and 400 ^{o}C. These procedures were repeated ten times and some of the recorded glow curves are seen in Fig. 5.2. The all glow curves were analysed by CGCD method and the obtained results are given in Fig. 5.3. It is seen that the intensities of P2+P3 and P4 increase slowly with increasing experimental cycles whereas the intensity of P1 quickly increases. On the other hand, the intensity of P5 has a good stability during successive readings (Fig. 5.3). The obtained repeatability of this peak over 10 cycles is within 5%.
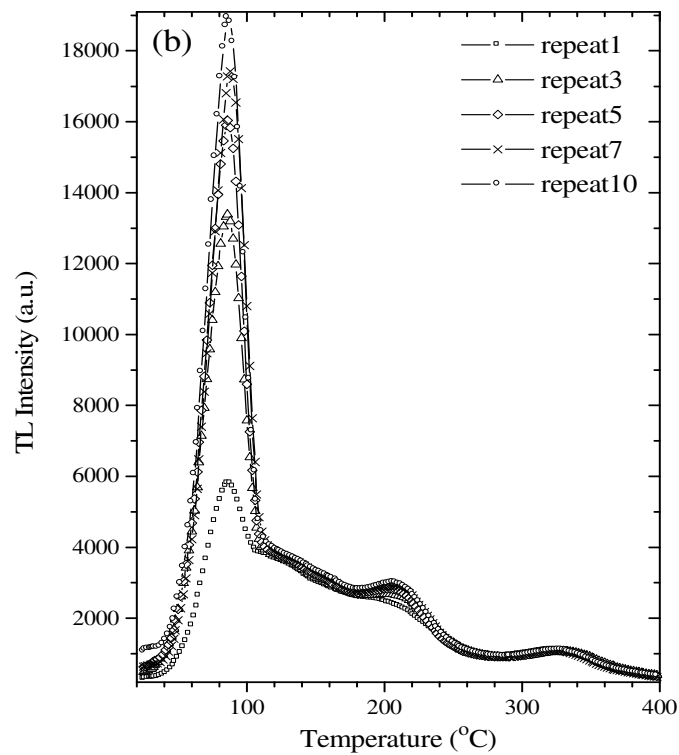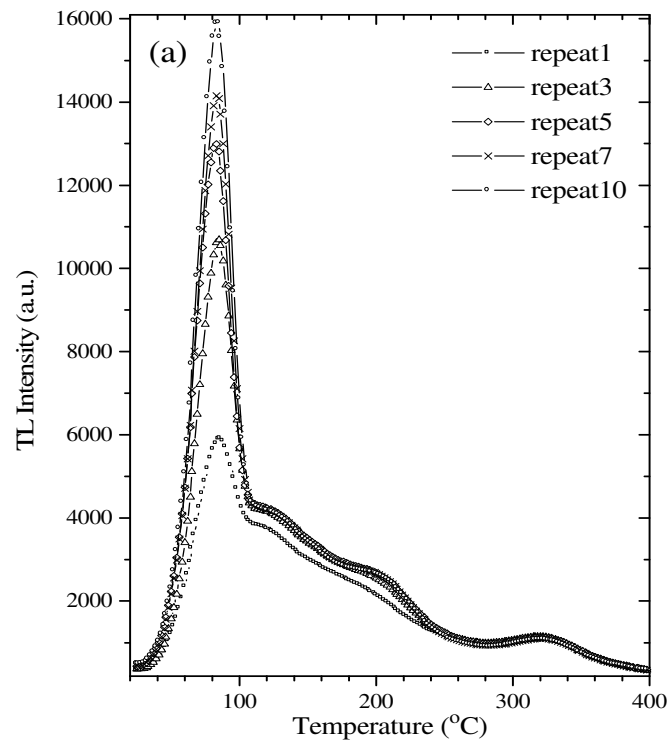
Figure 5.2 Some of the selected glow curves of synthetic quartz as a function of experimental cycle. The samples were annealed at (a) 500 ^{o}C (b) 600 ^{o}C for 1 h before irradiation
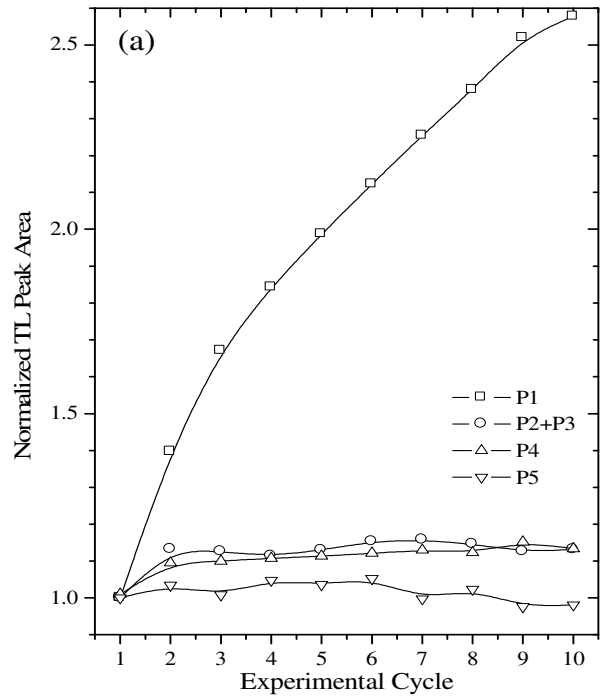
Figure 5.3 Reproducibility of deconvoluted peak areas of some glow peaks of synthetic quartz through ten repeated cycles of pre-irradiation annealing (a) 500 ^{o}C (b) 600 ^{o}C for 1 h -irradiation-readout

5.1.2 Annealing time

In this part of our investigation, we have observed the influence of the annealing time on the kinetic parameters and intensities of TL glow peaks. We have used 20 samples for these experiments. Ten of them were used for annealing time (30, 45, 60, 90, 120, 240, 360,480, 660 and 1500 minutes) at 500 $^{\circ}$C and the others were for 600 $^{\circ}$C with the same durations.
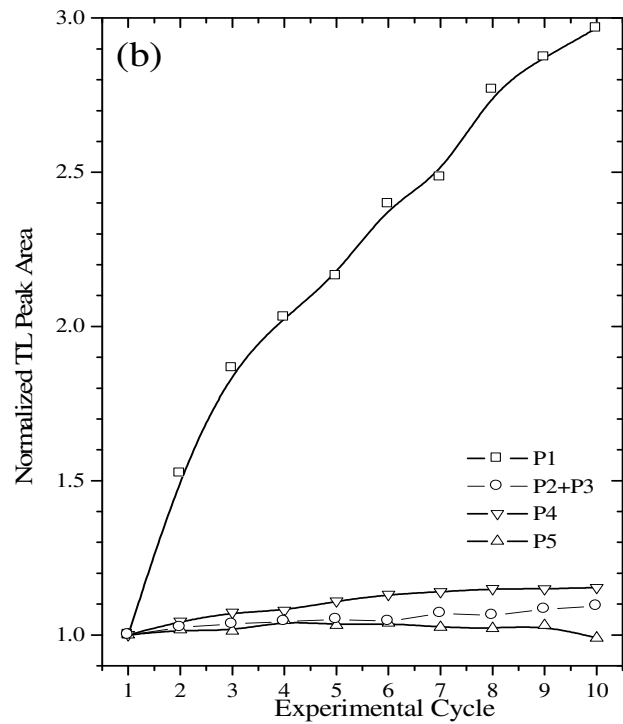
To obtain an optimum annealing procedure, the annealing experiments before irradiation were carried out at 500 and 600 $^{\circ}$C for different durations. It is well known that an optimum annealing procedure must satisfy reproducibility and high sensitivity for the TL peaks. Figure 5.4 shows two sets of glow curves measured immediately following irradiation after pre-irradiation heat treatments at 500 $^{\circ}$C and 600 $^{\circ}$C for different times of annealing. It can be seen that the shapes of the glow curves are not highly changed as a result of annealing time in both temperatures. In some of the previous works, it was mentioned that the peak temperatures of some glow peaks in quartz varied after the heat treatments before irradiation [21]. However, in the present study, any systematic changes in the peak temperatures of all glow peaks have not been observed after the heat treatments. As seen, the peak temperatures of all glow peaks are within the experimental errors. On the other hand, a small variation in the intensities of all glow peaks after heat treatment at 500 $^{\circ}$C is clearly seen in Fig.5.4(a). Moreover, the intensities and peak temperatures of all glow peaks are not affected from heat treatment at 600 $^{\circ}$C. In order to estimate the sensitivity changes of glow peaks at 500 $^{\circ}$C, the glow curves were analyzed by CGCD program.

The normalized peak areas of glow peaks with respect to pre-irradiation annealing time are shown in Fig.5.5. The intensities of all glow peaks increase with increasing annealing time up to 1 h and then they start to decrease with further annealing time above 1 h. For example, the intensity of peak 1 increases to ≈20% of its original value after annealing at 500 $^{\circ}$C for 1 h.
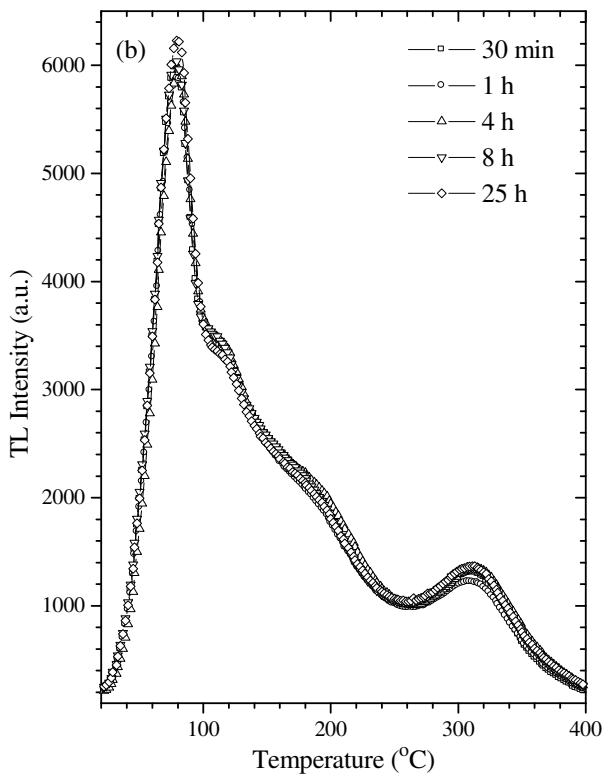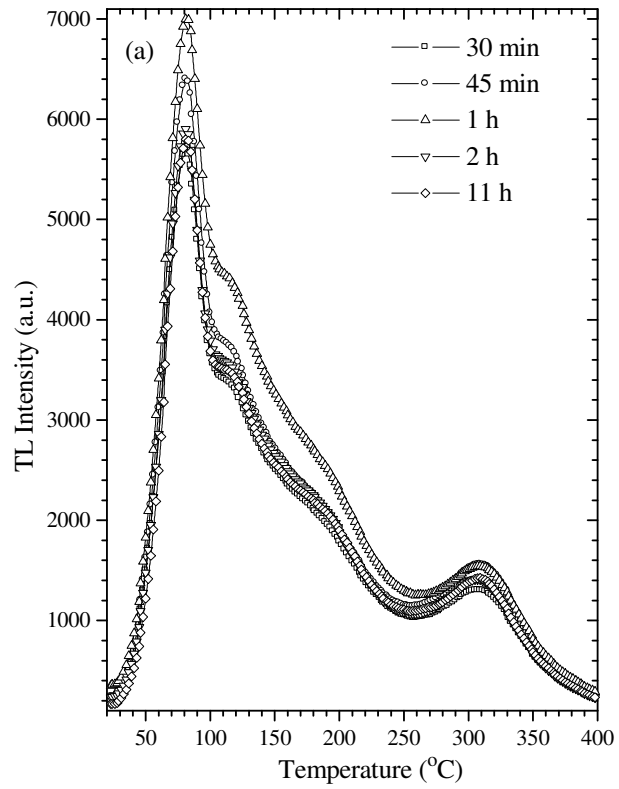
Figure 5.4 The glow curves of synthetic quartz after heat treatments at (a) 500 ^{o}C (b) 600 ^{o}C as a function of annealing time (dose levels are ≈30 Gy in all experiments)
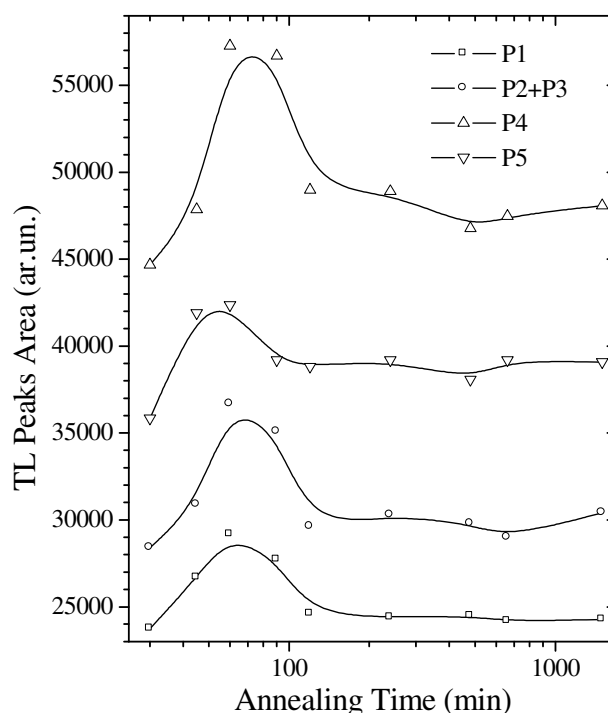
Figure 5.5 The variations of glow peak areas of synthetic quartz as a function of annealing time at 500 $^{\circ}$C

5.2 Effects of Thermal Treatment on the TL Intensity and Kinetic Parameters of Natural Quartz

In this study, the results were classified into three main groups according to desired aims:

5.2.1 Cycle of measurement experiments

The experiments were again performed at two different annealing temperatures, namely 500 and 600 $^{\circ}$C.

Figure 5.6 shows the glow curves of natural quartz sample after thermal treatment at 500 °C as a function of cycle of measurements. In this figure, three peaks at about 90, 216 and 360 °C are clearly seen. The variation of the TL intensity of glow peak 1 ($T_m \approx$ 90 °C) with repeat of experiment is also clearly seen in this figure. On the other hand, there is no systematic variation of TL intensity of this peak. Despite

62

of this result, the variations of TL intensities in peak 2 ($T_m \approx 216$ °C) and peak 3 ($T_m \approx 360$ °C) are not high with repeat of experiments when they are compared with P1.
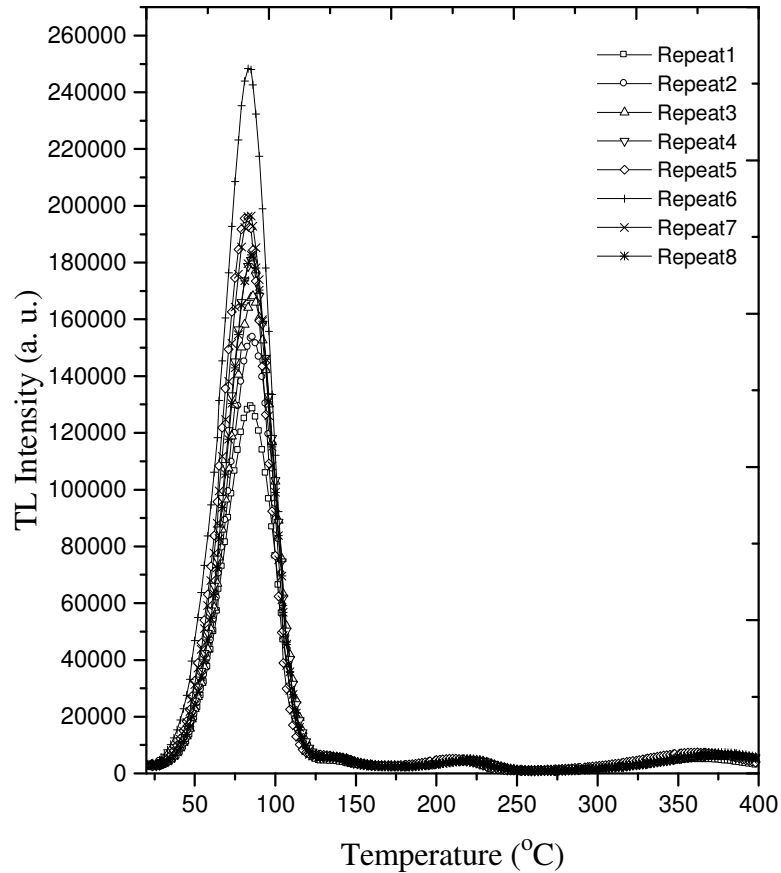
Figure 5.6 The variations of intensities of TL glow curves of annealed natural quartz sample at 500 °C for 1 h with experimental cycle of measurements

Fig.5.7 shows the variations of intensities of TL glow curves of the annealed quartz samples at 600 °C for 1 hour with respect to the experimental cycle of measurements. As seen, there are no variations in the TL intensities of all peaks with repeats of experiment. Therefore, it was decided that the annealing temperature at 600 °C gives the more stable results than the annealing temperature at 500 °C for the used quartz samples in this study. Fig.5.8 shows the variation of maximum TL intensity of peak 1 ($T_m \approx 90$ °C) of the annealed natural quartz sample at 500 and 600 °C for 1 hour with respect to cycle of measurement. As seen from this figure, the maximum TL intensity of peak 1 after annealing at 600 °C does not notably change with repeats of experiment although its intensity randomly changes at 500 °C.

Fig.5.9 shows the variation of maximum TL intensity of peak 2 ($T_m \approx 216$ °C) of the annealed quartz sample at 500 and 600 °C for 1 hour with respect to cycle of measurement. Similarly, the variation of peak intensity of glow peak ($T_m \approx 360$ °C) is shown in Fig.5.10. The last two figures represented that P2 and P3 were not significantly affected with the repeats of experiments after annealing at 500 and 600 °C. As seen, there are small changes after annealing at 500 °C but they can be ignored when they are considered together with the variation in the intensity of P1.
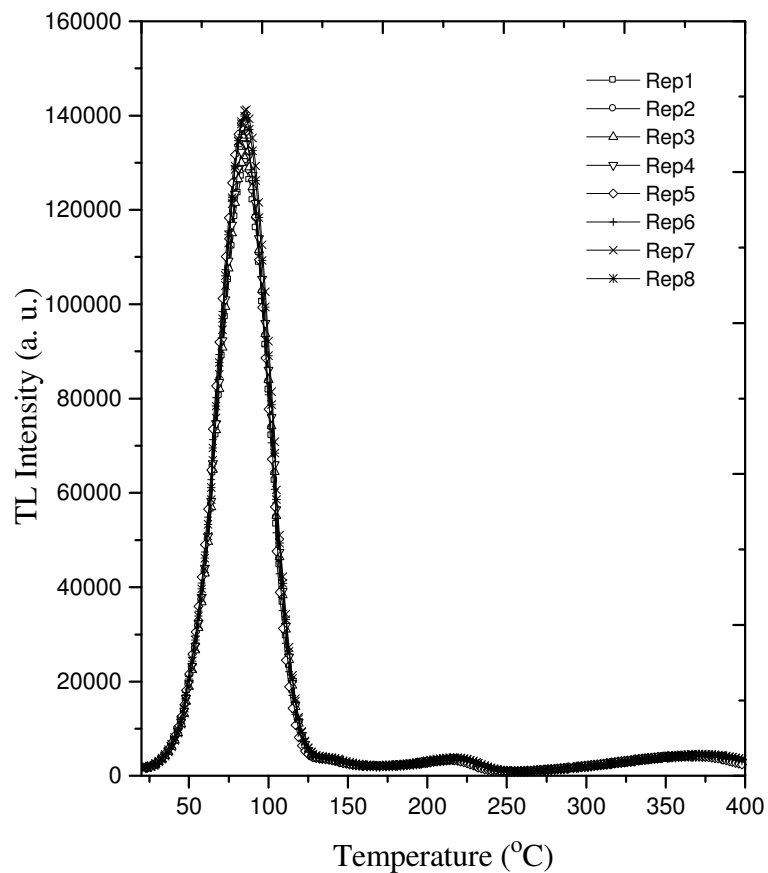
Figure 5.7 The variation of intensities of TL glow curves of annealed natural quartz sample at 600 °C for 1 h with cycles of measurements
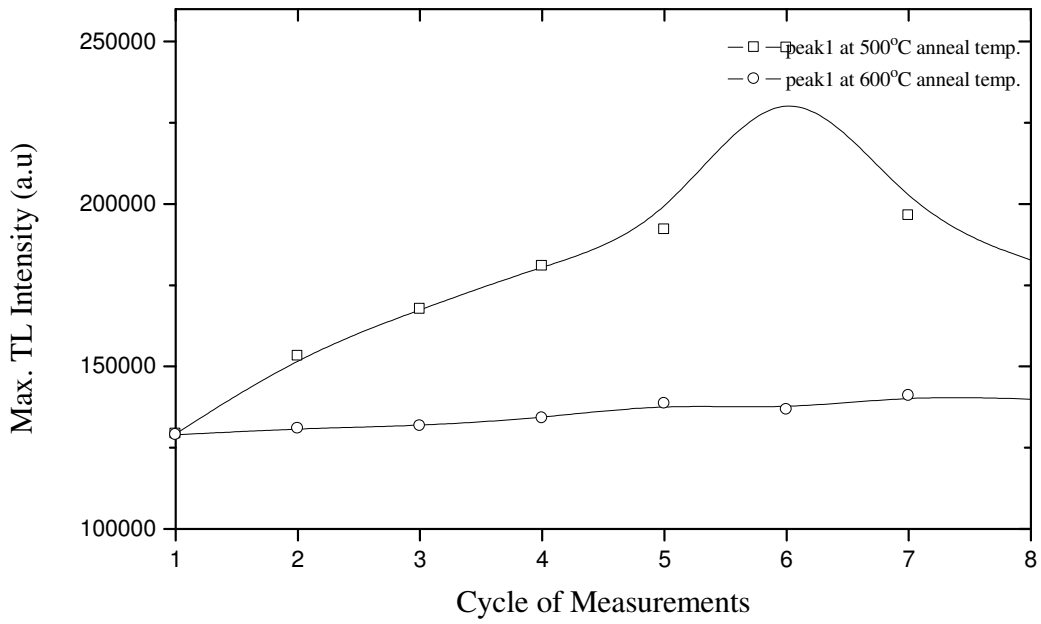
Figure 5.8 The variation of maximum TL intensity (I_m) of peak 1 of annealed quartz sample at 500 and 600 °C for 1 hour with respect to cycle of measurement
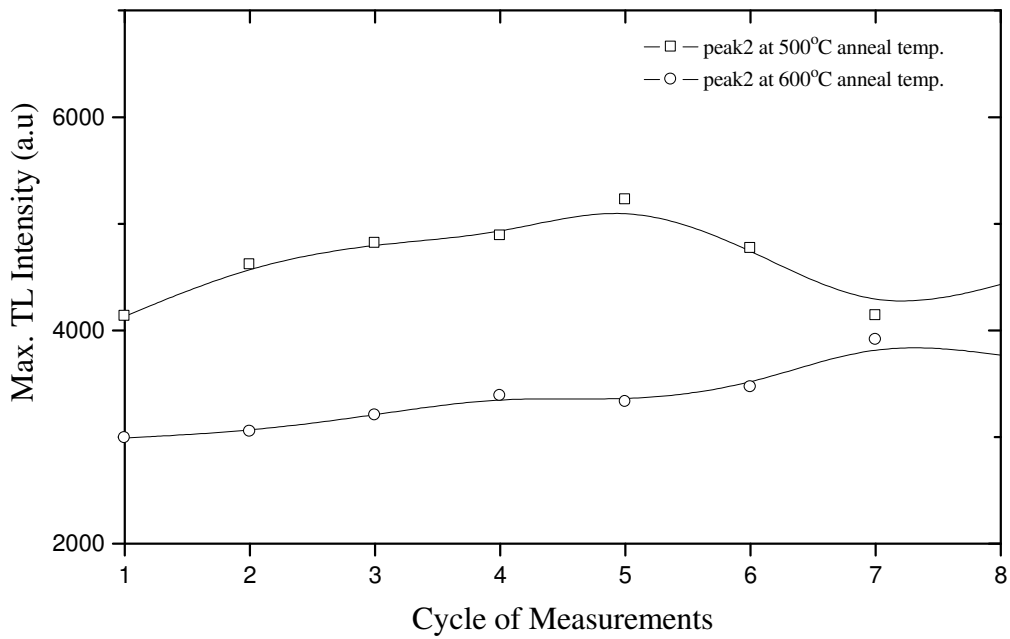
Figure 5.9 The variation of maximum TL intensity (I_m) of peak 2 of annealed quartz sample at 500 and 600 °C for 1 h with respect to cycle of measurement
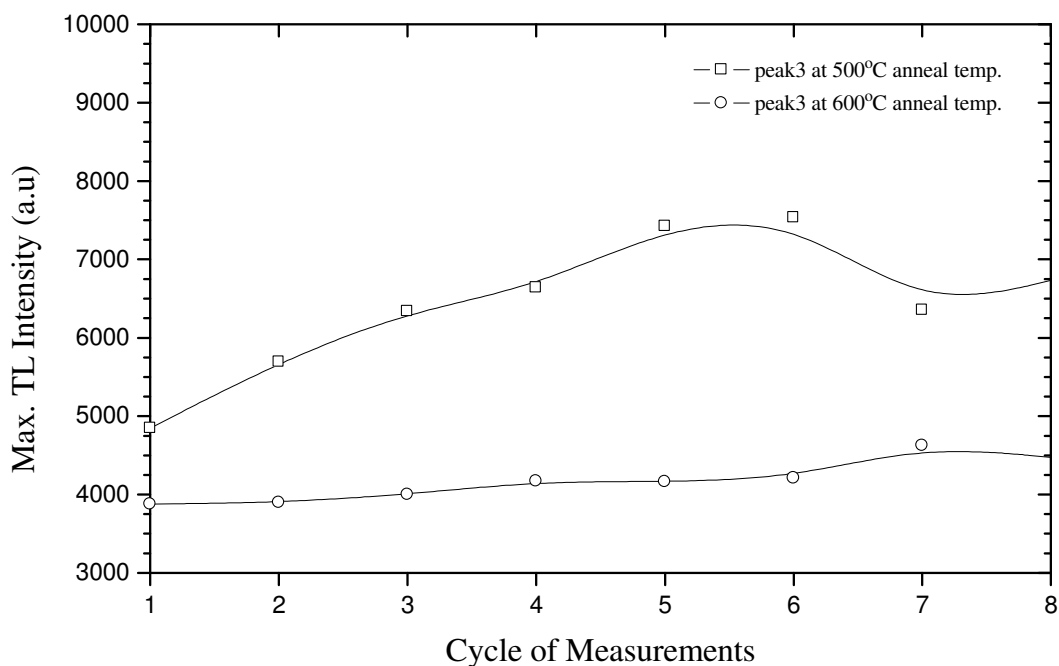
Figure 5.10 The variation of maximum TL intensity (I_m) of peak 3 of annealed quartz sample at 500 and 600 °C for 1 h with respect to cycle of measurement

Consequently, it was decided that the annealing at 600 °C is the best annealing temperature for natural quartz samples used in this study. Because, the intensities of glow peaks are not affected with the repeats of experiments at this annealing temperature. On the other hand, as seen from these figures, the variations in the intensities of glow peaks are high at annealing temperature at 500 °C.

The recorded TL glow curves were also analysed by CGCD method to observe the variations of the kinetic parameters (carrier population in a trap (n_o), trap depth (E_a) and frequency factor ($\ln(s)$)) as a function of experimental cycles at both annealing temperatures. The effect of experimental cycles on the trap depths (E_a) of main three TL peaks of the annealed quartz sample at 500 °C for 1 hour is shown in Fig.5.11. As seen, there are no stable results about the trap depth of glow peaks when the samples annealed at 500 °C. On the other hand, as seen from Fig.5.12, the trap depths are not affected with the experimental cycles when the samples where annealed at 600 °C for 1 h. In this case, it was observed that the trap depths of P1, P2 and P3 are approximately constant at 0.82±0.01, 0.78±0.02 and 0.69±0.01 eV, respectively.

66

Figure 5.11 The effect of experimental cycles on the trap depth (E_a) of traps of TL peaks of annealed quartz sample at 500 °C for 1h.

Figure 5.12 The effect of experimental cycles on the trap depth (E_a) of traps of TL peaks of annealed quartz sample at 600 °C for 1h.

Figure 5.13 shows the effect of experimental cycles on the carrier populations (n_o) in traps of TL peaks of annealed natural quartz sample at 500 °C for 1 h. This procedure

was also repeated after the annealing of natural quartz at 600 °C for 1 h and the obtained results are shown in Fig.5.14. As seen from Fig.5.13, there is an obvious change in the traps of peak 1 with repeat of experiment although the others are not significantly affected when the samples annealed at 500 °C for 1 h. On the other hand, when the samples where annealed at 600 °C for 1 h, the inconsistency in the P1 is disappeared and as seen from Fig.5.14 the carrier population of this peak is nearly constant with increasing experimental cycles.
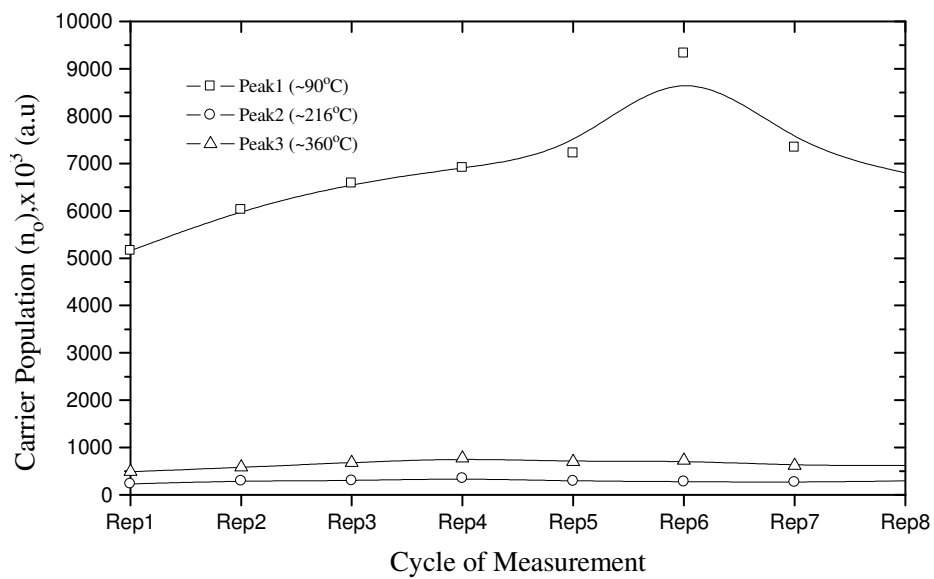
Figure 5.13 The effect of experimental cycles on the carrier populations (n_o) in traps of TL peaks of annealed quartz sample at 500 °C for 1 h.
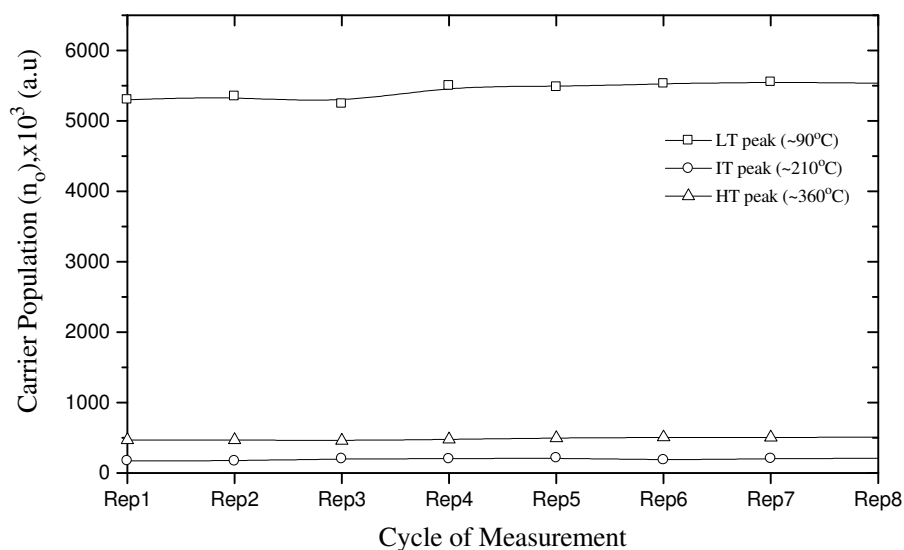
Figure 5.14 The effect of experimental cycles on the carrier populations (n_o) in traps of TL peaks of annealed quartz sample at 600 °C for 1 h.

68

Figures 5.15 and 5.16 show the effects of experimental cycles on the frequency factor (ln(s)) of main three TL peaks of quartz sample after annealing them at 500 °C and 600 °C for 1 h. Consequently, the similar results which were mentioned in above were observed for the frequency factors of glow peaks. As a result, it was observed the kinetic parameters of traps are not affected by repeats of experimental cycles after annealing at 600 $^{\circ}$C. Therefore, it was decided that the annealing temperature at 600 $^{\circ}$C for 1 h is the more suitable annealing temperature than annealing at 500 $^{\circ}$C for natural quartz that was used in our studies.
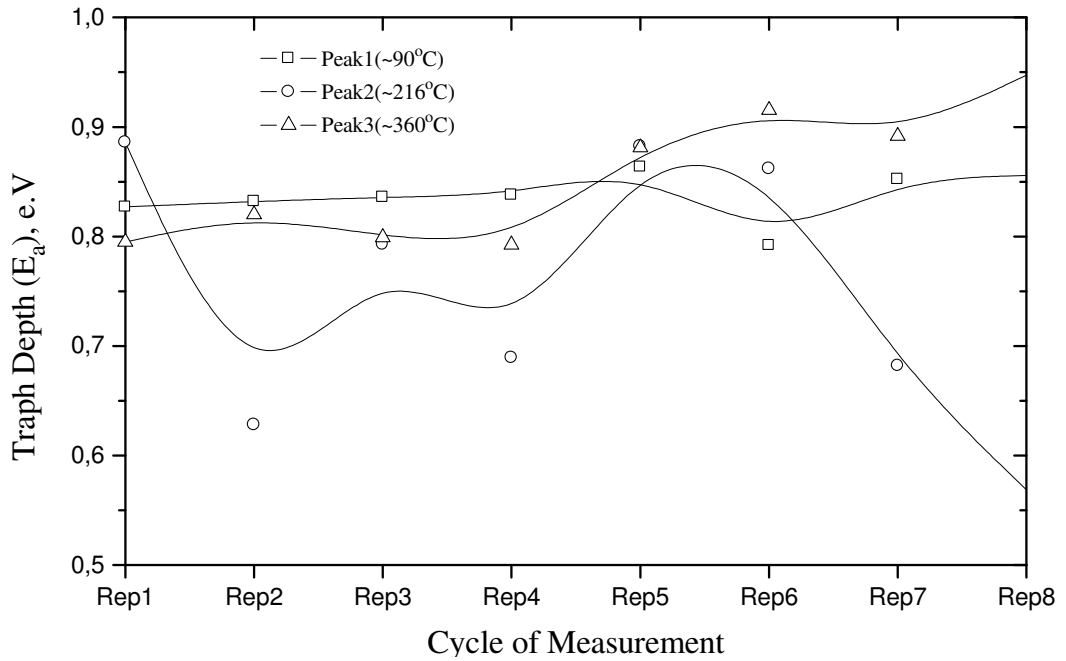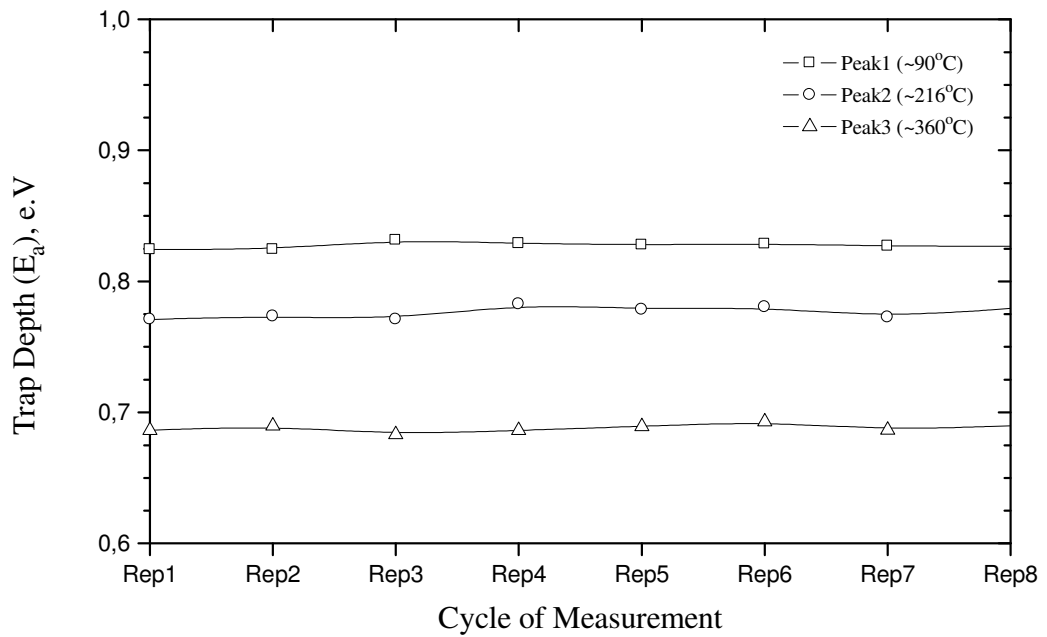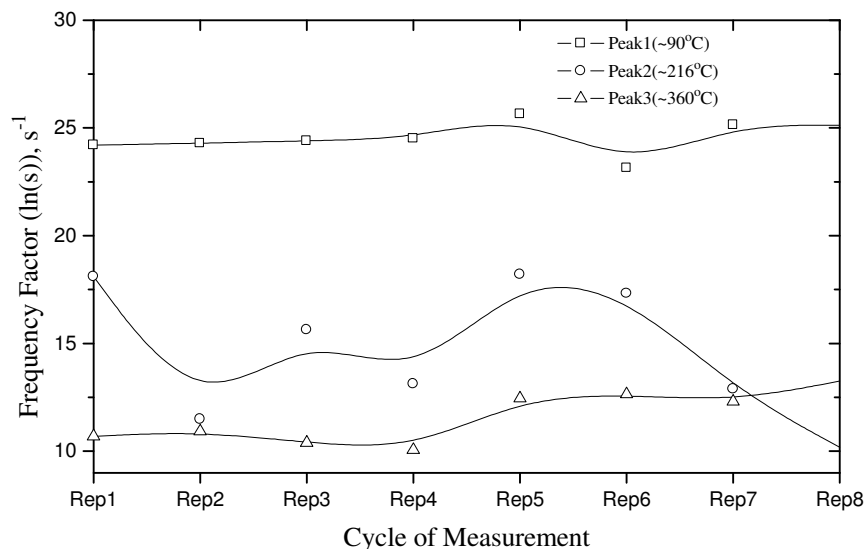

Figure 5.15 The effect of experimental cycles on the frequency factor (ln(s)) of TL peaks of annealed quartz sample at 500 °C for 1 h.
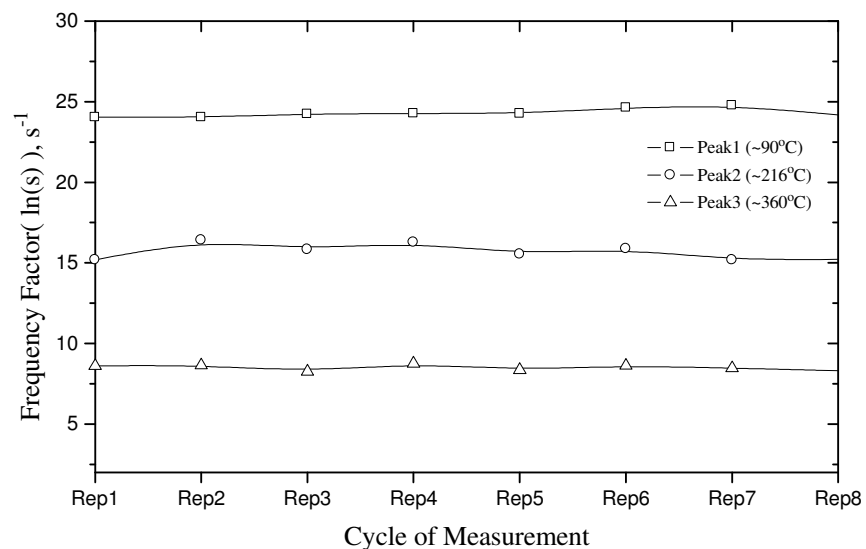
Figure 5.16 The effect of experimental cycles on the frequency factor (ln(s)) of TL peaks of annealed quartz sample at 600 °C for 1 h.

69

5.2.2 Annealing time experiments

In this part of the study, the samples were annealed at 600 °C for different durations to see their effects on the intensities of TL glow curves and kinetic parameters of traps in the natural quartz samples. This experiment wasn't done at 500 °C annealing temperature because it was decided that the annealing at 600 °C gave more stable results then annealing at 500 °C.

Figure 5.17 shows the variation of TL glow curves of annealed quartz sample at 600 °C as a function of different annealing times. As seen from this figure, it looks like there is no important change in the intensities of glow peaks of natural quartz with increasing the annealing time. However, when they were analyzed with CGCD program it was observed that there is a 17% increase between 30 minutes and 8 hours for peak 1. The increase in the intensities of peaks 2 and 3 were recorded as approximately 14.7% and 14.3%, respectively (Fig.5.18).
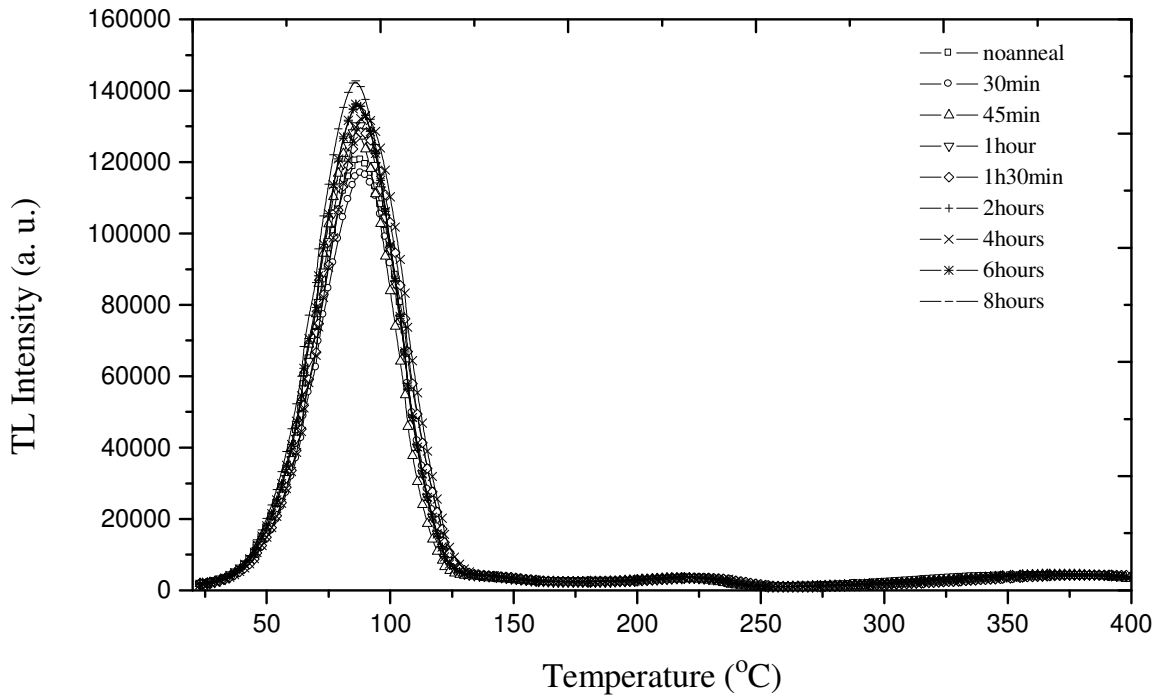
Figure 5.17 The variations of TL glow curves of natural quartz sample after annealing at 600 °C as a function of annealing times
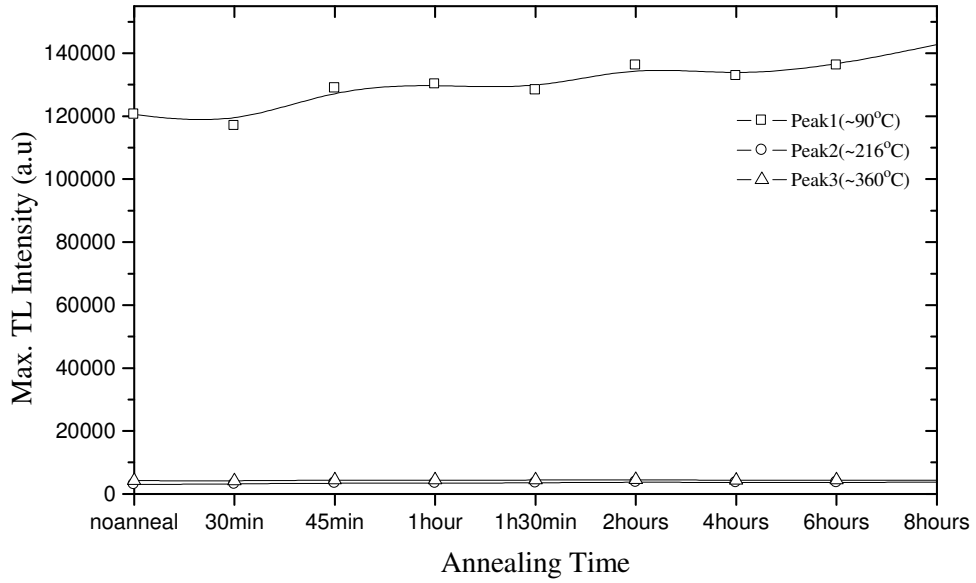
Figure 5.18 The variations of intensities of TL peaks of natural quartz sample after annealing at 600 °C as a function of annealing times

Figure 5.19, 5.20 and 5.21 show the variation of kinetic parameters (E_a, n_o and $\ln(s)$) of glow peaks as a function of annealing time at 600 °C. In Fig.5.19, there is no consistent result in E_a values when it is compared with Fig.5.12 due to the bad fitting in CGCD method.
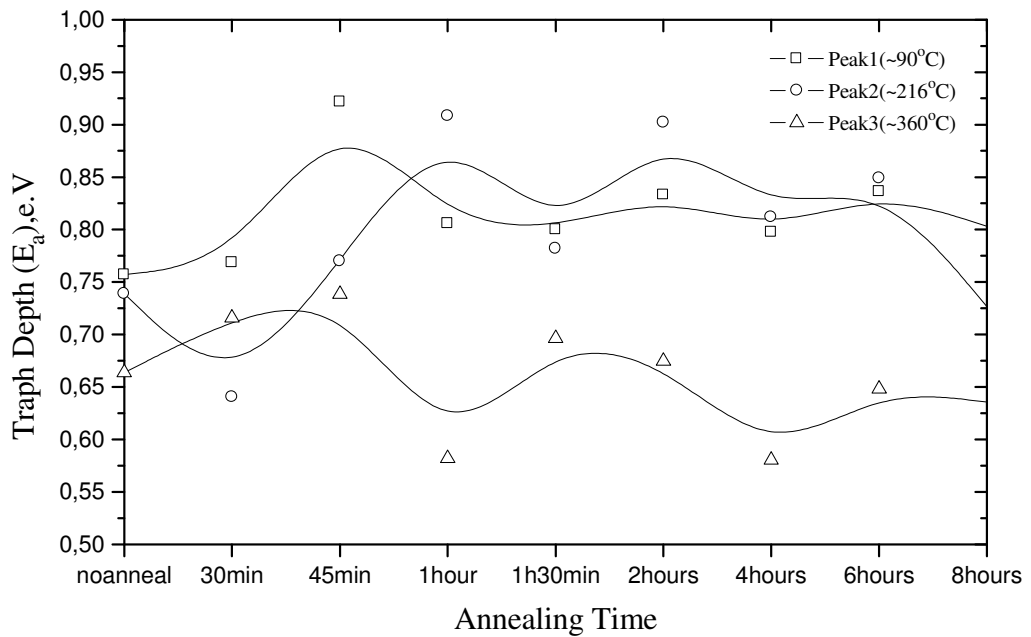
Figure 5.19 The effect of annealing time on the trap depth (E_a) of traps of TL peaks of quartz sample after annealing at 600 °C

71
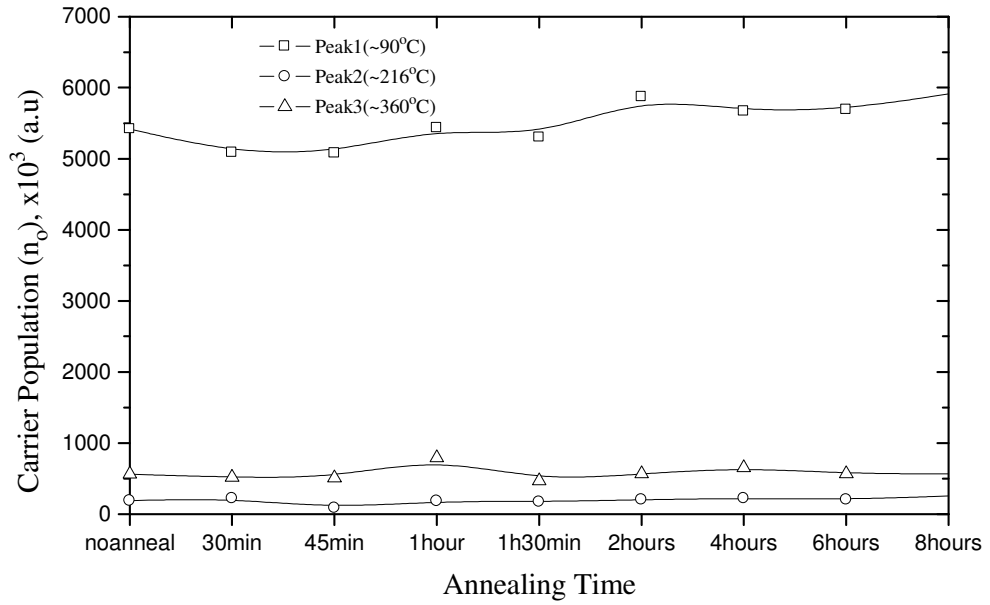
Figure 5.20 The effect of annealing time on the carrier populations (n_o) of traps of TL peaks of quartz sample after annealing at 600 °C
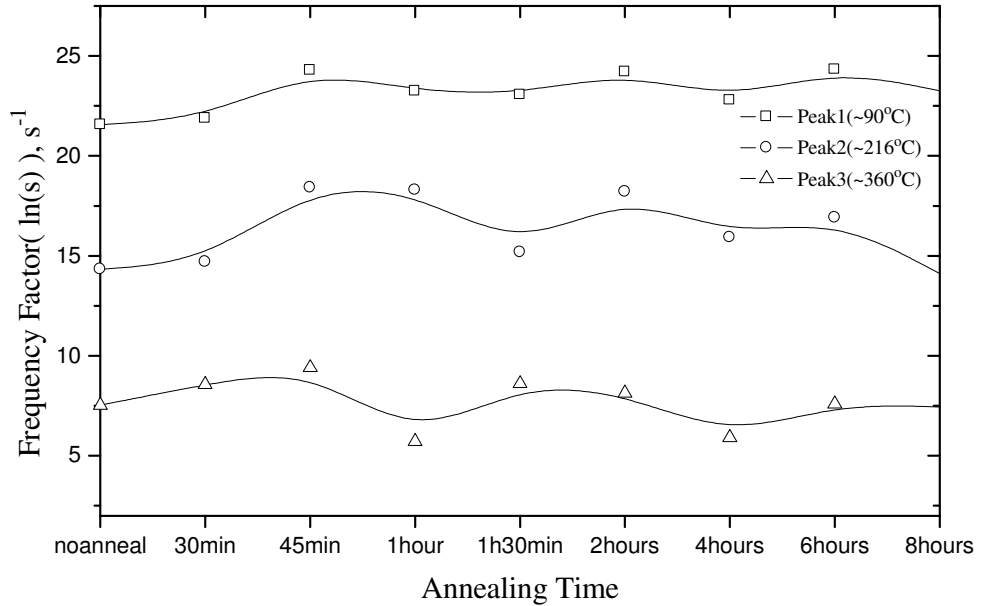
Figure 5.21 The effect of annealing time on the frequency factor ($\ln(s)$) of traps of TL peaks of quartz sample after annealing at 600 °C

5.2.3 Annealing temperature experiments

The possible effects of annealing temperatures on the intensities and kinetic parameters of TL glow peaks were also studied in the given study. Figures 5.22, 5.23 and 5.24 show the effect of different annealing temperatures between 200 and 1000 °C on the TL intensities of glow curves of quartz.
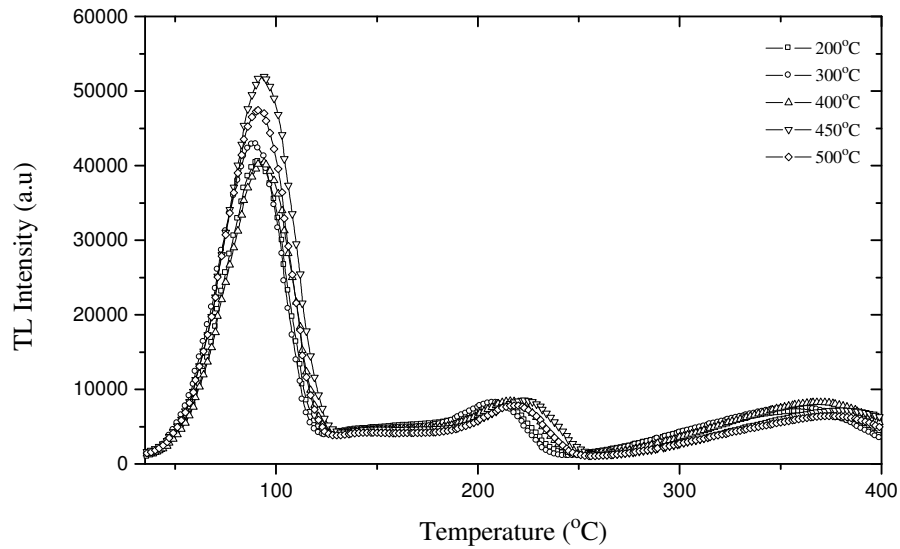
Figure 5.22 The effect of different annealing temperatures between 200 and 500 °C on the TL intensity of glow curves
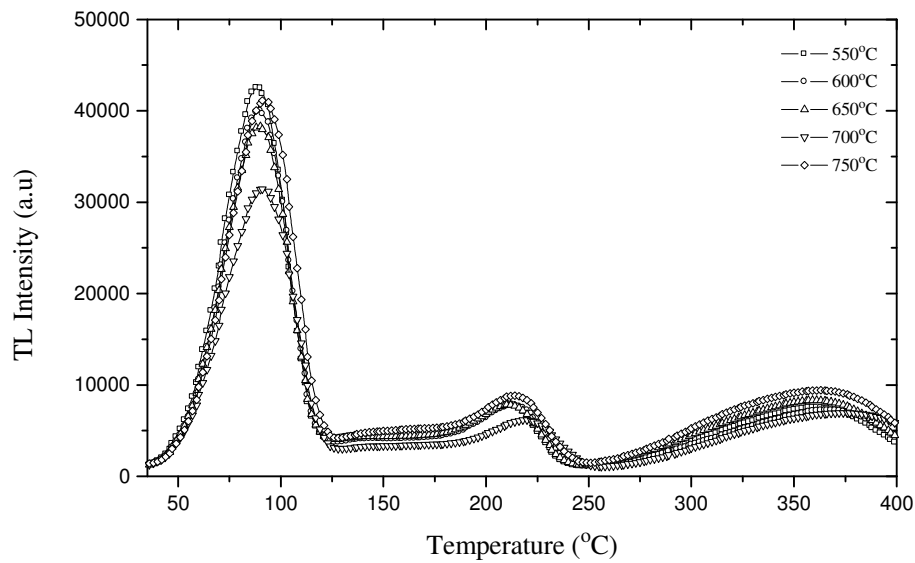
Figure 5.23 The effect of different annealing temperatures between 550 and 750 °C on the TL intensity of glow curves
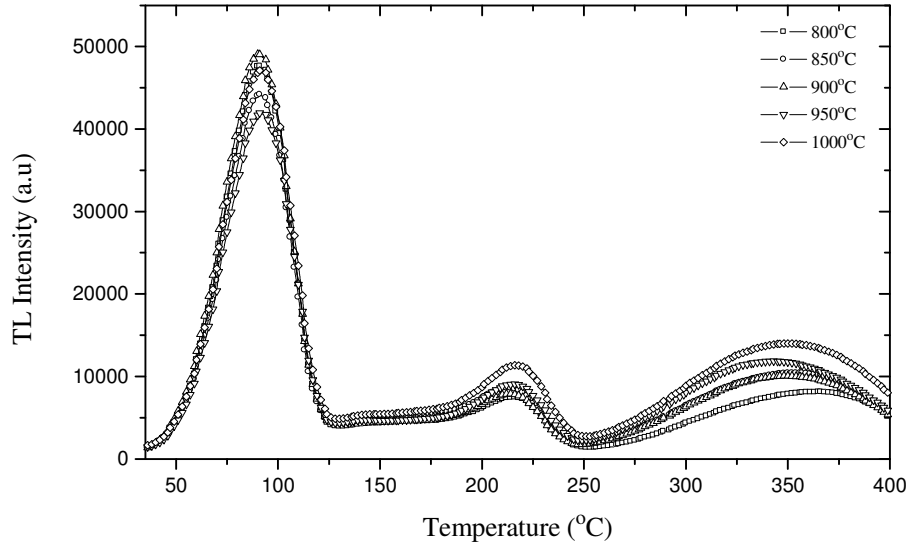
Figure 5.24 The effect of different annealing temperatures between 800 and 1000 °C on the TL intensity of glow curves

Figure 5.25 summarizes the effects of annealing temperatures on the intensities of TL glow curve peaks of quartz after different annealing temperatures. As seen, there is a sharp increase in the intensity of peak 1 after annealing at 450 °C but it then decreases up to 700 °C. Then it again starts to increase with increasing annealing temperature. The similar interpretations can be also made for peaks 2 and 3 for high temperature annealing region between 700 and 1000 °C. Moreover, the intensities of peak 2 and 3 are much more affected than the other peaks from the annealing temperatures between 850 and 1000 °C.
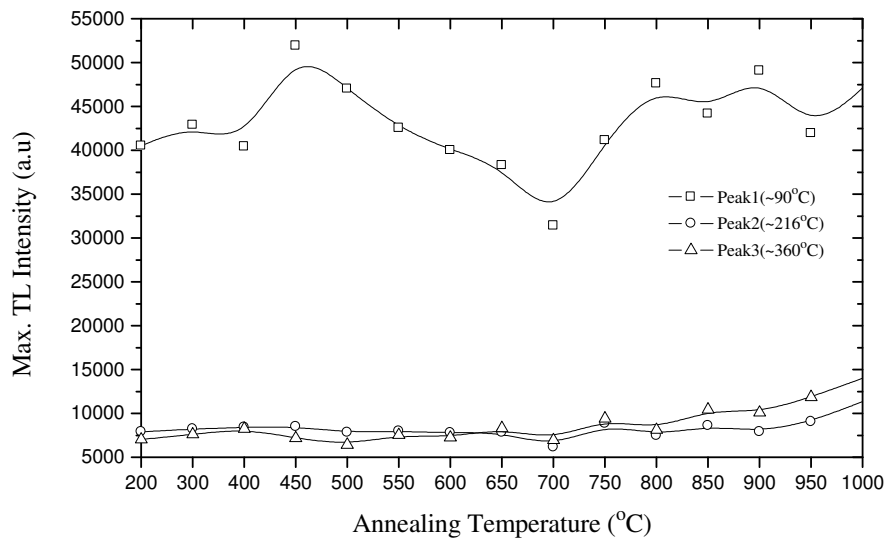
Figure 5.25 The variations of intensities of TL glow peaks of annealed quartz as a function of annealing temperatures

Figures 5.26, 5.27 and 5.28 show the kinetic parameters of glow peaks of quartz obtained by CGCD method after the annealing samples at different temperatures for 1 h. As seen from these figures, the trap depths and frequency factors of high temperature glow peaks above 200 ^{o}C were affected randomly from annealing temperatures because of the high variations of peak temperatures after different annealing temperatures.
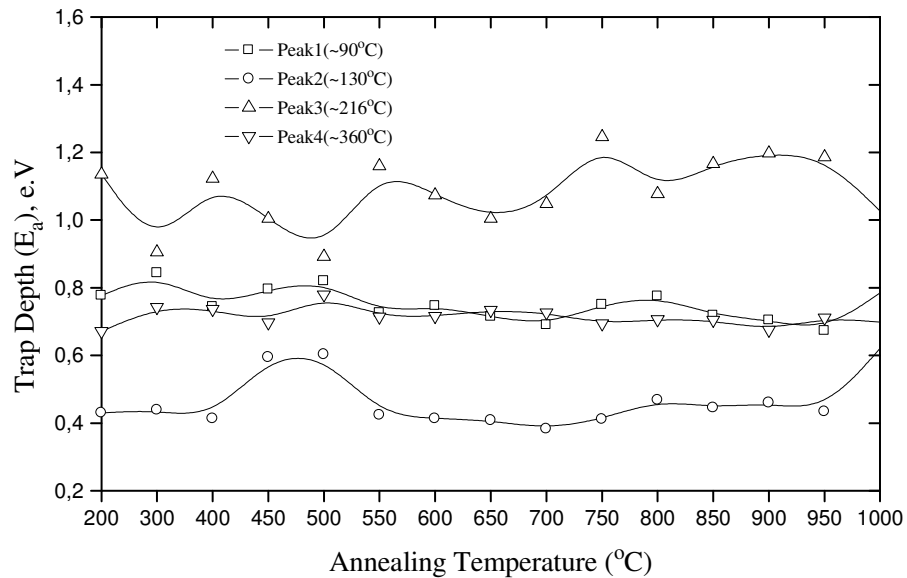
Figure 5.26 The effects of annealing temperatures on the trap depths (E_a) of traps of TL peaks of quartz. All data were obtained from a fitting program (CGCD method)
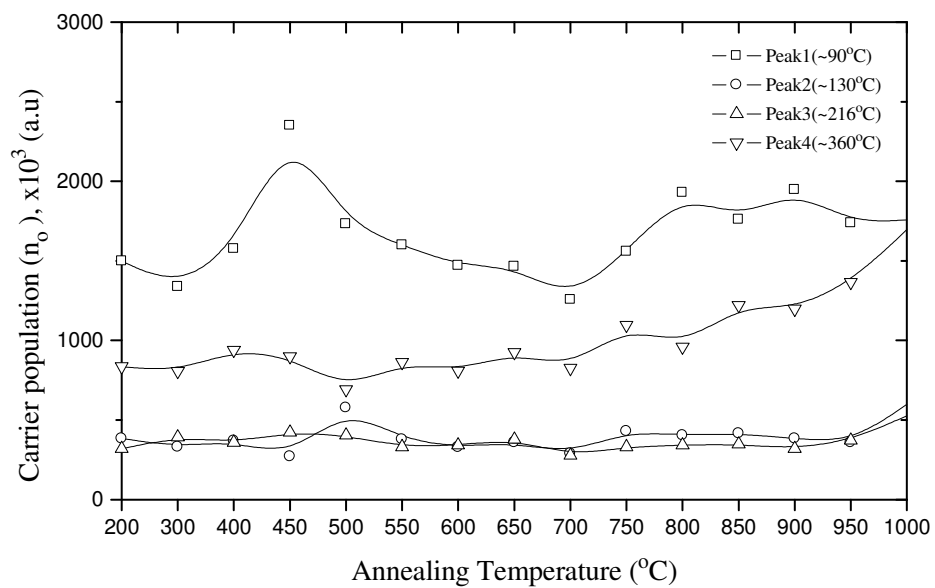
Figure 5.27 The effects of annealing temperatures on the carrier populations (n_o) of traps of TL peaks of quartz. All data were obtained from a fitting program (CGCD method)

75
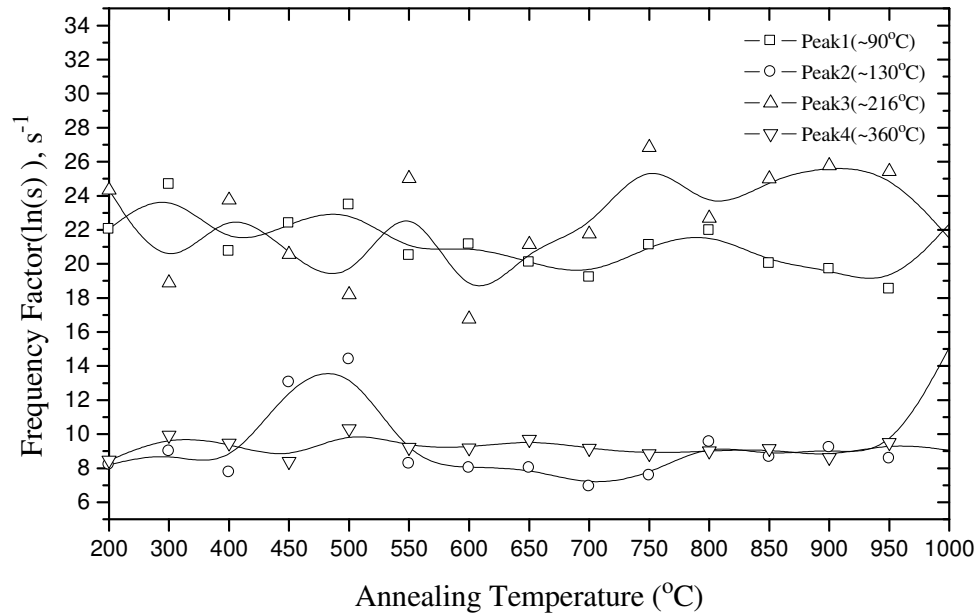
Figure 5.28 The effects of annealing temperatures on the frequency factor (ln(s))) of traps of TL peaks of quartz. All data were obtained from a fitting program (CGCD method)

5.3 Thermoluminescence Dose Responses of Synthetic and Natural Quartz

In this part of the study, the dose responses of glow peaks of synthetic and natural quartz samples were studied by three methods:

- Glow Curve Analysis
- Regions of Interest Area
- Maximum of TL Peak Intensity

5.3.1 Synthetic quartz

5.3.1.1 Glow curve analysis

In this part, fifteen dose implementations from 0.015Gy to 2.6 kGy were tried for four different samples underlined in the section 4.3.3. Some of the glow curves of unused synthetic quartz samples without heat treatment are shown Fig. 5.29.
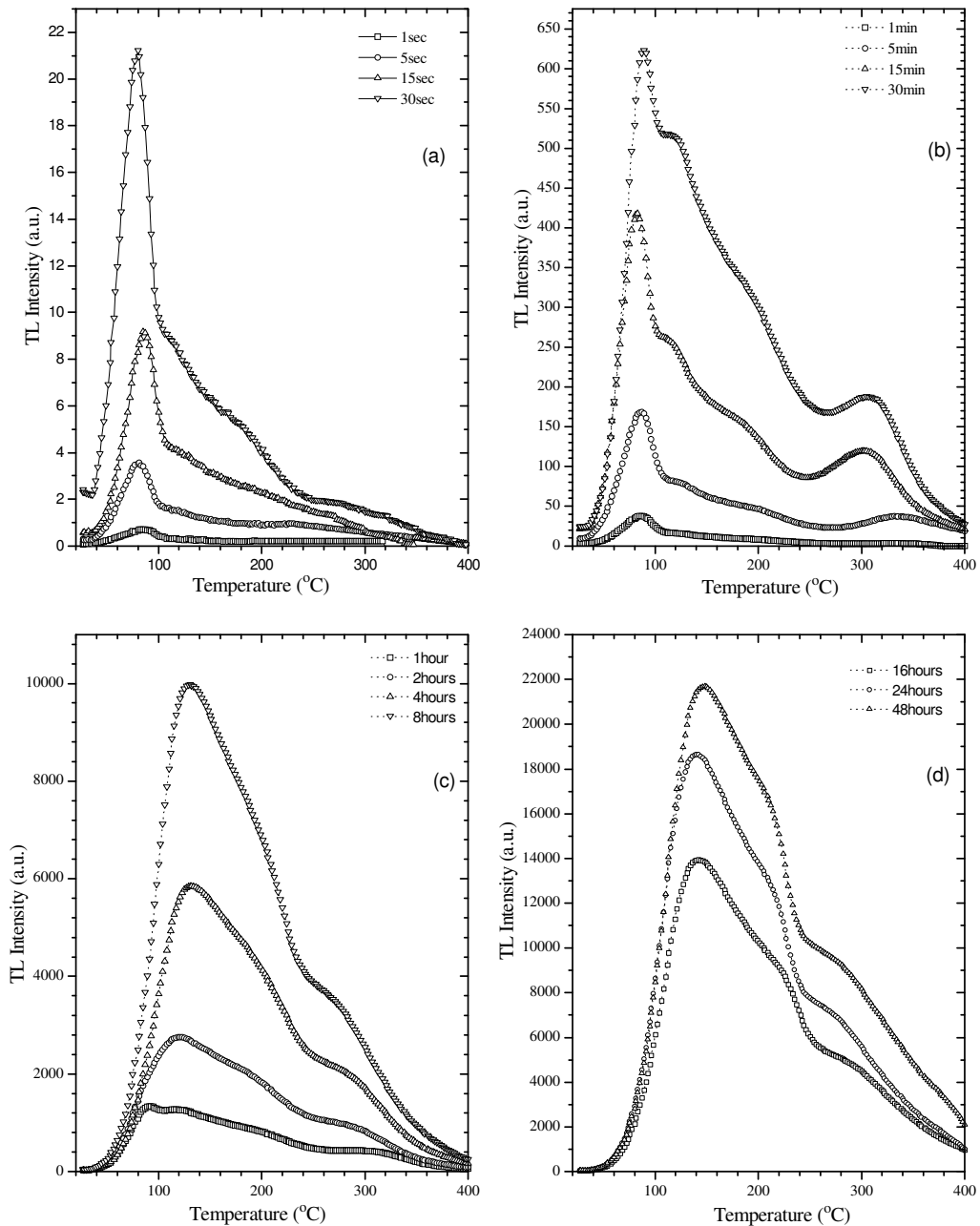
Figure 5.29 Variation of intensity of TL glow curves of fifteen unannealed synthetic quartz as a function of applied dose levels

In this figure, it is seen that all peaks increase clearly with increasing the applied dose levels. Peak 1 seems as a single peak at 83 $^{\circ}$C for lower doses (0.015~27 Gy) but when applied dose reaches to 1 h (54 Gy), it combines with peak 2 that appears at 120 $^{\circ}$C. Then, the peak temperature of combined peak slides to higher temperature region. As seen, the peak temperature have been observed at 144 $^{\circ}$C after 48 hours irradiations. The high temperature peak that appears at 310 $^{\circ}$C is most explicit between 15 mins (13.5 Gy) and 30 mins (27 Gy) doses.

Fig 5.30 shows the variation of the intensity of TL glow curves of unannealed synthetic quartz after different dose levels between 0.015 Gy and 2.6 kGy.
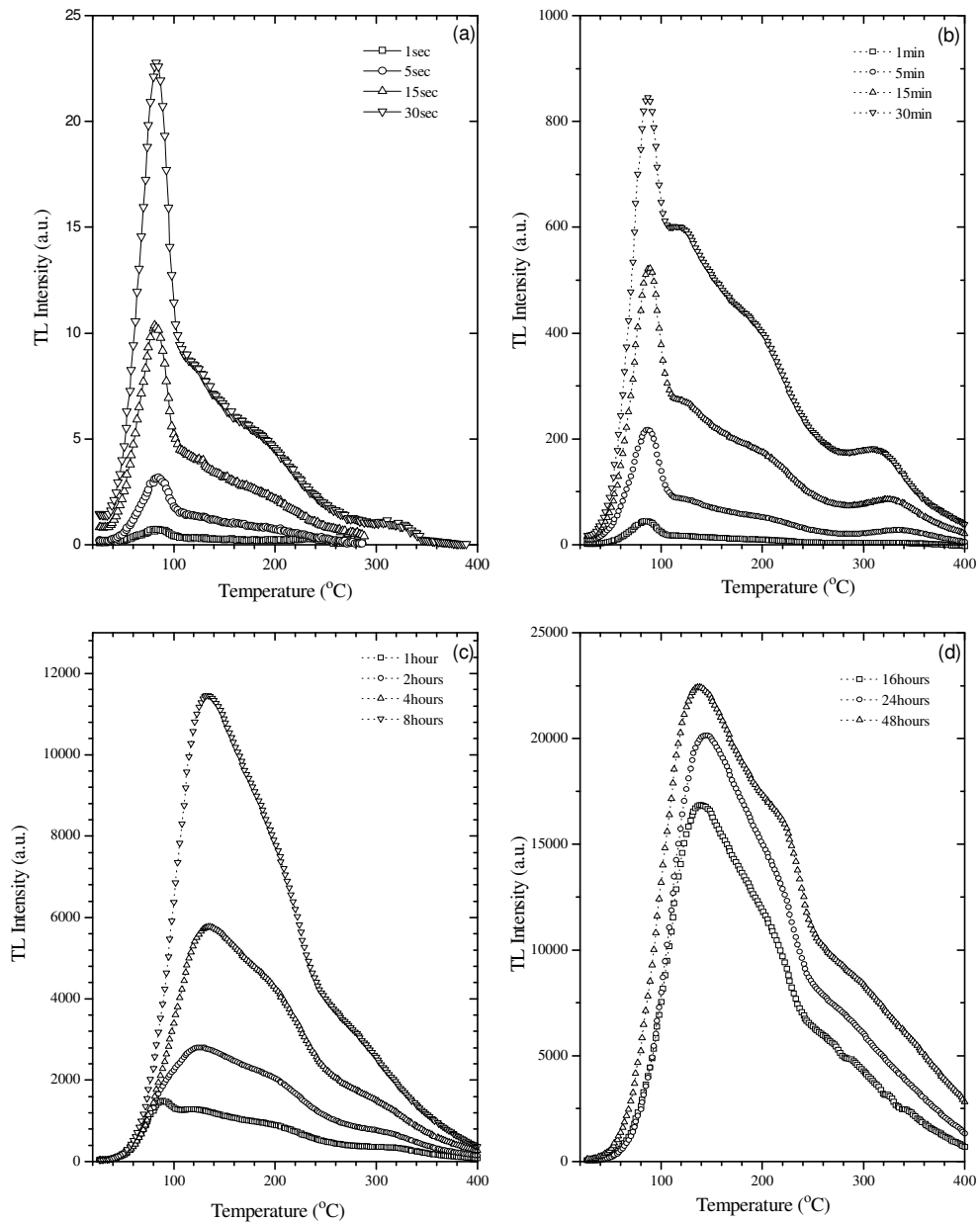
Figure 5.30 Variation of intensity of TL glow curves of unannealed synthetic quartz after different dose levels

In all glow curves in fig. 5.30, the peak intensities increase with increasing applied dose as shown in fig. 5.29. When the intensities of peak 1 in both figures 5.30 and 5.29 are compared for the same applied doses, it is seen that peak 1 intensity in Fig.5.30 is greater than peak 1 intensity in Fig.5.29. This increase varies between 5% and 40%. For example, there is an increase for 5 mins (4.5 Gy) and 30 mins (27 Gy) about 40%. This ratio becomes 20% for 16 h (864 Gy), 10% for 24 h (1296 Gy), 5% for

48 h (2592 Gy) but no increase was observed for 2 h (108 Gy) and 4 h (216 Gy). In brief, the using same (reused) sample in all dose studies affects the peak 1 intensities about 20% when it is compared with using different sample.
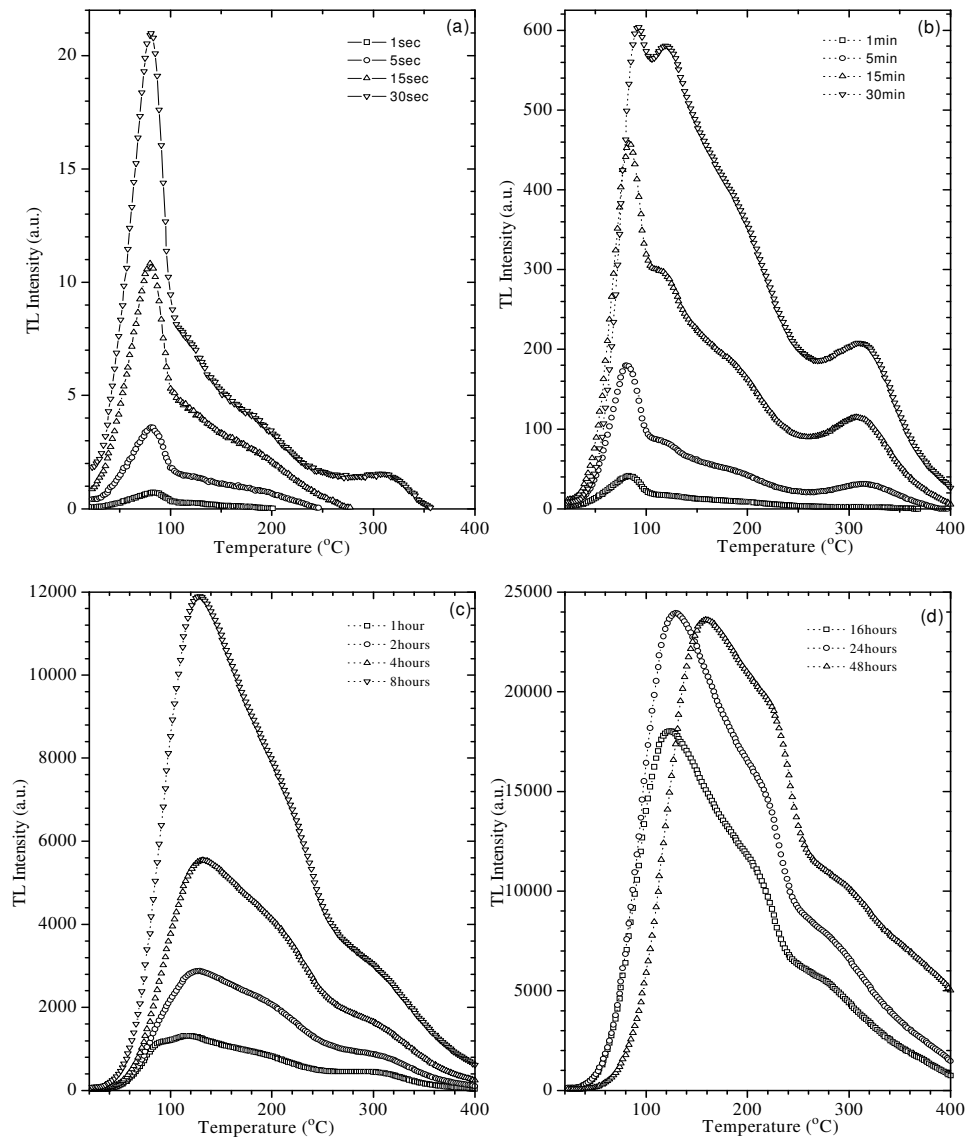
Figure 5.31 Variation of intensity of TL glow curves of fifteen annealed synthetic quartz at 600 ^{o}C for 1 hour for fifteen different applied doses

The process in *different samples without heat treatment* was also repeated in this section, but in addition, all samples were annealed at 600 ^{o}C for 1 h in an oven before they were exposed to dose. Fig. 5.31 gives us the variation of intensity of TL glow curves of fifteen annealed synthetic quartz for fifteen different applied doses. This part had been done to see the effects of annealing before irradiation.

When we compare figures 5.29 and 5.31, there is no important change in the peak 1 intensity until 8 hours (432 Gy) but its intensity increases dramatically about 20% at 8 h dose. This ratio becomes 30% for 16 h (864Gy) and 24 h (1296Gy). However, this increase wasn't seen at 48 h (2592Gy). Although we repeated this experiment, the same result had been observed, only 10% increase was seen and peak temperature slid near 30 °C to the higher temperature region. In brief, anneal process affects peak intensity at higher doses according to our results.

Figure 5.32 shows that the variation of intensity of TL glow curves of one annealed synthetic quartz at 600 °C for 1 hour for fifteen different applied dose
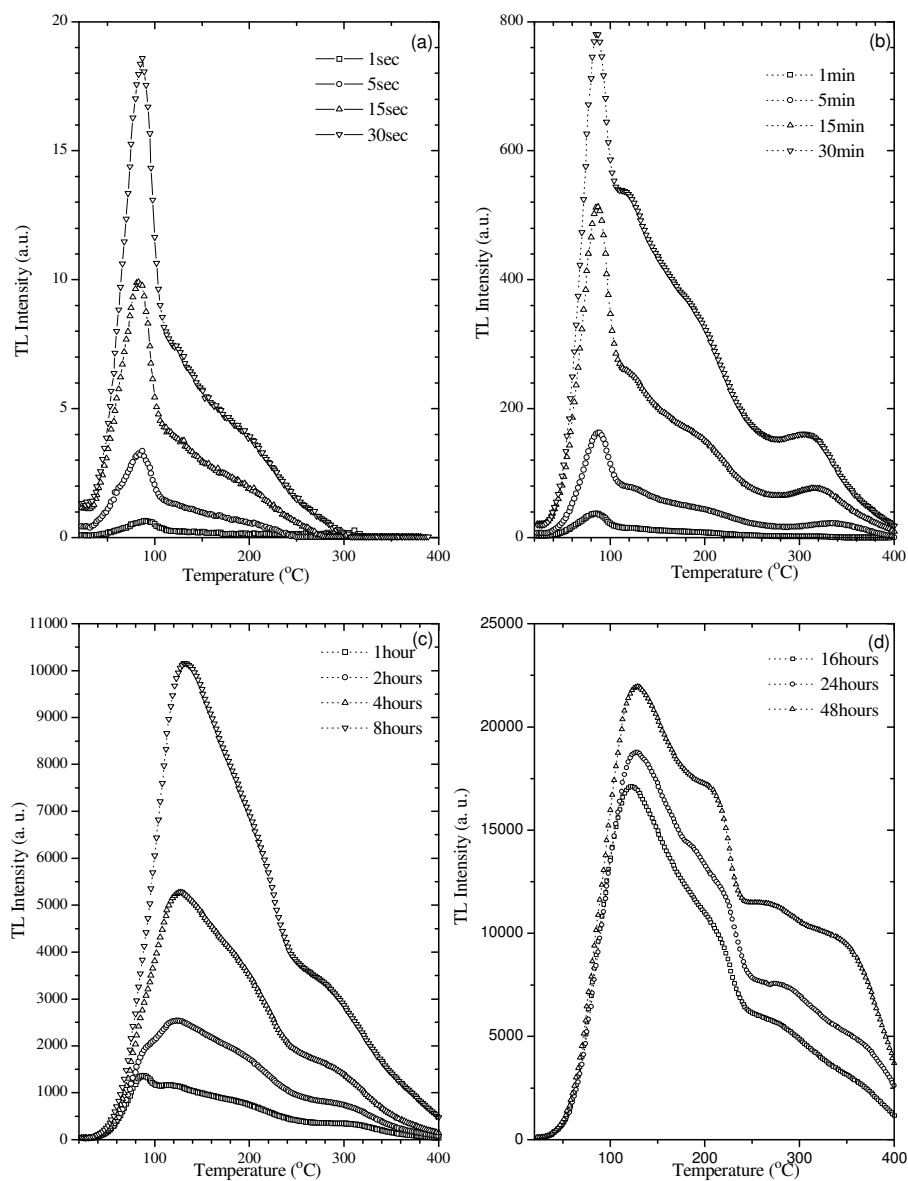
Figure 5.32 Variation of intensity of TL glow curves of one annealed synthetic quartz 1 h at 600 °C for fifteen different applied dose levels

80

levels. When this figure is compared with both Figs.5.30 and 5.31, it is seen that the intensity of peak 1 in Fig.5.32 is less than both in Figs.5.30 and 5.31 for all applied doses about 10% except for 15 mins (13.5 Gy) and 30 mins (27 Gy). These results show us the annealing process for re-used samples decreases the peak intensity.

5.3.1.2 Regions of interest area

Region of interest area is another method to investigate and obtain the variation of TL glow curve intensities with increasing applied dose level. To follow the sensitivity change by this method, the glow curve of quartz was separated into three regions.

- **Low temperature region:** The limits of this region vary between ≈36 ^{o}C and ≈102 ^{o}C at a heating rate 1 ^{o}C/s and it comprises the whole area of low temperature peak 1 in the glow curves.
- **Intermediate temperature region:** The limits of this region vary between ≈102 ^{o}C and ≈225 ^{o}C at a heating rate 1 ^{o}C/s. In this temperature region, there are at least one complete glow peak and the portions of two glow peaks.
- **High temperature region:** The limits of this region vary between ≈225 ^{o}C and ≈400 ^{o}C at a heating rate 1 ^{o}C/s and it is seen that it consists of one complete and one portion of glow peaks.

Fig.5.33 shows the alterations of interested region areas of glow curves of quartz as a function of applied dose levels after four different applications; 1-) for different samples without heat treatment, 2-) the same sample without heat treatment, 3-) the different samples with heat treatment, and 4-) the same sample with heat treatment.

As seen in Fig.5.33a, the area in the low temperature region increases linearly from low dose up to 50 Gy. This result is also valid for four different applications. On the other hand, the slope of each curve decreases after 50 Gy up to 100 Gy. And then the areas decrease exponentially with increasing applied dose levels up to 2.6 kGy and therefore they have sublinear characteristics. Beyond 2.6 kGy, there is a small difference between annealed and unannealed sample intensities. As seen, the annealed samples have greater area than the unannealed samples.

As seen in Fig.5.33b, the area of intermediate temperature region increases linearly at low doses below 5 Gy. However, the slope becomes superlinear between 5 and 110

Gy and then decreases and becomes sublinear up to applied max dose level in the given study. On the other hand, the area of the higher temperature region shows different behaviors at low doses for annealed and unannealed samples. As seen from Fig.5.33c, the slope is linear between 1 Gy and 216 Gy and then becomes sublinear.
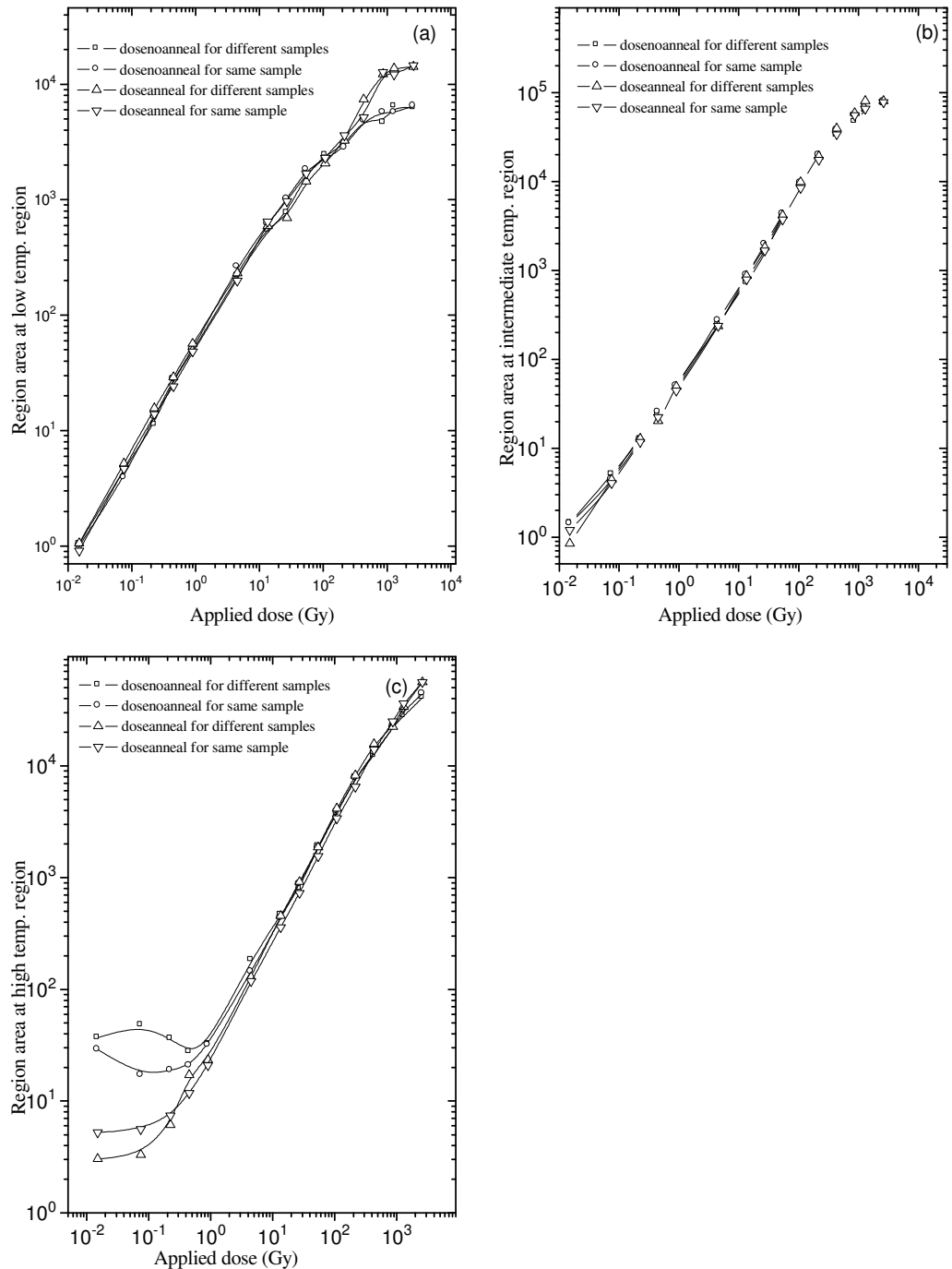
Figure 5.33 The variation of interested region areas of glow curves of synthetic quartz as a function of applied dose levels after four different applications

5.3.1.3 Maximum of TL peak intensity

This study has been also carried out to see the effects of applied dose levels on the peak intensities of glow peaks at $T_m \approx 83$, $T_m \approx 186$ and $T_m \approx 320\,^{\circ}\text{C}$ after four different applications. Fig. 5.34 shows that the variations of maximum peak intensity of glow peaks for four different applications which were explained in previous section (5.3.1.2) of this study.
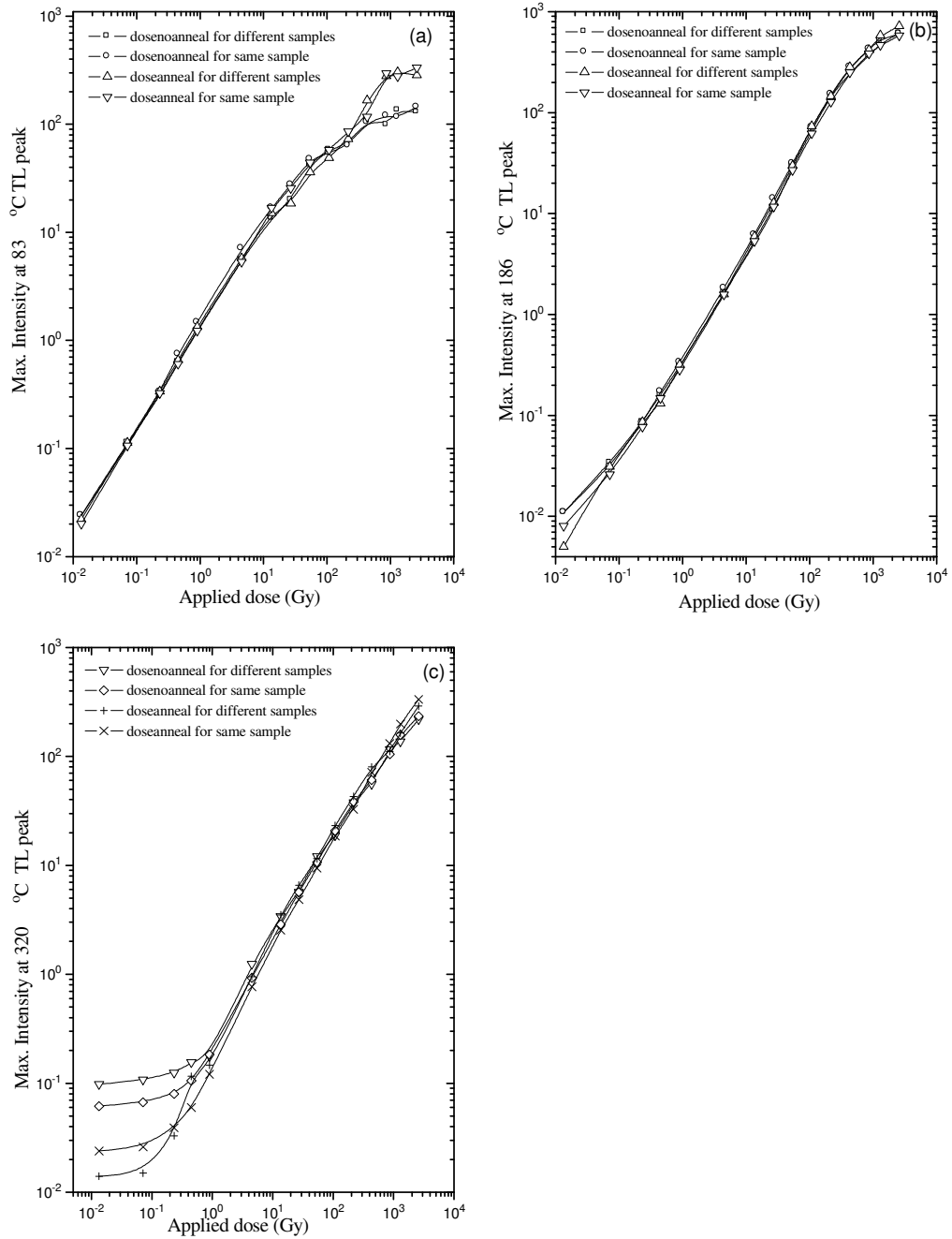
Figure 5.34 The variation of maximum peak intensities of glow peaks for four different applications

5.3.2   Natural quartz

All dose response analysis that has been mentioned for synthetic quartz were also repeated for natural quartz in the present study.

5.3.2.1 Glow curve analysis

In this part of the study, different dose implementations between 0.015 Gy to 2.6 kGy were also tried for four different studies underlined in the section 5.3.1.1. Fig.5.35 shows the glow curves of unannealed natural quartz samples after different dose levels.

As seen, there is an increase in the intensity of peak 1 ($T_m \approx 83$ ^{o}C) with increasing applied dose levels up to 1h (54 Gy), but the slope of increase is not equal to 1. For example, this value is greater than 1 up to 0.9 Gy dose (1 min). This value becomes smaller than one between 1 min (0.9 Gy) and 1 h (54 Gy). After 1 h (54 Gy), the intensity of peak 1 starts to decrease with increasing applied dose levels and this peak vanishes at higher doses.

The similar interpretations can be given for intermediate temperature peak at about 215 ^{o}C and high temperature peak at about 334 ^{o}C. Although a decreasing trend in the intermediate and high temperature peaks was seen, they didn't vanish in the studied dose range. In addition, saturation dose levels start at different dose levels.

Figure 5.36 shows the variation of the intensity of TL glow curves of one unannealed natural quartz samples after different dose levels between 0.015 Gy and 2.6 kGy. As seen, the TL intensity of low temperature peak 1 increases with increasing applied dose up to 1 h and then starts to decrease and one can estimate that it vanishes at higher doses above 2.6 kGy. The similar results are also valid for intermediate and high temperature peaks. However, these peaks are not visible up to 15 min (13.5 Gy) and the decrease starts after from 16 h (864 Gy).
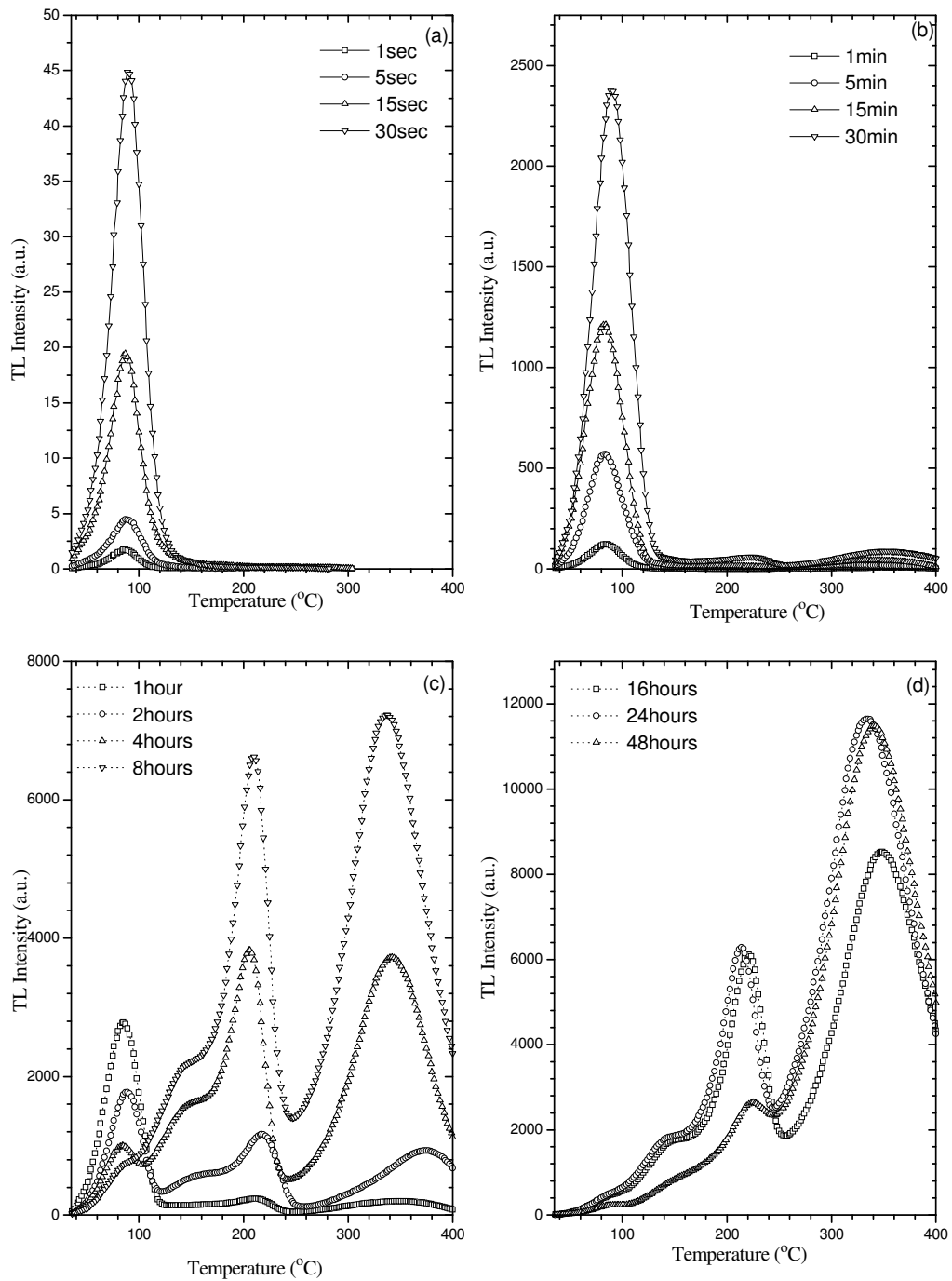
Figure 5.35 The variation of intensities of TL glow curves of unannealed natural quartz samples after different dose levels

Moreover, when we compare the glow curves in Fig.5.35 and 5.36, it was observed that the TL intensity of peak 1 is approximately 300% greater than in figure 5.35 at low doses below 0.45 Gy. This ratio immediately decreases above this dose level and becomes nearly zero at 13.5 Gy (15 min). The TL intensity of low temperature peak is smaller than in figure 5.35 about 5%~20% from 27 Gy to high doses (≈2.6 kGy).
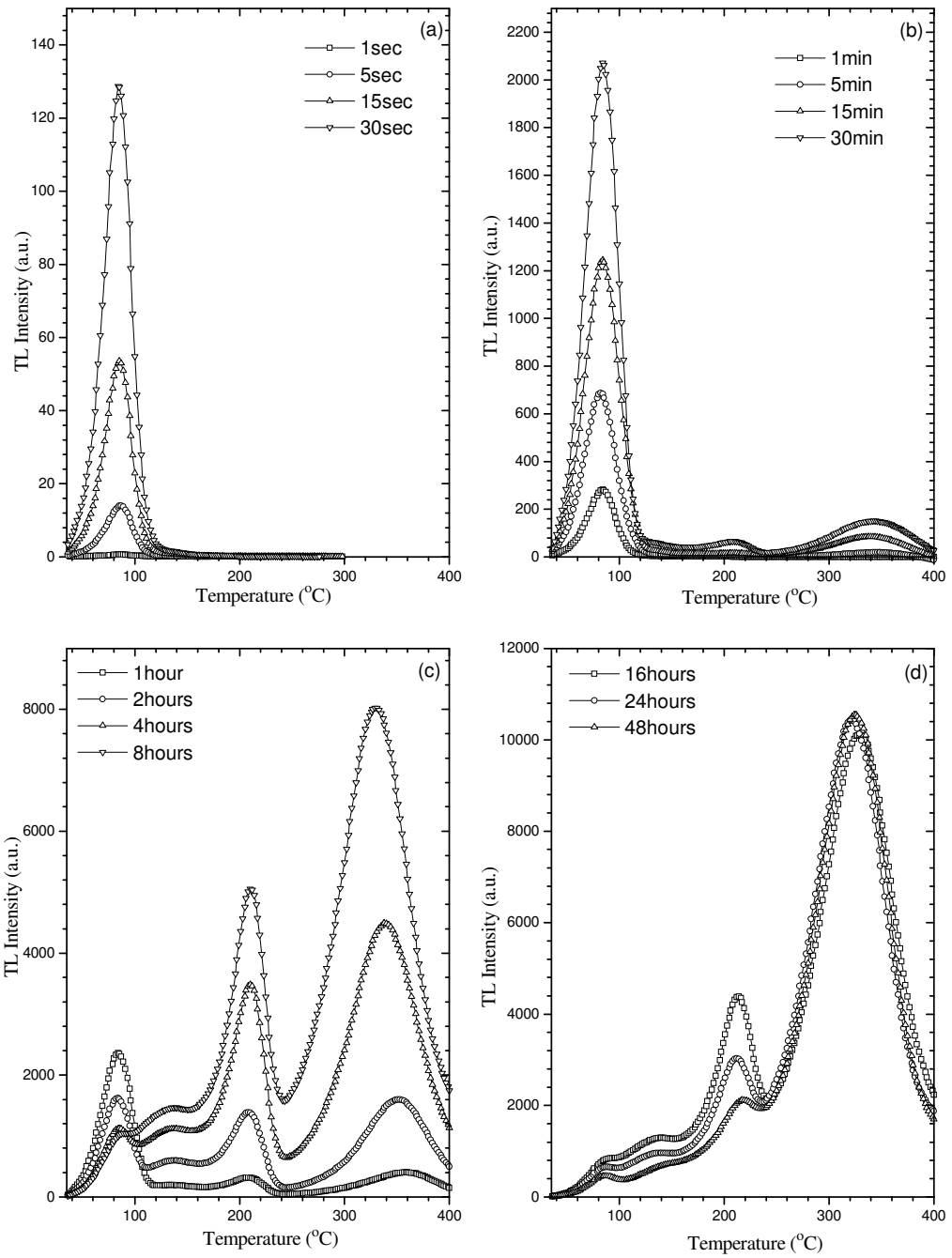
Figure 5.36 The variation of intensities of TL glow curves of one unannealed natural quartz samples after different dose levels

To understand the effects of annealing before irradiation on the glow curves of natural quartz samples, the above experiments were also repeated for different samples and only one sample with heat treatment at 600 °C for 1 h in a furnace. Figure 5.37 shows the variation of intensity of TL glow curves of annealed natural quartz samples after different dose levels. As seen, the intensity of peak 1 increases

with increasing applied doses up to 1 h (54 Gy). Beyond this value, its intensity decreases and then vanishes at high doses. The decrease in the intensity of intermediate temperature peak is started to seen at 16 h (864 Gy). On the other hand, we did not observe any decrease in the intensity of high temperature peak. In other words, the intensity of high temperature peak increases permanently with increasing dose level.
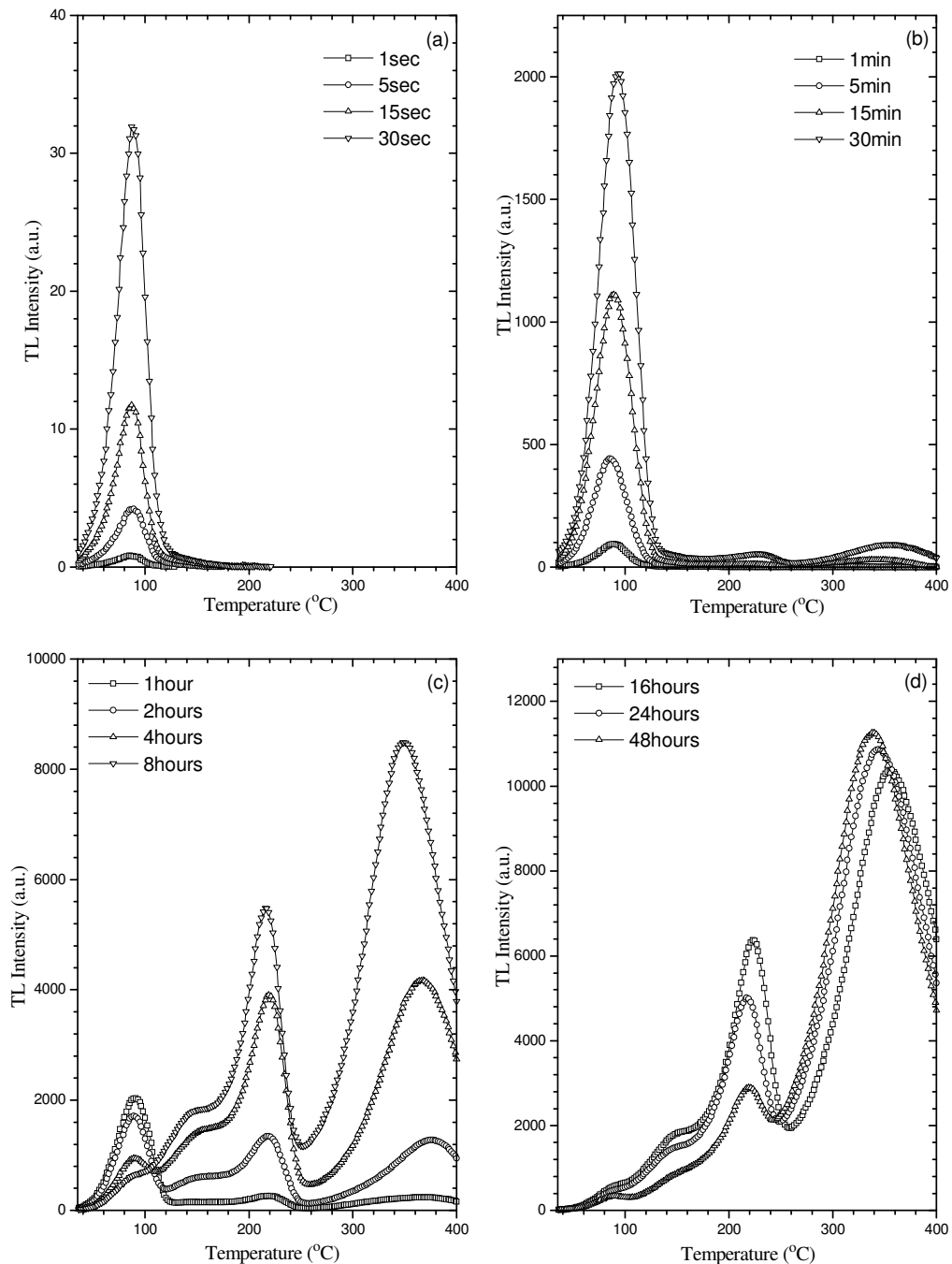
Figure 5.37 The variation of intensities of TL glow curves of annealed natural quartz samples after different dose levels

Moreover, an important analysis can be done when the differences between the glow curves of annealed and unannealed samples were discriminated. If Fig.5.35 and 5.37 are carefully compared, it is seen that the intensity of peak 1 in Fig.5.37 is smaller than in Fig.5.35 by about 40%~20% for low doses below 54 Gy (1 h). Above this level, the intensity of this peak is seen as on the same order. Besides, the intensities of intermediate and high temperature glow peaks are greater than in Fig.5.37 for all dose levels about 30%~10%. Fig.5.38 shows that the variation of intensities of TL glow curves of one annealed natural quartz at 600 ^{o}C for 1 hour after different dose levels. As seen, the intensity of peak 1 increases with increasing applied dose levels up to 1 h (54 Gy) and then starts to decrease up to 8 h (432 Gy). The intensity of intermediate temperature peak is increased between 1 min (0.9 Gy) and 16 h (864 Gy) and then it starts to decrease. The high temperature peak intensity has increasing trend for all applied doses.

In addition, if we compare the low, intermediate and high temperature peak intensities between in Fig.5.38 and 5.36, it was observed that the annealing process reduces the low temperature peak intensity about 80%~10% up to 2 h (108 Gy) but between 4 h and 48 h , the annealing process increases the low temperature glow peak intensity about 50%~300%. The intensity of intermediate temperature peak for annealed sample that is shown in Fig.5.38 is smaller about 25%~6% than unannealed sample shown in Fig.5.36 up to 8 h (432 Gy). However, it is greater than unannealed sample about 42%~15% between 16 h (864 Gy) and 48 h (2.6 kGy). The high temperature peak intensity for annealed sample is smaller than unannealed sample about 13%~5% until 48 h. It is greater than unannealed sample about 10% for 48 h.
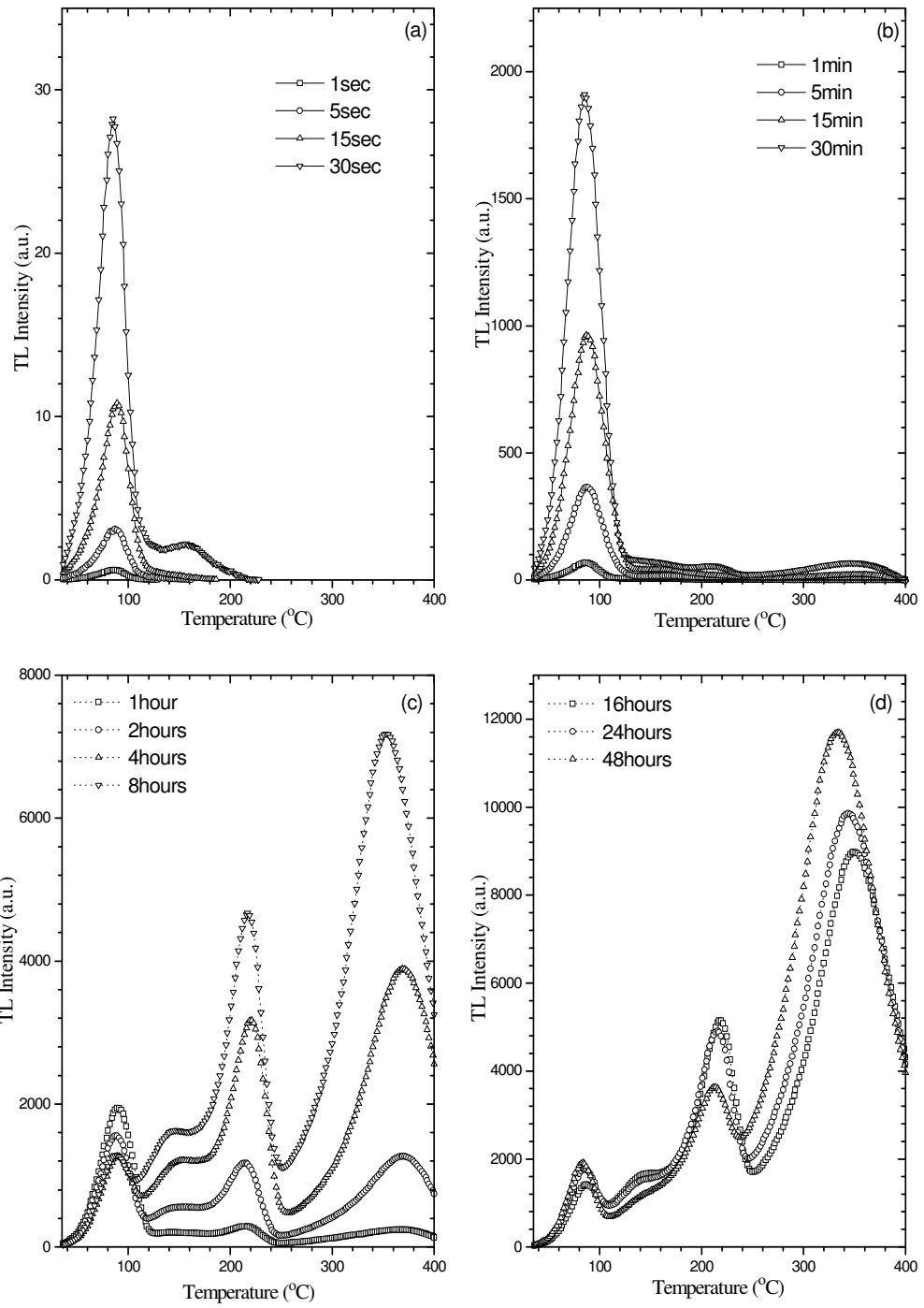
Figure 5.38 The variation of intensities of TL glow curves of one natural quartz samples after annealing at 600 ^{o}C for 1 before irradiation after different dose levels.

5.3.2.2 Regions of interest area

In this part, the glow curve of natural quartz samples was divided into 3 regions:

- **Low temperature region:** The limits of this region vary between $\approx$35 ^{o}C and $\approx$119 ^{o}C at a heating rate 1 ^{o}C/s. This temperature region comprises the whole area of peak 1.

- **Intermediate temperature region:** The limits of this region vary between $\approx$119 ^{o}C and $\approx$251 ^{o}C. In this temperature region, there are at least one complete glow peak and the portions of two glow peaks.

- **High temperature region:** The limits of this region vary between $\approx$251 ^{o}C and $\approx$400 ^{o}C. In this temperature region, there is a whole peak which appears at $T_m \approx 334$ ^{o}C.

Fig.5.39 shows the alterations of interested region areas of glow curves of quartz as a function of applied dose levels after four different applications; 1-) for different samples without heat treatment, 2-) the same sample without heat treatment, 3-) the different samples with heat treatment, and 4-) the same sample with heat treatment.

As seen in Fig.5.39a, the area of low temperature region increases linearly from low dose up to 27 Gy (30 min). This result is valid for four different applications but there is a difference between annealed and unannealed samples. As seen, both of them are linear but the slope of linearity of annealed samples is bigger than the slope of unannealed samples. In Fig. 5.39b, the difference between annealed and unannealed samples is also seen clearly at low doses from 0.015 Gy (1 sec) to 1 Gy (1 min). The areas of the intermediate temperature region of annealed samples are smaller than of unanealed samples. The area of this region increases linearly with dose between 1 Gy and 27 Gy but the slope of linearity between 1 Gy and 13.5 Gy is smaller than between 13.5 Gy and 27 Gy. The sublinear phenomena start above $\approx$27 Gy for four different applications. Fig.5.39c shows different behaviors of the area of higher temperature region at low doses for annealed and unannealed samples.
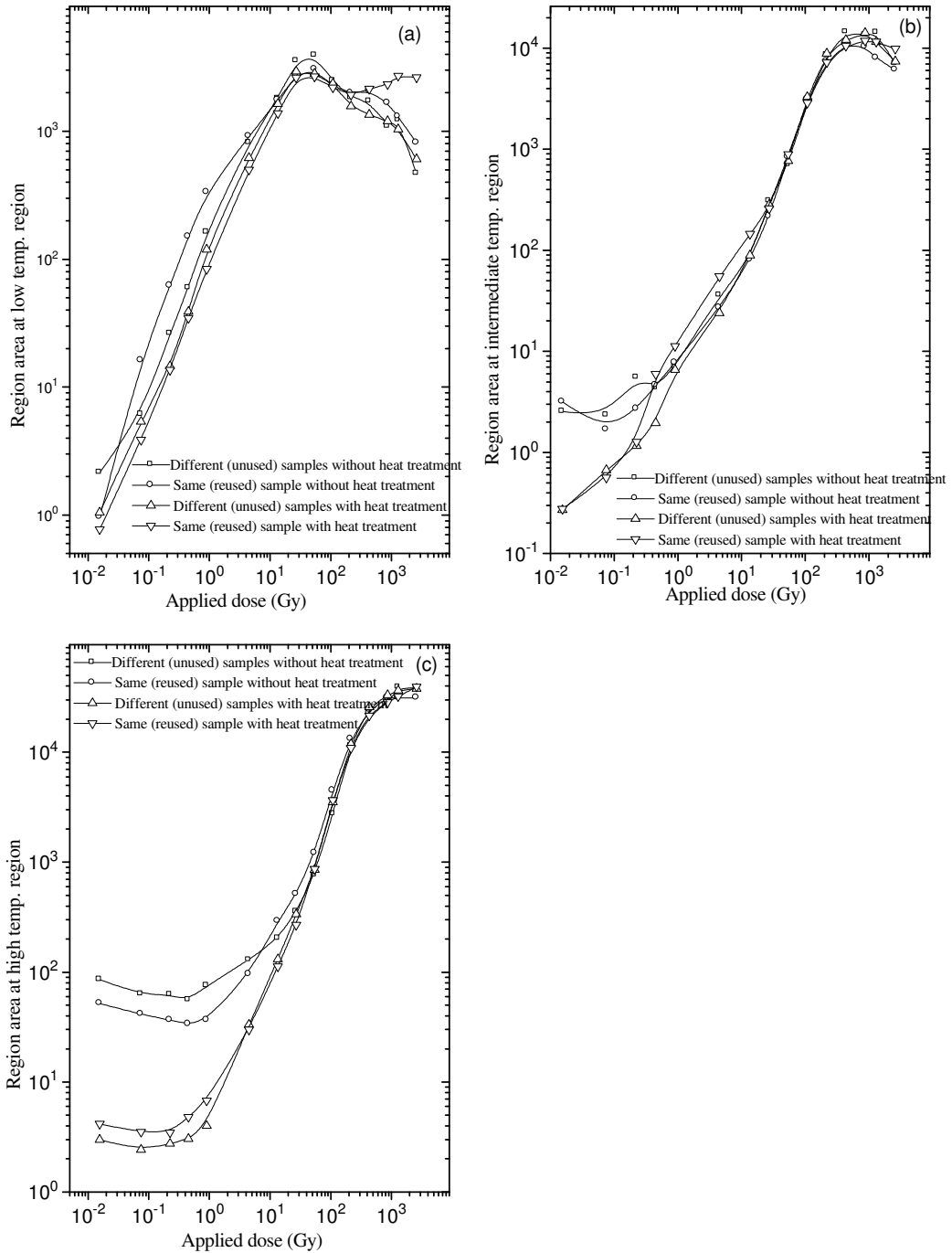
Figure 5.39 The variation of interested region areas of glow curves of natural quartz as a function of applied dose levels after four different applications

5.3.2.3 Maximum of TL peak intensity

This study has been carried out to see the effects of applied dose on the maximum thermoluminescence peak intensities at $T_m \approx 83$, $T_m \approx 215$ and $T_m \approx 334$ ^{o}C for the four different applications. The obtained results are shown in Fig.5.40.

91
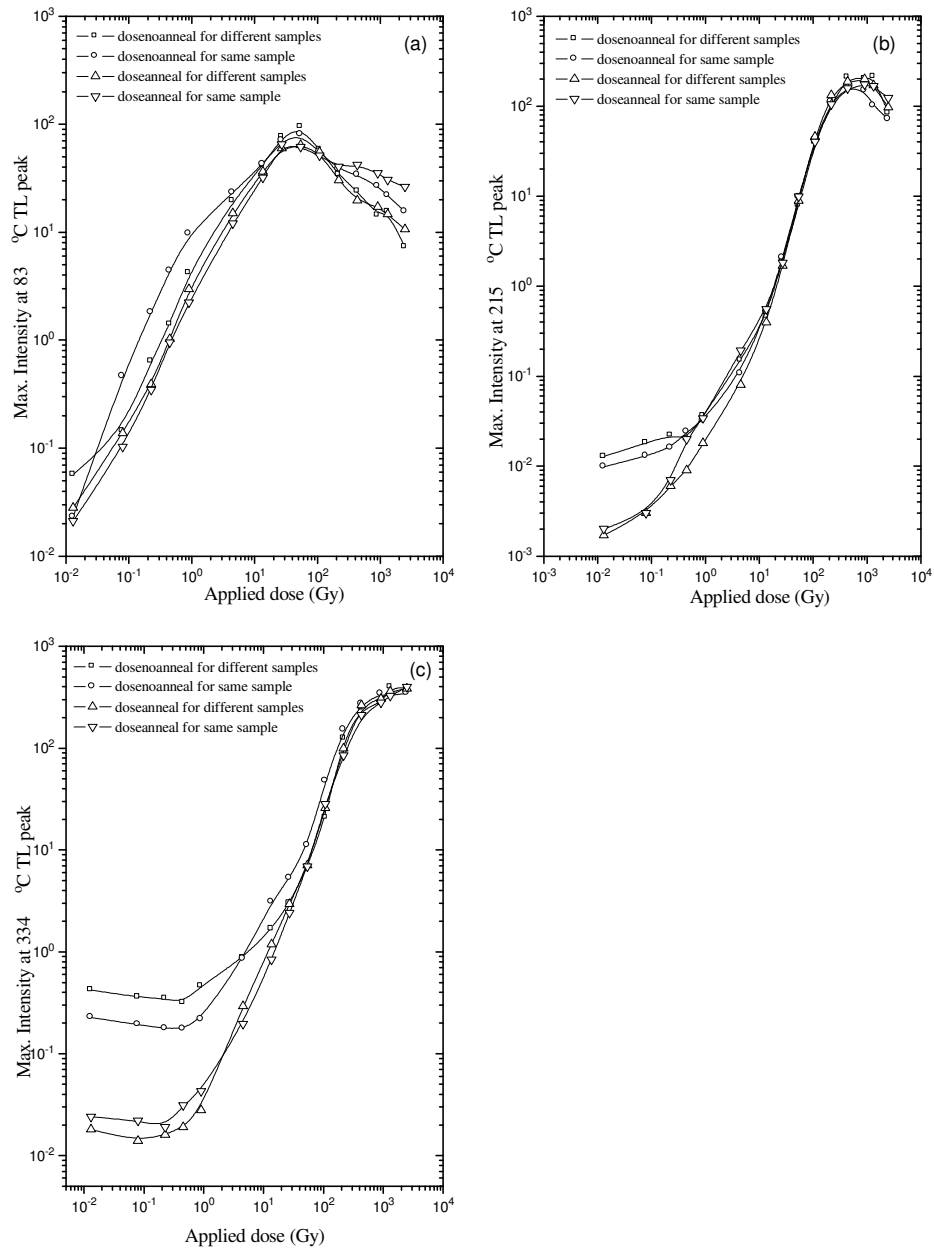
Figure 5.40 The variation of maximum peak intensities of glow peaks for four different applications

5.4   Heating Rate Effects on the TL of Synthetic and Natural Quartz

In this part of study, the effect of heating rate (β) on the shape and intensities of glow curves of both natural and synthetic quartz samples was studied. Five different heating rates (β=1, 2, 4, 8 and 16 $^{\text{o}}$C/sec) were applied to observe the

alterations on the glow curves shapes, areas of region, carrier population in traps and peak temperatures.

5.4.1 Synthetic quartz

In this part, ten unused synthetic quartz samples (each 20 mg) were used. Five of them were annealed in a furnace at 600 ^{o}C 1 h before irradiation and the others are not annealed. Fig. 5.41 shows the variations of the shapes of glow curves of five unannealed synthetic quartz samples after different heating rates: 1, 2, 4, 8 and 16 ^{o}C/sec. As seen that the intensities of all peaks decrease clearly with increasing heating rate.
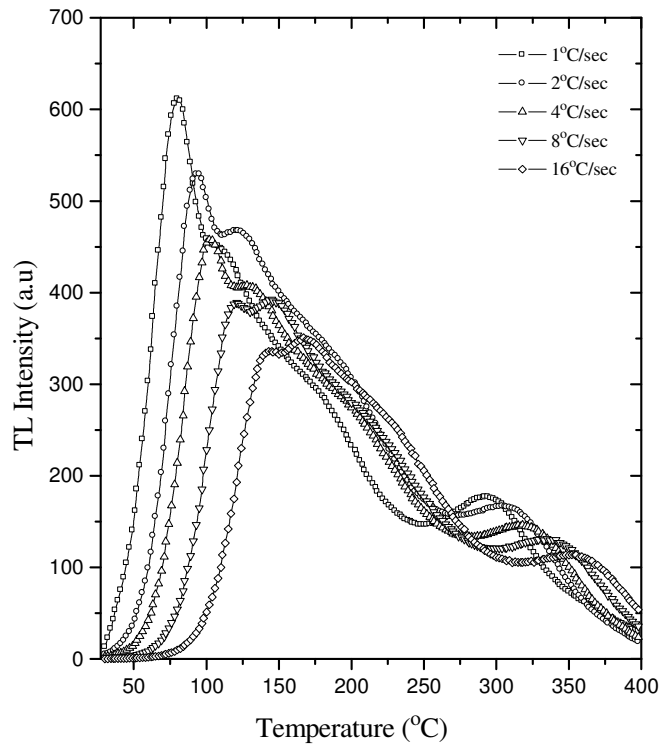
Figure 5.41 The variation of the shapes of TL glow curves of five unannealed synthetic quartz measured by different heating rates at 1, 2, 4, 8 and 16 ^{o}C/sec

Although the intensity of first peak is much bigger than intensity of second peak at low heating rates (β<5 ^{o}C/s), their intensities become comparable at high heating rates, (i.e. β>8 and 16 ^{o}C/s). At the same time, the peak temperatures of all peaks shift to high temperature sides with increasing heating rate.

93

Fig. 5.42 shows the variation of the shapes of TL glow curves of five annealed synthetic quartz after different heating rates at 1, 2, 4, 8 and 16 ^oC/sec. As seen the annealing process highly affects the intensities of TL peaks, especially the first peak. Indeed, the intensity of the first peak of unannealed samples is sharper than the annealed samples.
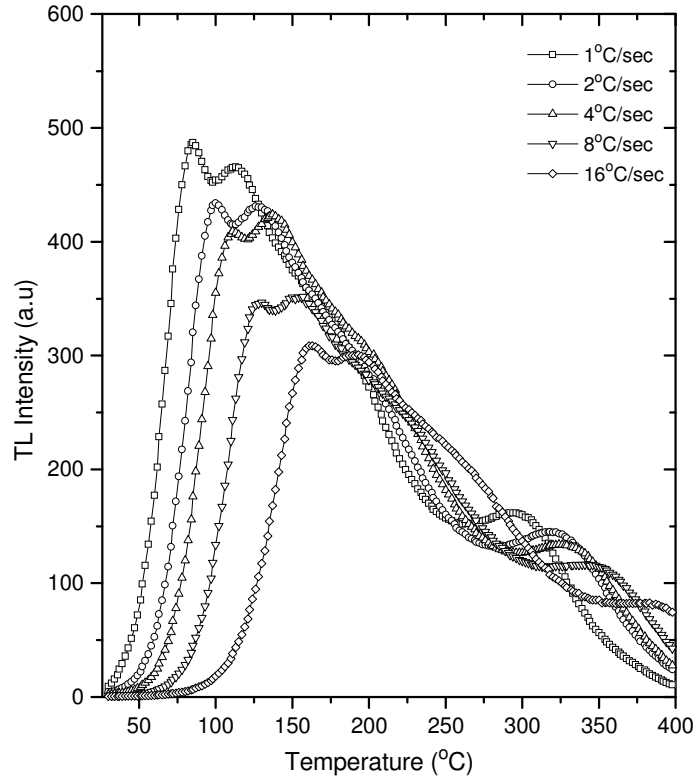
Figure 5.42 The variation of the shapes of TL glow curves of five annealed synthetic quartz measured by different heating rates at 1, 2, 4, 8 and 16 ^oC/sec

The effects of heating rate on the glow curves were also tested by using the region of interested method. In this case, the glow curve of quartz samples were divided into three regions:

- **Low temperature region:** The limits of this region vary between ≈30 ^oC and ≈100 ^oC for β=1 ^oC/sec. This region is suitable because it includes whole area of peak 1 and varies with increasing heating rate and chosen according to its peak temperature.

- **Intermediate temperature regions:** This region was also separated into two parts, IT1 and IT2. The limits of region IT1 vary between ≈100 ^oC and ≈160 ^oC,

- which consists of the peak 2 and 3 whereas the limits of IT2 vary between ≈160 °C and ≈250 °C. It only consists of the area of peak 4.
- **High temperature region:** This region includes only peak 5 and its limits vary between ≈225 °C and ≈330 °C.

Figs. 5.43 and 5.44 show that the variations of interested region areas of five unannealed and annealed synthetic quartz samples as a function of heating rate, respectively. As seen all region areas decrease with increasing heating rate.
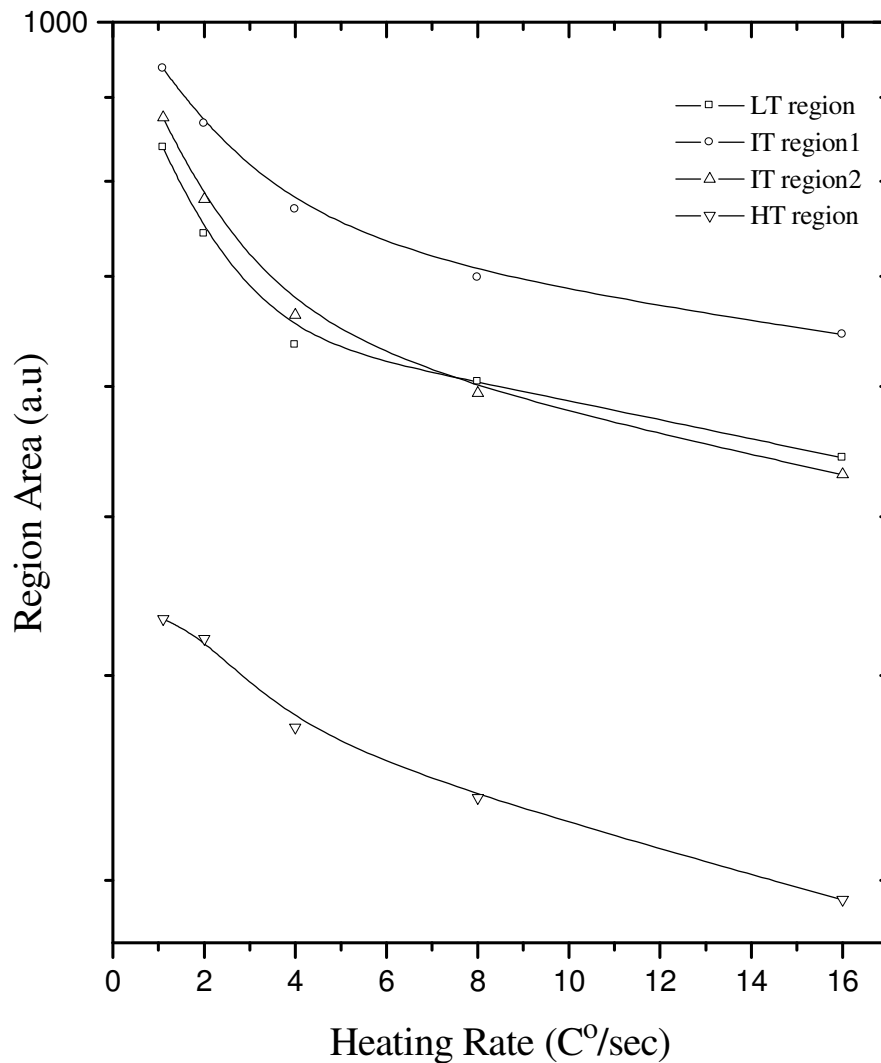
Figure 5.43 The variations of the intensity of interested region areas of TL glow curves of five unannealed synthetic quartz samples as a function of heating rates
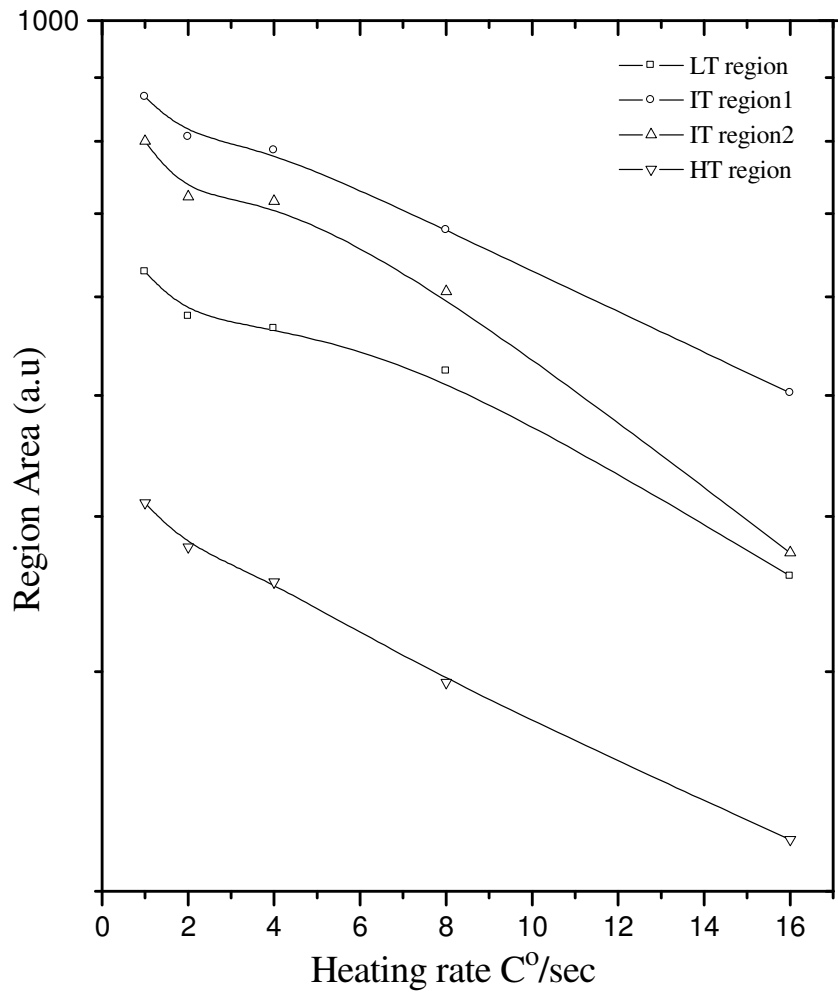
Figure 5.44 The variations of the intensity of interested region areas of TL glow curves of five annealed synthetic quartz samples as a function of heating rates

The all glow curves were also analyzed by using a Computer Glow Curve Deconvolution (CGCD) program to get possible number of carrier population in the traps. Figure 5.45 shows one of the analyzed glow curves of synthetic quartz sample with five peaks. Figures 5.46 and 5.47 show that the variations of carrier populataions in five traps as a function of heating rates for unannealed and annealed synthetic quartz, respectively. It is seen clearly that all carrier concentrations in the traps decrease with increasing heating rate.
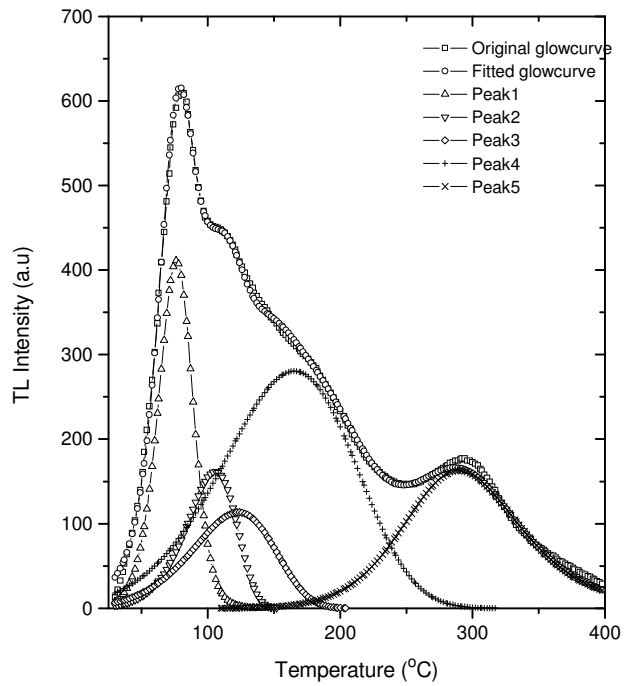
Figure 5.45 An analyzed glow curve of synthetic quartz sample using five glow peaks in the CGCD program
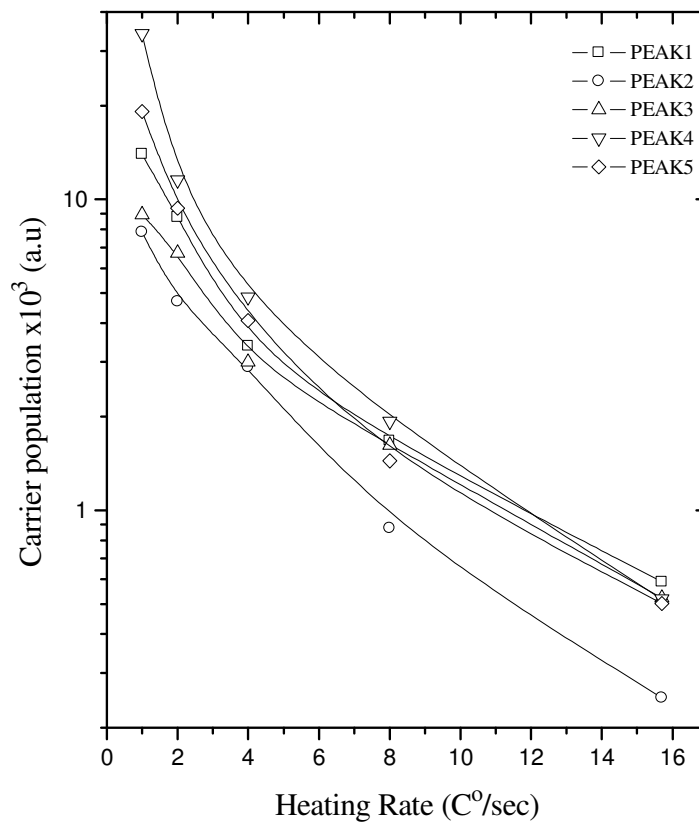
Figure 5.46 The variations of carrier concentrations in the traps of unannealed synthetic quartz as a function of heating rates
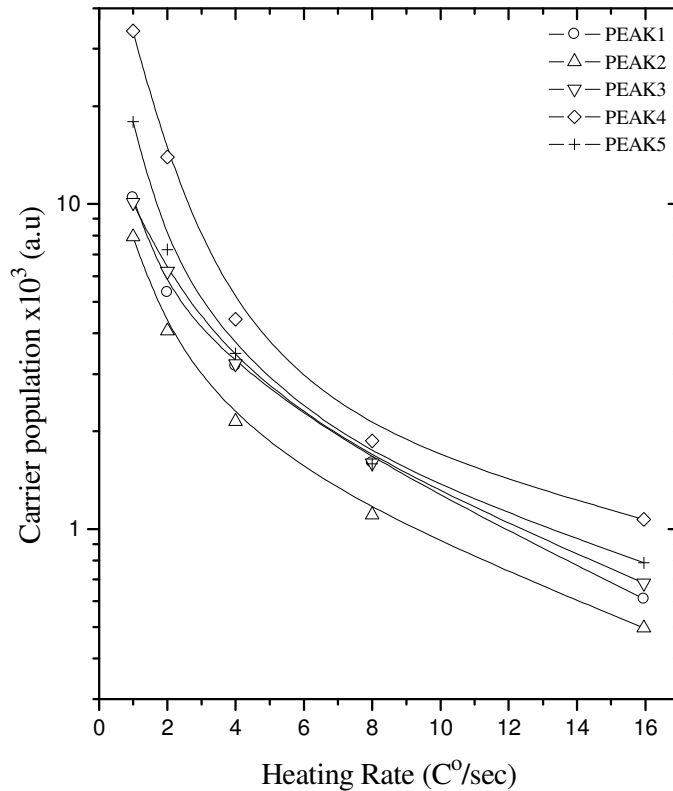
Figure 5.47 The variations of carrier concentrations in the traps of annealed synthetic quartz as a function of heating rates

The peak temperature of a TL glow peak is associated with trap depth (E_a) of trap and frequency factor (s) of electrons in the trap. In general, the higher value of peak temperature results the higher trap depth (activation energy). In this part, the effect of the heating rate on the peak temperatures of TL glow peaks was investigated as a function of heating rates. Figures 5.48 and 5.49 show the alterations in the peak temperatures of low temperature (LT), intermediate temperature (IT) and high temperature (HT) peaks versus heating rates for the unannealed and annealed synthetic quartz samples, respectively. As shown in both figures, the peak temperatures of all peaks are approximately linearly increased with the increasing heating rate. In addition, when the heating rate is increased from 1 ^{o}C/s to 16 ^{o}C/s, the peak temperatures of LT, IT and HT peaks are shifted to high temperature sides by about 50 ^{o}C. However, the shift in the peak temperatures of annealed samples is approximately 75 ^{o}C for LT and IT peaks and 100 ^{o}C for HT peak. This result is possibly caused by the annealing process and it explains the effects of annealing on peak temperatures. If these figures are also compared, it is seen that the peak temperatures of glow peaks of the annealed synthetic quartz are always bigger than

the peak temperatures of glow peaks of unannealed synthetic quartz at each heating rate.
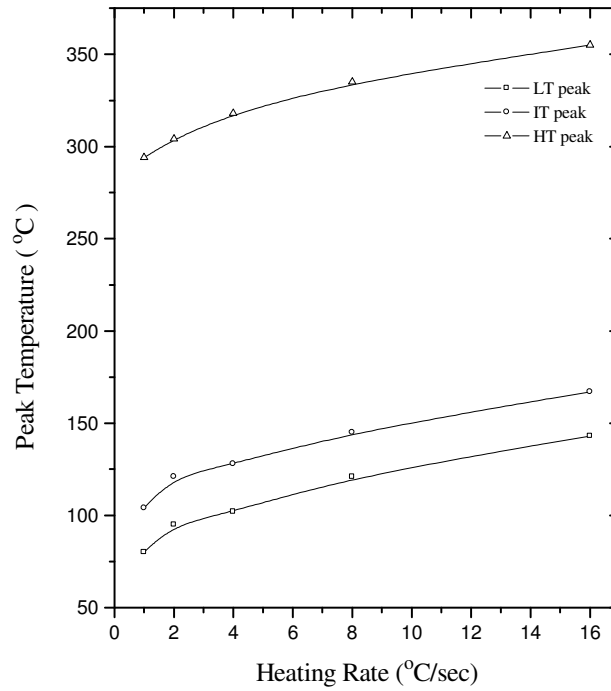
Figure 5.48 The alteration in the peak temperatures of glow peaks of unannealed synthetic quartz samples versus heating rates
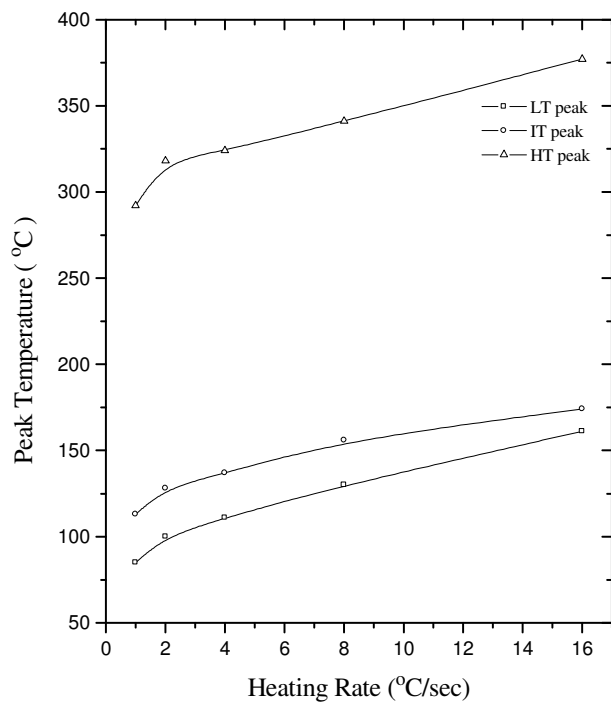
Figure 5.49 The alteration in the peak temperatures of glow peaks of annealed synthetic quartz samples versus heating rates

The effect of annealing on the peak variation:

Figure 5.50 shows the effect of the annealing process on the peak temperatures of the TL glow curves of synthetic quartz samples; (a) for low temperature peak, (b) intermediate temperature peak and (c) high temperature peak.
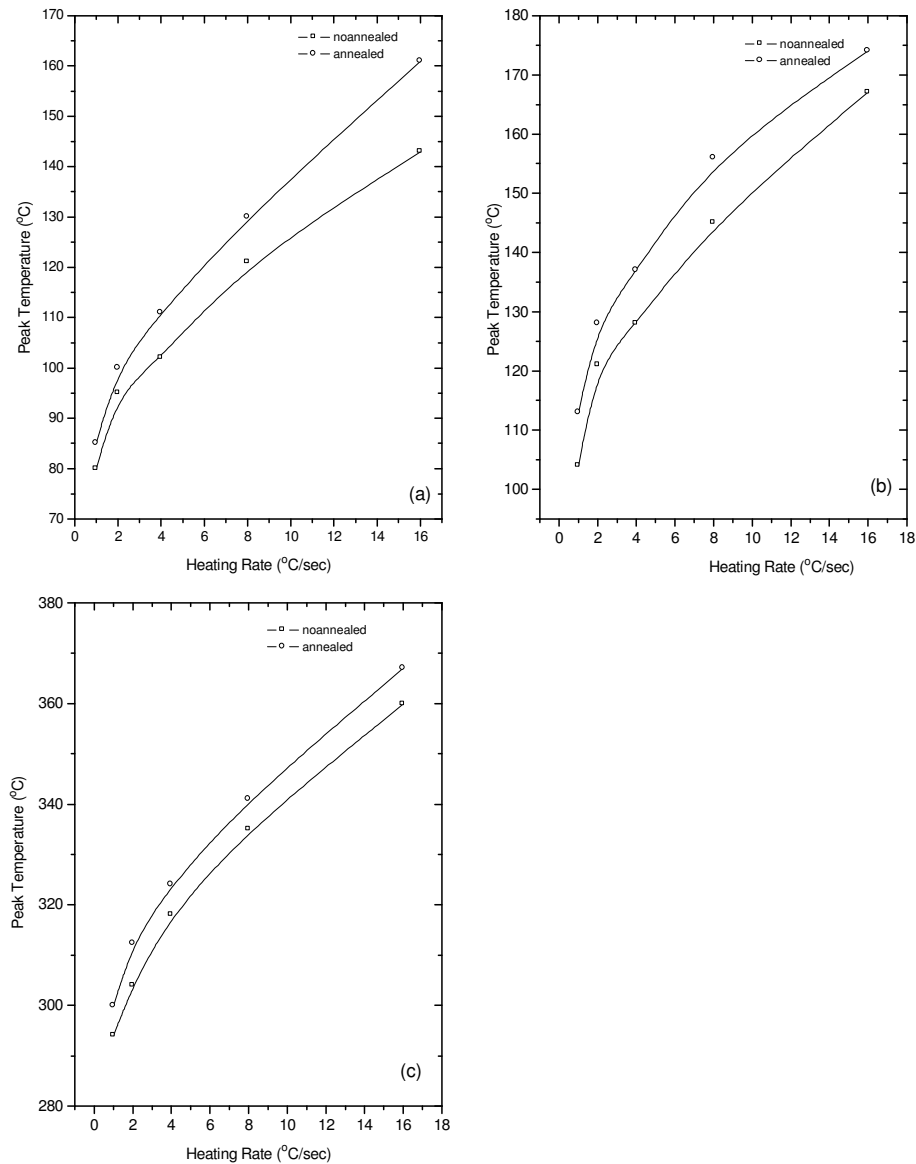
Figure 5.50 The effect of the annealing process on the peak temperatures of the TL glow curves of synthetic quartz samples; (a) for low temperature peak, (b) intermediate temperature peak and (c) high temperature peak

This figure explains that the annealing process shifts the peak temperature of glow curve. In all figure, the peak temperatures of the annealed synthetic quartz for each heating rate values is bigger than that of unannealed synthetic quartz.

100

5.4.2 Natural quartz

All the analysis which had been mentioned in previous section for synthetic quartz samples were also repeated for natural quartz samples. Fig.5.51 shows the variation of the shapes of TL glow curves of unannealed natural quartz samples after different heating rates (β=1, 2, 4, 8 and 16 ^{o}C/sec). As seen, the intensities of all peaks are also decreased with increasing heating rate. However, when the decreasing values of the intensities of glow peaks of both unannealed synthetic and natural quartz samples are compared, it is seen that the decreasing in the natural quartz samples is very small than the synthetic quartz samples. Moreover, the peak temperatures of all peaks shifted with the same ratio by the increasing heating rate. Fig.5.52 shows the TL glow curves of annealed natural quartz after different heating rates.
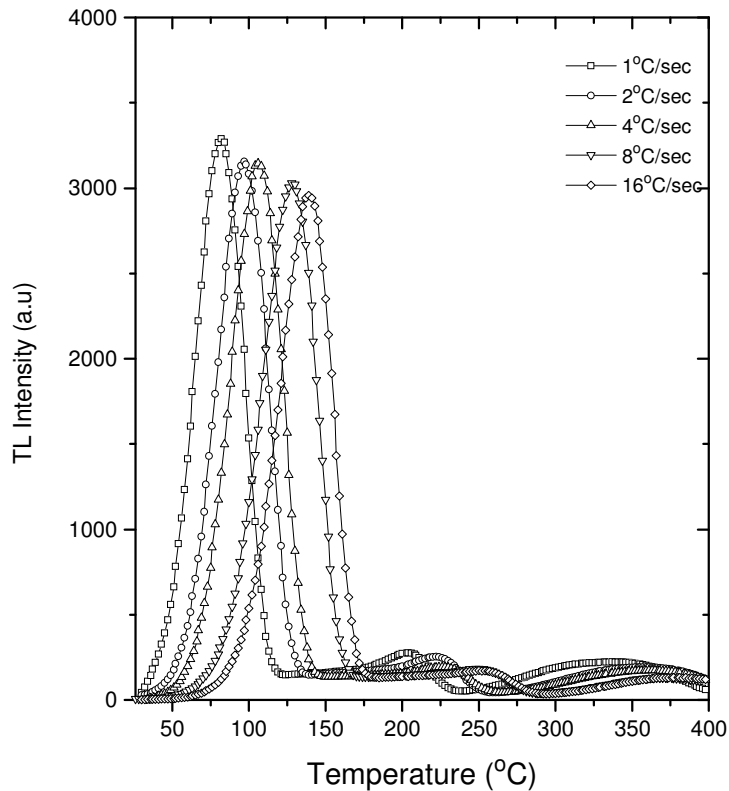
Figure 5.51 The TL glow curves of unannealed natural quartz samples after different heating rates (β=1, 2, 4, 8 and 16 ^{o}C/s)

As seen, the annealing process affects dramatically the intensities of all glow peaks, especially the intensity of low temperature peak 1.
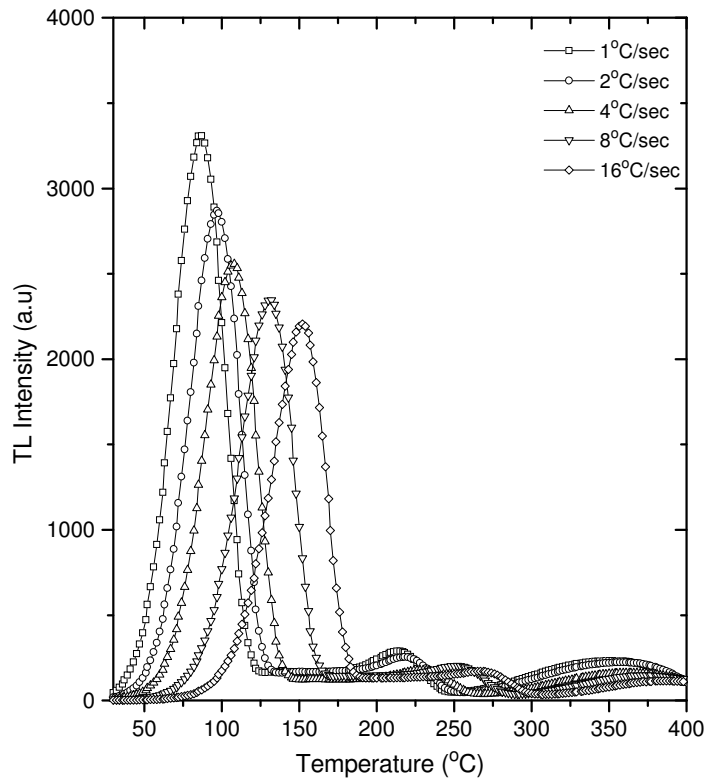
Figure 5.52 The TL glow curves of annealed natural quartz samples after different heating rates (β=1, 2, 4, 8 and 16 °C/s)

The effects of heating rate on the intensity of glow peaks of annealed and unannealed natural quartz samples were also investigated by using region of interested area method. In this method, the glow curves were again separated into three regions:

- **Low temperature region:** The limits of this region vary between ≈30 °C and ≈119 °C at β=1°C/sec.

- **Intermediate temperature regions:** This region was again separated into two parts, IT1 and IT2. The limits of region IT1 vary between ≈119 °C and ≈170 °C whereas the limits of IT2 vary between ≈170 °C and ≈239 °C.

- **High temperature region:** This region includes only peak 4 and its limits vary between ≈239 °C and ≈330 °C.

Fig.5.53 shows the variations of the areas of the chosen interested regions of unannealed natural quartz samples as a function of heating rate. It is seen that the areas of all regions are not much affected with increasing heating rate if the heating rate is grater than 2 °C/s. On the other hand, the areas of chosen regions of annealed

quartz samples decreases up to $\beta \approx 4$ ^{o}C/s and then they become nearly stable with increasing heating rate (see Fig.5.54).
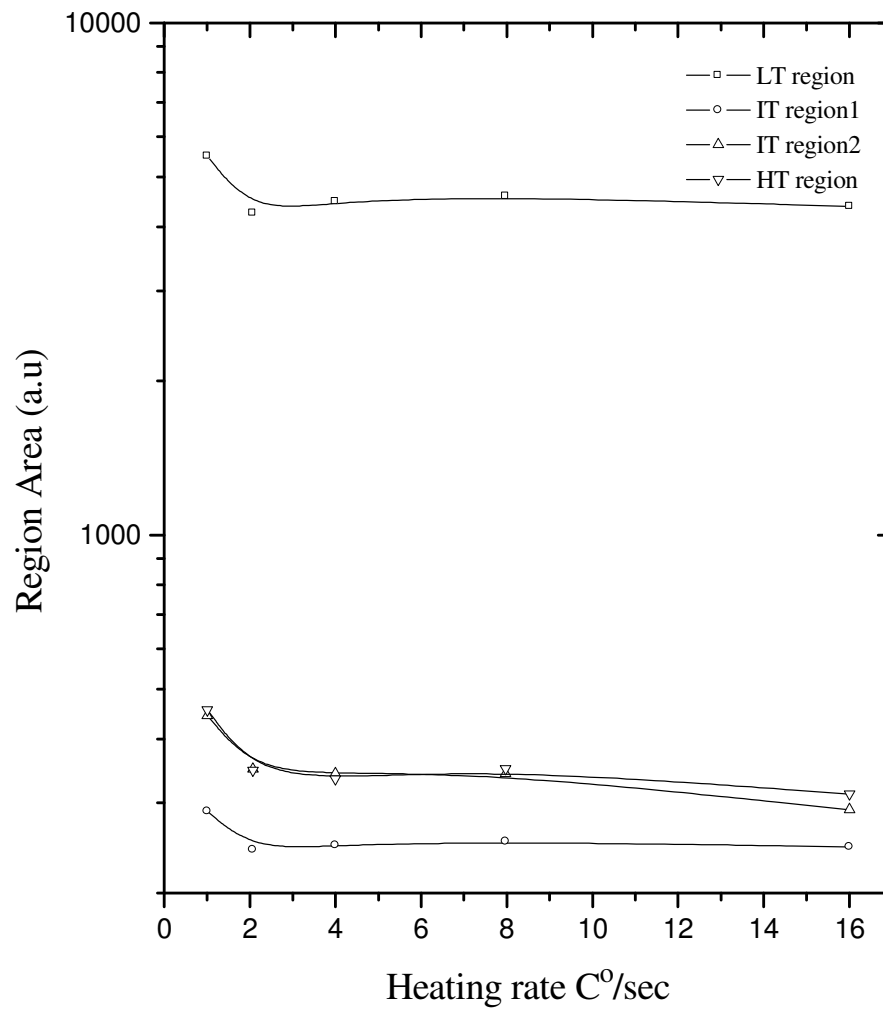
Figure 5.53 The variations of the chosen region areas of TL glow curves of unannealed natural quartz samples as a function of heating rates
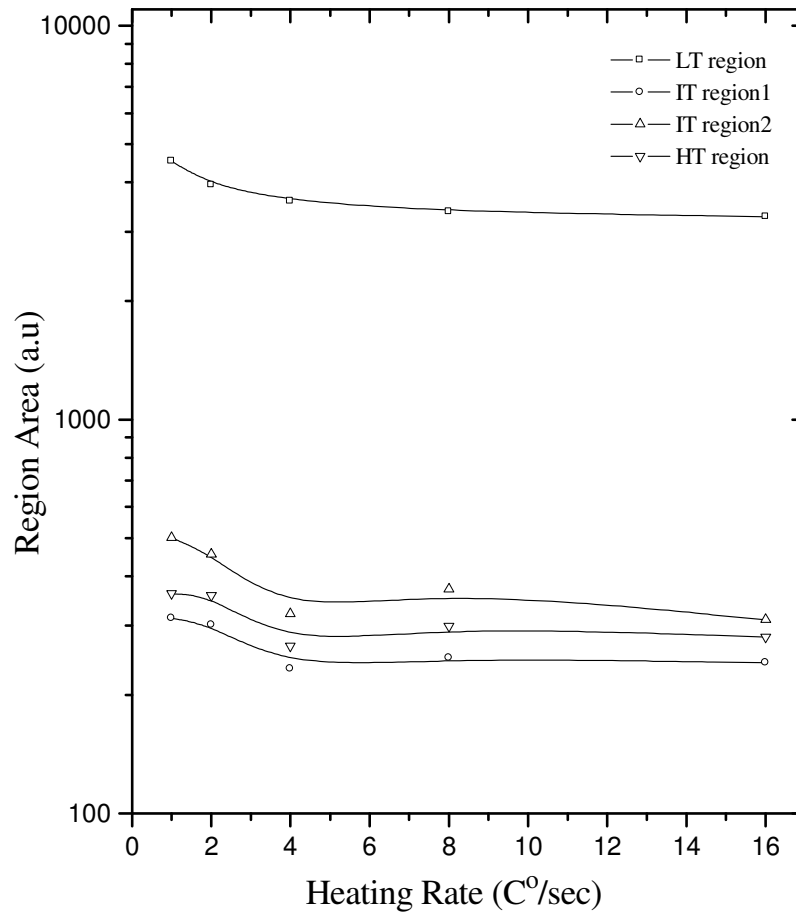
Figure 5.54 The variations of the chosen region areas of TL glow curves of annealed natural quartz samples as a function of heating rates

The effects of heating rate on the intensity of glow peaks of annealed and unannealed natural quartz samples were also investigated by using CGCD method. Figure 5.55 shows one of the fitted glow curves of natural quartz sample by CGCD program. The glow curves of natural quartz samples were analyzed by using four glow peaks in the CGCD program. The obtained results from the glow curves of unannealed and annealed quartz samples are shown in figures 5.56 and 5.57, respectively. As seen in both figures, the intensity of all peaks decreases with increasing heating rate, as in synthetic quartz samples.
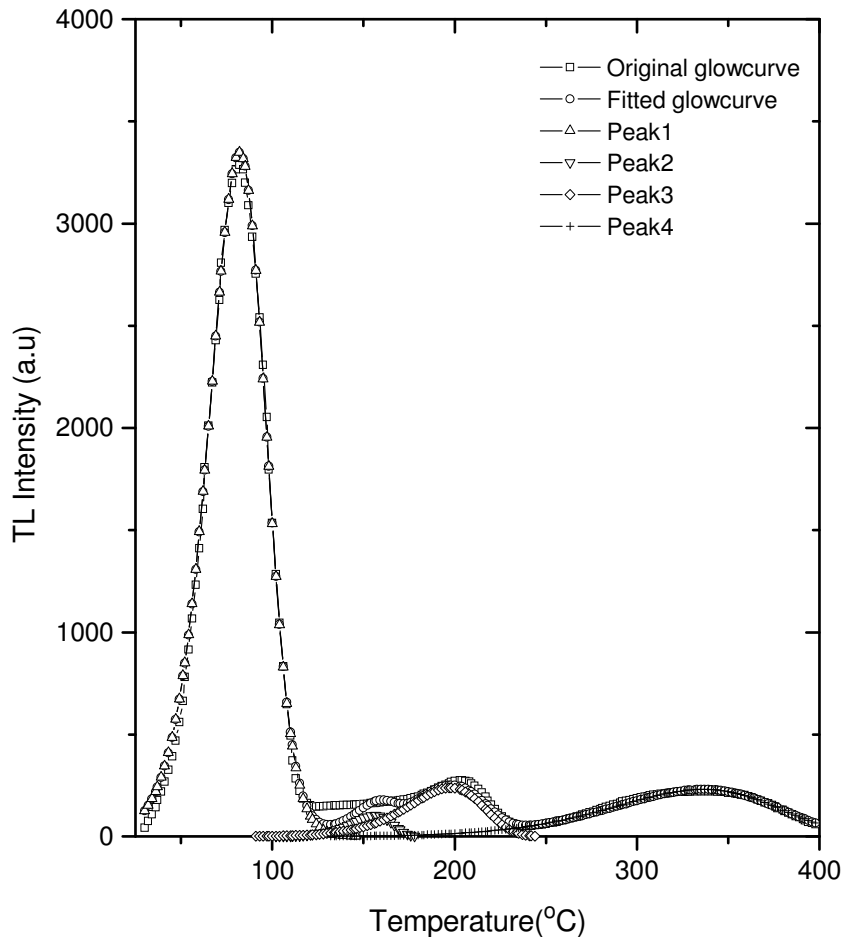
Figure 5.55 An analyzed glow curves of natural quartz sample without annealing by CGCD program
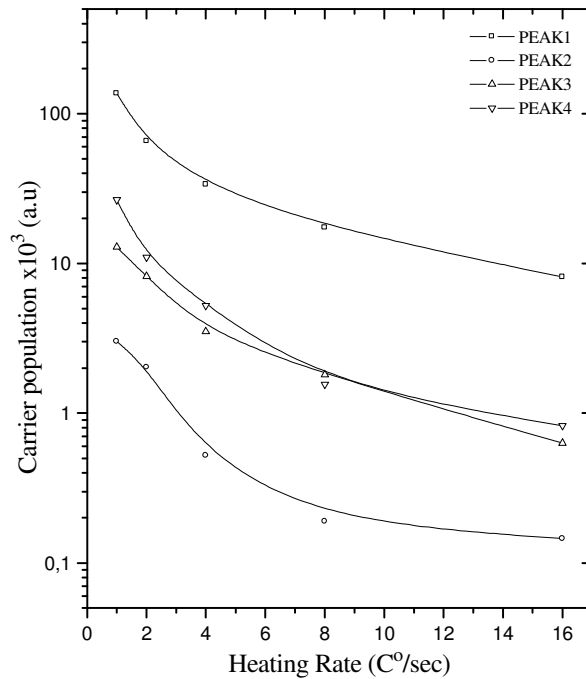
Figure 5.56 The variations of intensities of glow peaks of unannealed natural quartz samples as a function of heating rate obtained by CGCD method
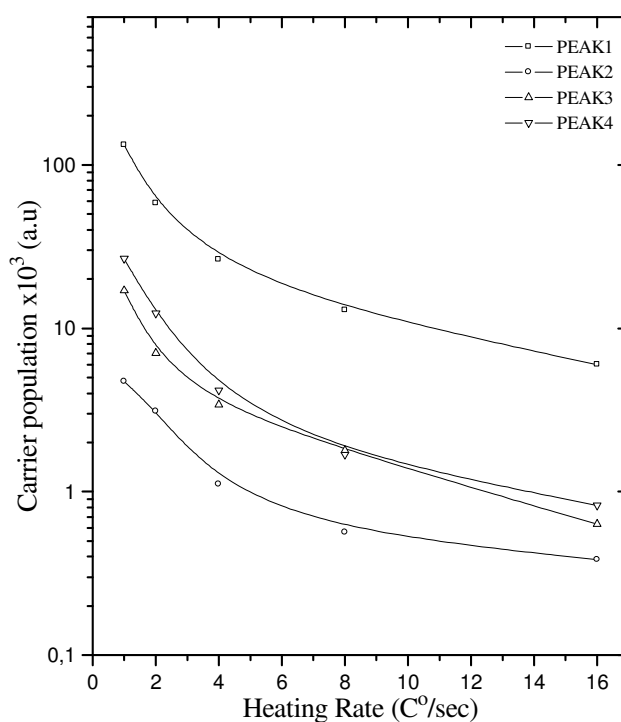
Figure 5.57 The variations of intensities of glow peaks of annealed natural quartz samples as a function of heating rate obtained by CGCD method

5.4.3 Calculation of trap depth

The trap depth (activation energy, E_a) can be derived from the graph of $ln(T_m^2/\beta)$ versus $1/T_m$ and the slope of this graph gives us the E_a/k value. Figure 5.58 and 5.59 show the graphs of $ln(T_m^2/\beta)$ versus $1/T_m$ of low temperature and high temperature peaks of unannealed and annealed synthetic quartz samples. As seen in both figures, there is a linear ramp but the annealing has slightly affected the slopes. In the both of two figures, all graphs were fitted by a curve fitting program (Origin 4.0). The trap depths (E_a) of low and high temperature peaks were calculated using the slopes of these graphs for annealed and unannealed samples. The results were given in the Table 5.1.
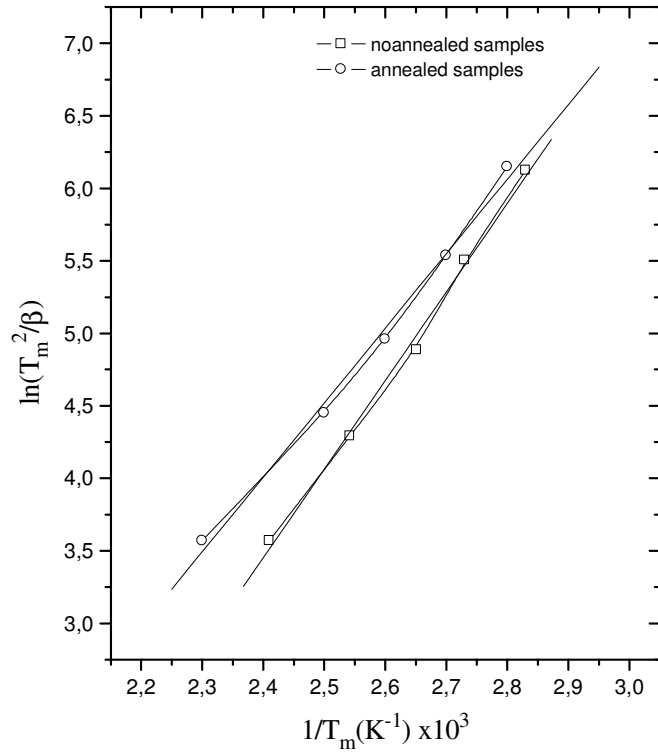
Figure 5.58 The graph of *ln(T$_m$²/β)* versus *1/T$_m$* of low temperature peak of unannealed and annealed synthetic quartz samples
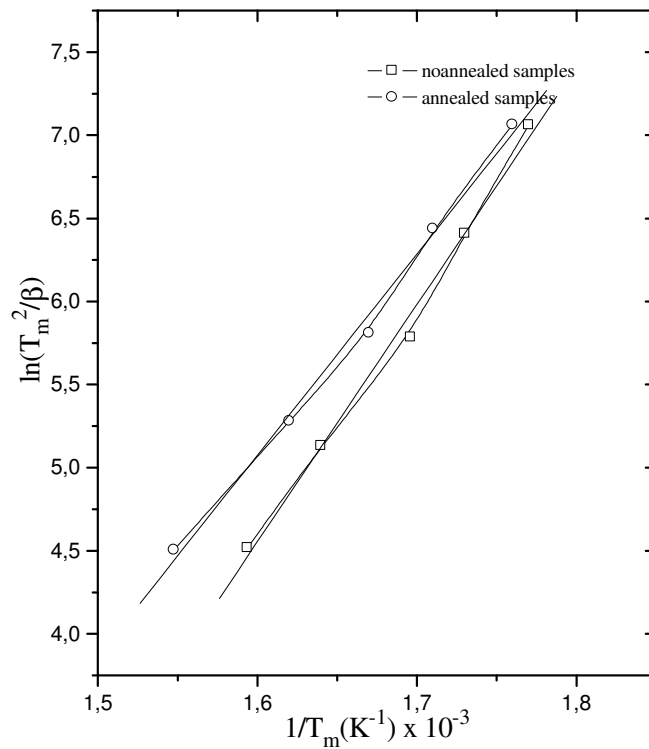
Figure 5.59 The graph of *ln(T$_m$²/β)* versus *1/T$_m$* of high temperature peak of unannealed and annealed synthetic quartz samples

107

Table 5.1 The values of trap depths of low and high temperature peaks of unannealed and annealed synthetic quartz

Low Temperature Peak		High Temperature Peak	
E_a (e.V) (noanneal)	E_a (e.V) (anneal)	E_a (e.V) (noanneal)	E_a (e.V) (anneal)
0.526	0.443	1.231	1.043

Figures 5.60 and 5.61 show the graphs of $ln(T_m^2/\beta)$ versus $1/T_m$ of low temperature and high temperature peaks of unannealed and annealed natural quartz samples. The similar trends as in the synthetic quartz samples were also observed in this case.
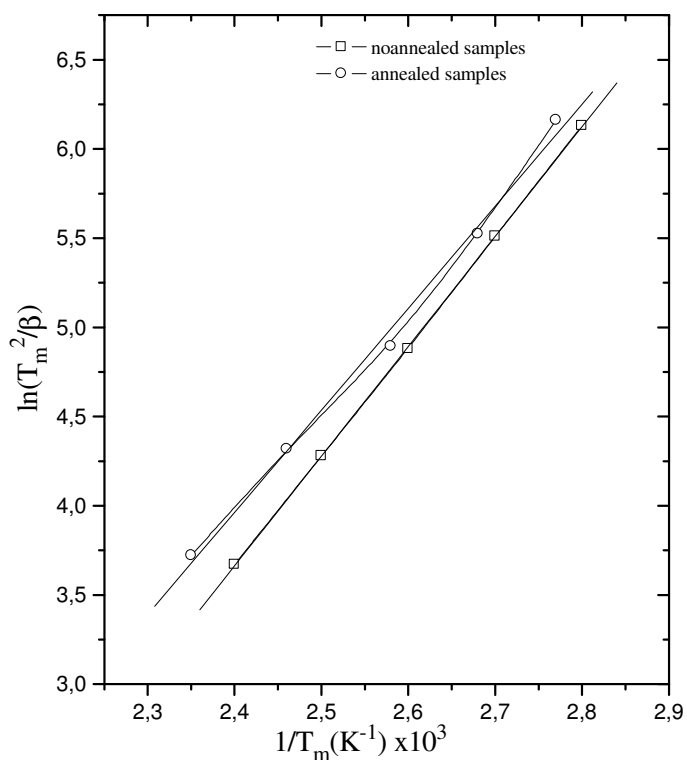
Figure 5.60 The graph of $ln(T_m^2/\beta)$ versus $1/T_m$ of low temperature peak of unannealed and annealed natural quartz samples

108
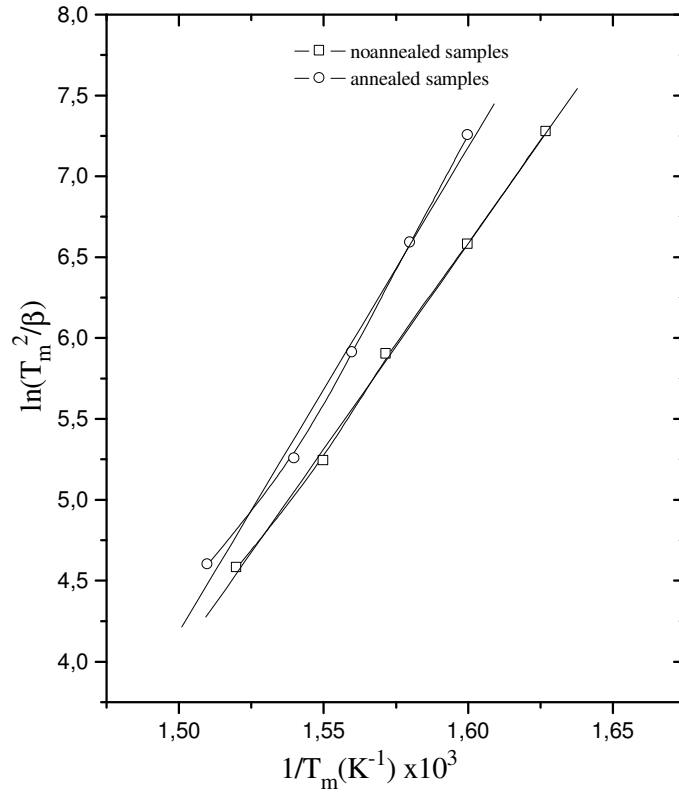
Figure 5.61 The graph of $ln(T_m^2/\beta)$ versus $1/T_m$ of high temperature peak of unannealed and annealed natural quartz samples

Table 5.2 shows the values of trap depths of low and high temperature peaks of unannealed and annealed natural quartz. These values were calculated from the slopes of graphs in figure 5.60 and 5.61.

Table 5.2 The values of trap depths of low and high temperature peaks of unannealed and annealed natural quartz

Low Temperature Peak		High Temperature Peak	
E_a (e.V) (noanneal)	E_a (e.V) (anneal)	E_a (e.V) (noanneal)	E_a (e.V) (anneal)
0.53	0.493	2.19	2.07

CHAPTER 6

CONCLUSION

One of the most important mineral in dosimetric investigation is quartz, which is found abundantly in archaeological and geological materials. Although there are many studies about its thermoluminescence (TL) properties in the literature, studies are still being done on the quartz because each quartz mineral extracted from the different region of the world.

It is well known that the thermal treatment highly affects the intensity of TL glow curves in all dosimetric materials and therefore its effects have been investigated by a number of scientist [90, 91, 95, 99, 101]. Natural quartz is one of the most important samples for dosimetric investigations and dating of ancient ceramics and pottery. The TL intensity of natural quartz is affected by the thermal treatments but quartz samples which have been collected from different region of world can not show the same results after applied thermal treatments.

This thesis was based on four main experimental works, each having different aims. These experiments were carried out to investigate the effects of the thermal treatment, dose response, heating rate and predose on the thermoluminescence (TL) intensity, glow curves and kinetic parameters of synthetic and natural quartz.

In the first work of this thesis, we have investigated the effect of thermal treatment on the kinetic parameters and intensity of TL peaks of the annealed synthetic quartz crystal at 500 $^{\circ}$C and 600 $^{\circ}$C. During this study, all samples were exposed to ^{90}Sr-^{90}Y beta source. This study was considered under two parts: cycle of measurement and annealing time.

The cycle of measurement experiment is done to see the reproducibility of a sample. If the sensitivity of a sample or at least its dosimetric peak does not change after several cycles of exposures and readouts, it can be considered as a good

phosphor. In this part, there is a big altering in the intensity of peak 1 after annealing at 500 ^{o}C for 1 h. The same experiment was repeated after annealing at 600 ^{o}C for 1h but a good enhancement was observed in the stability of peak5 shown in Fig. 5.3. The obtained repeatability of this peak over 10 cycles is within 5%. The intensity of peak 1 after annealing at 500 ^{o}C and 600 ^{o}C increases with increasing experimental cycles.

During the investigation of the influence of the variation of annealing time on the kinetic parameters and intensity of TL glow peaks, it was observed that the areas of all glow peaks increase with increasing annealing time up to 1 hour (54Gy) and then they start to decrease with further annealing time above 1 h shown in Fig.5.5. For example, the intensity of peak 1 increases to ≈20% of its original value after annealing at 500 ^{o}C for 1 h. The reason of these results can be explained with Zimmerman model. In this model, the carriers in the reservoir trap move to the luminescence center with annealing. But this transfering continues until reservoir traps depleted. The depletion time could be considered 1hour for this study. The presence of competitor traps caused the decreasing area (TL intensity). After 1hour annealing, the anneling process may create competitor traps.

In the second work of our thesis, we have tried to see the effects of thermal treatment on the TL intensity and kinetic parameters of natural quartz which have been extracted from ceramics of Kubad Abad palace, Beyşehir, Konya. In this part, the stabilities of TL peak intensities of the quartz minerals extracted from the tiles of Kubad Abad Palace were investigated. The stability is defined as the variation of radiation sensitivity with annealing temperature does not change with the repeats of experiment. To do this, the two annealing temperatures at 500 ^{o}C and 600 ^{o}C for 1 hour were tried before irradiation of samples. According to the obtained results, the intensities of all glow peaks are not stable after the samples annealed at 500 ^{o}C for 1 hour shown in Fig.5.6. Their intensities vary dramatically with increasing the number of experimental cycles. On the other hand, it was observed that there is no significant change in the intensities of LT and HT glow peaks when the samples are annealed at 600 ^{o}C for 1 hour before irradiation shown in Fig.5.7. Moreover, the intensities of IT peaks are not significantly affected by the repeat of experiment. Nevertheless, the annealing at 600 ^{o}C gets more stable peak intensities than at 500 ^{o}C. The increase in

the peak intensity with increasing experimental cycles can be explained by pre-dose effect and the presence of competitors in the quartz. Pre-dose effect is shortly termed as sensitization that means the change in sensitivity of the ~110 ^{o}C TL peak in quartz [125]. The pre-dose effect in quartz was firstly explained by Zimmerman [9]. According to this model, a reservoir hole trap, which has large cross section, accumulates all the free holes. This trap is not deep and enough close to valance band. When the sample is heated up to 500 ^{o}C, all the free holes escape and go to luminescence center. Therefore, an increase in the intensity of 110 ^{o}C peak is observed due to the increase of the concentration of holes in the luminescence center. Samples were annealed at 500 and 600 ^{o}C and examined to find the most suitable annealing temperature for natural quartz sample. Moreover, the studies, which are about kinetic parameters, support this result shown in figures between 5.8 and 5.12. Consequently, it was decided that the annealing at 600 °C is the best annealing temperature for natural quartz samples used in this study because the peaks were not affected by the repeats of experiment. This result was not observed after the annealing at 500 °C.

The effect of annealing time on the TL intensity and kinetic parameters of traps was also investigated in the second part of the study. The experimental results were shown that the intensities of all glow peaks between RT and 400 ^{o}C vary approximately 15% for the annealing time between 30 min and 8 hours.

In the second work of the thesis, the behaviors of TL intensities and kinetic parameters of traps were also observed at different annealing temperatures which vary from 200 and 1000 °C. As seen in figure 5.25, there is a sharp increase of low temperature peak at 450 °C annealing temperature but it decreases until 700 °C. Then it increases with increasing annealing temperature. The same interpretation can be made for intermediate and high temperature peaks. Moreover, high temperature peaks are affected by high annealing temperature between 850 and 1000 °C.

Dose responses of synthetic and natural quartz have been investigated widely by many authors. They have tried to find the effects of applied dose on the linearity, superlinearity, supralinearity and sublinearity of glow curves peaks under different conditions, i.e, annealing, irradiation temperature, etc.

In the third part of this thesis, we have investigated dose responses of annealed and unnealed synthetic and natural quartz, which have been mentioned in

chapter 5, and the analyzed behaviors of TL glow peaks. Also the changes in the areas of glow peaks were examined.

As a result of this study, it is obviously seen that all peak intensities increase with increasing applied dose between 15 mGy and 2.6 kGy. This observation was valid both of synthetic and natural quartz. However, in natural quartz, the increases in the intensities decrease and tend to vanish or convert to higher temperature peaks (>400 ^{o}C) after 27 Gy for low temperature peak, 864 Gy for intermediate temperature peaks and 1.3 kGy for high temperature peaks due to the competitor traps [89, 40, 126, 127, 109]. This is the most important difference between synthetic and natural quartz. In synthetic quartz, low temperature peak disappears after 27 Gy. Two interpretations can be done to explain this situation; the one is fading of peak intensity with increasing of time. But, this is weak possibility because of short time during irradiation. The second is the conversion of peak1 to peak2 and 3.

The heat treatments before irradiation show different results for synthetic and natural quartz. On the other hand, the low temperature peak intensity of annealed natural quartz is smaller than unannealed natural quartz about 40%~20% up to 54 Gy dose. But their intensities become equal to after this point up to applied maximum dose. Besides, the intermediate and high temperature peaks intensities in annealed natural quartz are greater than in unannealed natural quartz for all dose levels about 30%~10%. The reason of this enhancement is probably the presence of competitors [109]. The competitors of the low temperature region seem to have been removed up to a firing temperature of 600 ^{o}C. The competitors are electron traps and essential entities for the appearance of superlinearity in the recombination during heating model. As the firing temperature removes the competitors, the sensitivity is increased due to the absence of competition and superlinearity is reduced [109].

If the effects of pre-irradiation heat treatments were examined on synthetic quartz, it was observed that there is no any important change in the low temperature peak intensity up to 432Gy (8 hours). On the other hand, the effects of heat treatment were clearly observed after high dose levels (D>432Gy). In brief, the annealing process enhances peak intensity at higher doses for synthetic quartz according.

Moreover, the comparison was done between using one sample and using fifteen unused sample for fifteen experiments. In the synthetic quartz, when intensity

of low temperature peak of same sample after different dose levels without annealing is compared with the intensity of low temperature peak of different samples, it was observed that there is approximately 20% difference between them. But after 1hour annealing at 600°C, the low temperature peak intensity of re-used sample is smaller than of unused sample about 10% of its original value. Therefore, the annealing process for re-used samples decreases the low temperature peak intensity. However, in natural quartz, this difference becomes approximately 300% between 0.015 and 0.45Gy. The annealing process reduces the low temperature peak intensity in re-used sample about 80%~10% until 2 hour (108Gy) dose when it is compared with unused sample.

The peak areas show different behaviors at low, intermediate and high-applied doses for synthetic and natural quartz. At low and intermediate doses, synthetic quartz shows superlinearity behavior both low and intermediate temperature peaks and it becomes sublinear at high dose levels (430Gy~2.6kGy). For high temperature peaks, it shows supralinearity at low doses and becomes linear for intermediate doses and then sublinear for high doses. The similar interpretation can be done for natural quartz. This analysis shows that the annealing process affects the supralinearity for both synthetic and natural quartz.

The last part of this thesis was done to see effect of the heating rate on the thermoluminescence glow peaks of the both samples. In this part, it was observed that the intensities of all peaks decrease clearly with increasing the heating rate in both unannealed synthetic and annealed quartz samples. This decrease has also been observed by some authors [109,115,118] and well described using a Mott-Seitz theory. According to these authors this decrease is due to the thermal quenching. Thermal quenching is the process such that the luminescence efficiency decreases with temperature, due to the increased probability of non-radiative transitions due to killer centres. But annealing process has an influence on low temperature peak. Indeed, the low temperature peak intensity in the unannealed samples is sharper than the annealed samples as shown in Fig.5.41 and 5.42. When the effect of heating rate was performed on the natural quartz sample, the similar results were seen as in synthetic quartz samples. But, in this case the alteration is very small (see fig.5.41). When the natural quartz samples were annealed in a furnace, the intensity of low

temperature peak decreased much more than the unannealed sample. In brief, the TL intensities of all glow peaks decrease with increasing heating rate in both samples.

Also, we have investigated that how carrier populations in chosen regions of glow curves change with increasing heating rate by region of interest area method. The results were shown in figures 5.43, 5.44, 5.53 and 5.54. As seen from these figures, there is a high decrease with increasing heating rate.

When the results of heating rate experiments were also checked, it is seen that carrier concentration in all traps decreses dramatically with increasing heating rate for both samples. It is known that the peak intensity and area of a glow peak depend on the carrier population in a trap. Therefore, a decrease in the carrier population reveals decreasing the TL intensity and area under the peak.

If the heating rate was varied from 1 to 16 ^{o}C/sec, it was also seen that the peak temperature of glow peaks of unannealed samples vary approximately 50 ^{o}C toward the high temperature sides. However, in the shifts in peak temperatures become 75°C for LT and IT peaks, 100 ^{o}C for HT peak. When the figures 5.50 and 5.60 are carefully checked, the effect of annealing on the peak temperatures seen clearly. Our results obey to literature [109-119].

Finally, the the graphs of $ln(T_m^2/\beta)$ versus $1/T_m$ of low temperature and high temperature peaks of unannealed and annealed samples were drawn to obtain the activation energies of these traps. The calculated trap depths were given in Tables 5.1 and 5.2.

In brief, the last part of this thesis shows that:

1. The intensities of TL glow peaks decrease with increasing heating rate.
2. The peak temperatures of TL glow peaks shift to higher temperature region with increasing heating rate.
3. The annealing process affects the peak temperatures of TL glow peaks.
4. The carrier population in a trap and there upon area of interested region decrease with increasing heating rate.

REFERENCES

[1] Bos, A. J. J. (2007). Theory of thermoluminescence. *Rad. Meas.* **41,** 45-56.

[2] McKeever, S. W. S. (1985). Thermoluminescence of solids. *Cambridge university Press.* Cambridge.

[3] Daniels F. and Boyd C. A. (1953). Thermoluminescence as aresearch tool. *Science*, **117**, 343-349.

[4] Aitken M. J., Tite M. S. and Reid J. (1964). Thermoluminescencent dating of ancient ceramics, *Nature*, **202**, 1032-1033.

[5] Aitken M. J., Zimerman D. W. and FlemingS. J. (1964). Thermoluminescencent dating of ancient pottery, *Nature*, **219**, 442-444

[6] Mejdahl V. (1969). Thermoluminescence dating of ancient Danish ceramics. *Archaeometry*, **11**, 99-104

[7] Wintle A. G. and Huntley D. J. (1985). Thermoluminescencent dating of ocean sediments. *Canadian journal of earth sciences*

[8] Chen, R. (2001). Advantages and disadvantages in the utilization of TL and OSL for radiation dosimetry. *IRPA Regional Congress on Radiation Protection in Central Europe.*Dubrovnik, Croatia.

[9] Zimmerman, J. (1971). The radiation-induced increase of the 100°C thermoluminescence sensitivity of fired quartz. *Phys. C: Sol. St. Phys.* **4**, 3277.

[10] Cameron, J. R., Zimmerman, D. W. and Bland, R. W. (1965). TL vs. R in LiF: A Proposed mathematical model. Rept. COO-1105-102, USAEC.

[11] Braunlich, P. (1983). *Thermally stimulated relaxation in solids*, Springer-Verlag,

[12] HalpBran A. (1985). Evaluation of thermal activation energies from glow curves, *Phys. Rev*., **117**, 40

[13]   Wintle A. G. (1985). Anomalous fading of thermoluminescence in mineral samples, *Nature*,**245**, 143-144

[14]   Wintle A. G. (1985). Thermal quenching of thermoluminescence in quartz,*Geophys. J. R. Ast. Soc.*,**41**,107-113

[15]   Botter-Jensen L. (1997). Luminescence technique: instrumentation and methods. *Rad. Meas.*, **17**, 749-768

[16]   Randall J.T. and Wilkins M.H.F. (1945). Phosphorescence and Electron Traps. I. The Study of Trap Distributions. *Proc.R.Soc.London Ser. A* **184**, 366

[17]   Chen R. and McKeever S.W.S. (1997). *Theory of Thermoluminescence and Related Phenomena*, World Scientific, Singapore.

[18]   Furetta, C. and Kitis G. (2004). Rewiev of Thermoluminescence. *Journal of Materials Science.* **39**, 2277-2294.

[19]   Garlick G.F.J. and Gibson A.F. (1948). The Electron Trap Mechanism of Luminescence in Sulphide and Silicate Phosphors. *Proc.Phys.Soc.* **60**, 574

[20]   May C.E. and Partridge J.A. (1964). Thermoluminescent kinetics of alpha;- irradiated alkali halides *J.Chem.Phys.* **40**, 1401.

[21]   Kitis G., Gomez-Ros J.M. and Tuyn J.W.N. (1998). Thermoluminescence glow-curve deconvolution functions for first, second and general orders of kinetics *J.Phys.D:Appl.Phys.* **31**, 2636.

[22]   Chen R. and Winer A.A. (1970). Effects of Various Heating Rates on Glow Curves .*J.Appl.Phys.* **41**, 5227.

[23]   Piters T.M. and Bos A.J.J. (1993). A model for the influence of defect interactions during heating on thermoluminescence in LiF:Mg,Ti (TLD-100) *J.Phys.D:Appl.Phys.* **26**, 2255.

[24]   Chen R (1969). On the Calculation of Activation Energies and Frequency Factors from Glow Curves *J.Appl.Physics* **40**, 570.

[25]   Grossweiner L. I. (1953). A Note on the Analysis of First-Order Glow Curves *J.Appl.Physics* **24**, 1306.

[26]   Bunghkbardt B., Singh D. and Piesch E. (1977). *Nuclear Instrumentations and Methods, 141, 363*

[27]   Halperin A. and Braner A. A. (1960). Evaluation of Thermal Activation Energies from Glow Curves *Phys.Rev.* **117**, 408

[28]   Kathuria S. P. and Sunta C. M. (1979).Kinetics and Trapping Parameters TL in LiF TLD-100 *J.Phys.D:Appl.Phys.* **12**, 1573.

[29]   Bos A. J. J., Piters J. M., Gomez Ros J. M. and Delgado A. (1993) GLACANIN, and Intercomparision of Glow Curve Analysis Computer Programs IRI-CIEMAT Report, 131-93-005 IRI Delft.

[30]   Mahesh K, Weng P. S. and Furetta C. (1989) *Thermoluminescence in Solids and its Applications*, Nuclear Technology Publishing Ashford.

[31]   Hsu P C and Wang T K. (1986). On the Annealing Procedure for CaF_2:Dy *Radiat.Protect.Dosim.* **16**, 253.

[32]   Dana, J.D. (1993). *Manual of Mineralogy*, 21st Ed., John Wiley & Sons, USA.

[33]   Khan, H.M. and Ehlermann (1993). Food irradiation dosimetry using thermoluminescence of quartz sand *D.A.E* ,**16,** 76-81

[34]   Cadogan, P. (1981). *The Moon: Our Sister Planet*, Cambridge University Press.

[35]   Cordani, U.G. and Sıgolo, J.B. (1997). *Marte: Novas descobertas*, Institute Astronomico e Geofisico – IAG/SP, Sao Paulo.

[36]   Aitken, M.J. (1985). *Thermoluminescence Dating. Academic Press*, Oxford.

[37]   Leite, R.C.C., Szulc, A., Lemos, C.R., Machado, E., Arcoverde, W.L. (1992). *Quartzo: Da Magia Pas Fibras M Opticas* – Livraria Duas Cidades, SP.

[38]   Franklin, A.D., Prescott, J.R., ScholeDeld, R.B. (1995). The mechanism of thermoluminescence in an Australian sedimentary quartz. *J. Lumin* **63**, 317–326.

[39]   Fleming, S.J. (1970). Thermoluminesce dating: refinement of the quartz inclusion technique. *Archeometry* ,**12**, 133–145.

[40]   Yang, X.H., McKeever, S.W.S. (1990). The predose effect in crystalline quartz. *J. Phys. D*, **23**, 237–244.

[41]   Evans, R. C. (1966). *An introduction to Crystal Chemistry.* Cambridge University Press, Cambridge.

[42]   Paradysz, R. E. and Smith, W. L. (1975). Crystal Controlled Oscillators for Radiation Environments. *Radiat. Effects, 26,* 213-218.

[43]   Lell, E., Kriedl, N. J. and Hensler, J. R. (1966). Radiation effects in quartz and slica glasses. *Progr. Ceram. Soc.*,**4**, 3-40.

[44]   Griscom, D. L. (1978). Defects and impurities in ∝-quartz and fused slica. *Pergammon,N.Y*, 232-252

[45]   Chandler, P. J., Jaque, F. and Townsend, P. D. (1979). Ion beam induced Luminescence in fused slica. *Radiat. Effects,***42**, 45-53.

[46]   Jaque, F. and Townsend, P. D. (1981). Luminescenece during ion implantation of slica. *Nucl. Inst. Meths.,***182/183**, 781-786.

[47]   Yokoyama Y., Falgueres C. and Quaegebeur J. P. (1985). *ESR Dating and Dosimetry*, Tokyo, 197-204

[48]   Figel, F. J., Fowler, W. B. and Yip, L. K. (1974). Oxygen vacancy model for the E_1' centre in SiO_2. *Solid state commun.*, **14**, 225-229.

[49]   Ruffa, A. R. (1973/74). Models for electronic processes in SiO_2. *J. Non-cryst. Solids,***13**, 37-54

[50]   Isoya, J., Weil, J. A. and Halliburton, L. E. (1981). EPR and Ab inititio SCF-MO studies of the Si-H-Si system in the E_4 centres of $\propto$-quartz. *J.Appl. Phys*,**74**, 5436-5448.

[51]   Greaves, G. N. (1978). Colour centres in vitreous slica. *Phil. Mag*, **B37**, 447-466.

[52]   Lucovsky, G. (1979). Spectroscopic evidence for valance- alteration- pair defect states in vitreous SiO_2. *Phil. Mag*, **B39**, 513-530.

[53]   Lucovsky, G. (1980). Intimate valance alteration pairs in amourphous SiO_2 *J. Non-cryst. Solids,***35/39**, 825-830

[54]   McKeever, S. W. S. (1984). Thermoluminescence in quartz and silica. *Radiat. Protect. Dosimetry,* **8.**, 81-98.

[55]   Weil, J. A. (1975). The aliminium center in $\propto$-quartz. *Radiat Effect,* **26.**, 261-265.

[56]   Martin, J.J., Hwang, H. B., Bahadur, H. and Berman, G.A. (1989). Room temperature acoustic loss peaks in quartz. *J.Appl. Phys.* **65,** 4666 -4671.

[57]   Mackay, J. H. (1963). EPR study of impurity-related colour centres in germanium-doped quartz. *J. Chem. Phys.,* **39.**, 74.

[58]   Griscom, D. L. (1979) Proceedings of the Third International Frequency Control Symposium.*Electronic Industries Association*, Washington, D. C., p. 98.

[59]   Tanimura, K., Tanaka, T., and Itoh, N. (1983). Creation of Quasistable Lattice Defects by Electronic Excitation in SiO_2 *Phys. Rev. Lett.* ,**51**, 423.

[60]   Trukhin, A. N. (1987). Temperature Dependence of Luminescence Decay Kinetics of Self-Trapped Excitons, Germanium and Aluminium Centres in Crystalline Quartz Phys. Status Solidi B, **142**, K83.

[61]   Fleming, S. J. (1973). The pre-dose technique: A New TL Dating. *Archaeometry* **15**, 13

[62]   Franklin, A. D.(1998). A kinetic model of the rapidly bleaching peak in quartz thermoluminescence *Radiat. Meas.*, **29**, 209.

[63]   Huntley, D. J., Hutton, J. T. and Prestcott, J. R. (1993). The stranded beach-dune sequence of south-east South Australia: a test of thermoluminescence dating *Quart. Sci. Rev.* **12**, 1.

[64]   Huntley, D. J., Hutton, J. T. and Prestcott, J. R. (1984). Further thermoluminescence dates from the dune sequence in the south-east of South Australia *Quart. Sci. Rev.* **13**, 201.

[65]   Krbetschek, M. R., Gotze, J., Dietrich, A. and Trautmann, T. (1997). Spectral information from minerals relevant for luminescence dating *Radiat. Meas.,***27**, 695.

[66]   Alanso, P. J., Halliburton, L. E., Kohnke, E. E. and Bossoli, R. B. (1983). X-ray-induced luminescence in crystalline SiO_2 .*J. Appl.Phys.* **54**, 5369.

[67]   Halperin, A. and Sucov, E. W. (1993). Temperature dependence of the X-ray induced luminescence of Al-Na-containing quartz crystals *J. Phys. Chem. Solids*, **54**, 43.

[68]   Itoh, N., Stoneham, D. and Stoneham, A., M. (2002). Ionic and electronic processes in quartz. *J. Appl.Phys.* **92**, 5036

[69]   Stevens Kalceff, M. A. and Phillips, M. R. (1995). Cathodoluminescence microcharacterization of the defect structure of quartz *Phys. Rev. B*, **52**, 3122.

[70]   Scholefield, R. B. and Prescott, J. R. (1999). The red thermoluminescence of quartz: 3-D spectral measurements. *Radiat. Meas.* **30**, 83.

[71]   Franklin, A. D., Prescott, J. R. and Robertson, G. B. (2000). Comparison of blue and red TL from quartz *Radiat. Meas*. **32**, 633.

[72]   Martini, M., Paleari, A., Spinolo, G. and Vedda, A. (1995). Role of $[AlO_4]^o$ centers in the 380-nm thermoluminescence of quartz *Phys. Rev. B* ,**52**, 138.

[73]   Bailey, R. M. (2001). Towards a general kinetic model for optically and thermally stimulated luminescence of quartz. *Rad. Meas.,***33**, 17-45.

[74]   Malik, D.M., Kohnke, E.E. and Sibley, W.A. (1981). Low-temperature thermally stimulated luminescence of high-quality quartz. *Journal of Applied Physics,* **52**, 3600-3605.

[75] Alexander, C.S., Morris, F. and McKeever, S.W.S. (1997). The time and wavelength response of phototransferred thermoluminescence in natural and synthetic quartz. *Radiation Measurements*, **27 (2)**, 153-159.

[76] Rhodes, E.J., Bailey, R.M., (1997). Thermal transfer effects observed in the luminescence of quartz from recent glaciofuvial sediments. *Quaternary Science Reviews (Quaternary Geochronology)*, **16**, 291-298.

[77] Bailey, R.M. (1997). Optical detrapping of charge from the 110°C PTTL trap.,*Ancient TL,* **15** (1), 7-10.

[78] Bailey, R.M. (1998). The form of the optically stimulated luminescence signal of quartz: implications for dating. Ph.D. Thesis, University of London

[79] Dussel, G.A. and Bube, R.H. (1967). Theory of thermally stimulated conductivity in a previously photoexcited crystal. *Physical Review,* **155,** 764-799.

[80] Kelly, P.J., Laubitz, M.J. and Braunlich, P., (1971). Exact solutions of the kinetic equations governing thermally stimulated luminescence and conductivity. *Physical Review* **B4**, 1960-1968.

[81] Sunta, C.M, Ayta, W.E.F.F. and Watanabe, S. (1997). Interactive trap system model and the behavior of thermoluminescence glow peaks. *Materials Science Forum*, **239,** 745-748.

[82] Huntley, D.J., Short, M.A. and Dunphy, K. (1996). Deep traps in quartz and their use for optical dating. *Canadian Journal of Physics*, **74**, 81-91.

[83] Scholefield, R.B., Prescott, J.R., Franklin, A.D. and Fox, P.J. (1994). Observations on some thermoluminescence emission centers in geological quartz. *Radiation Measurements*, **23**, 409-12.

[84] Huntley, D.J., Godfrey-Smith, D.I. and Thewalt, M.L.W. (1985). *Optical dating of sediments. Nature*, **313**, 521-524.

[85] Aitken, M.J. and Smith, B.W. (1988). Optical dating: recuperation after bleaching. *Quaternary Science Reviews*, **7,** 387-393.

[86] Stokes, S. (1994). The timing of OSL sensitivity changes in a natural quartz. *Radiation Measurements*, **23**, 593-600.

[87] Wintle, A.G. and Murray, A.S. (1997). The relationship between quartz thermoluminescence, photo-transferred thermoluminescence and optically stimulated luminescence. *Radiation Measurements*, **27 (4)**, 611-624.

[88] Baili., I.K. (1994). The pre-dose technique. *Radiation Measurements,* **23 (2/3)**, 471-479.

[89]   Chen, R., Yang, X.H. and McKeever, S.W.S. (1988). Strongly supralinear dose dependence of thermoluminescence in synthetic quartz. *Journal of Physics D: Applied Physics,* **21**, 1452-1457.

[90]   Rendell, H.M., Townsend, P.D., Wood, R.A. and Lu., B.J. (1994). Thermal treatments and emission spectra of TL from quartz. *Radiation Measurements,* **23**, 441-449.

[91]   Bùtter-Jensen, L., Agersnap, Larsen N., Mejdahl, V., Poolton, N.R.J., Morris, M.F. and McKeever, S.W.S. (1995). Luminescence sensitivity changes in quartz as a result of annealing. *Radiation Measurements,* **24**, 535-541.

[92]   Sunta, C.M. and David, M. (1982). Firing temperature of pottery from pre-dose sensitization of TL. *PACT,* **6**, 460-467.

[93]   Watson, I.A. and Aitken, M.J. (1985). Firing temperature analysis using the $110^{o}C$ TL peak of quartz. *Nuclear Tracks,* **10**, 517-520.

[94]   Liritzis, Y. (1982). Non-linear TL response of quartz grains: some annealing experiments. *PACT* ,**6**, 209-213.

[95]   McKeever, S.W.S., Strain, J.A., Townsend, P.D. and Uvdal, P. (1983). Effect of thermal cycling on the TL and radioluminescence of quartz. *PACT,* **9**, 123-132.

[96]   Duller, G.A.T. (1991). Equivalent dose determination using single aliquots. *Nuclear Tracks and Radiation Measurements,* **18**, 371-378.

[97]   McKeever, S.W.S., Chen, C.Y. and Halliburton, L.E. (1985). Point defects and the pre-dose effect in natural quartz. *Nuclear Tracks,* **10**, 489-495.

[98]   Han, Z.Y., Li, S.H. and Tso, M.Y.W. (1999). TL dating technique based on a trap model and its application as a geochronometer for granitic quartz. *Radiation Protection Dosimetry*, **84**, 471-478.

[99]   Zhi-Young Han, Sheng- Hua Li, Man-Yin W. Tso. (2000). Effect of annealing on TL sensitivity of granitic quartz. *Radiation Meas.*, **32**, 227-231.

[100] Wintle, A.G. (1997). Luminescence dating: laboratory procedures and protocols. *Radiat. Meas.,* **27**, 769–817.

[101] de Lima, J. F., Navarro, M. S. and Valerio, M. E. G. (2002). Effect of thermal treatment on the TL emission of natural quartz. *Radiation Meas.*, **35**, 155-159.

[102] McKeever, S.W.S. (1991). Mechanisms of thermoluminescence production: some problems and a few answers? *Nucl. Tracks Radiat. Meas.* **18**, 5–12.

[103] Charitidis, C., Kitis, G., Furetta, C. and Charalambous, S. (1999). Superlinearityof quartz: dependence on pre-dose. *Radiat. Prot. Dosim.*, **84**, 95–98.

[104] Charitidis, C., Kitis, G., Furetta, C. and Charalambous, S. (2000). Superlinearityof synthetic quartz: dependence on the firing temperature. *Nucl. Instrum. Methods B,* **168**, 404–410.

[105] Chen, R. and Leung, P.L. (1999). Modeling the pre-dose effect in thermoluminescence. *Radiat. Prot. Dosim.*, **84**, 43–46.

[106] Zimmerman, J. (1971). The radiation induced increase of the thermoluminescence sensitivityof the dosimetry phosphor LiF (TLD-100). *J. Phys. C,* **4**, 3277–3291.

[107] Pagonis, V., Kitis, G. and Chen, R. (2003). Applicabilityof the Zimmerman predose model in the thermoluminescence of predosed and annealed synthetic quartz samples.*Rad. Meas.,* **37**, 267-274.

[108] Chen, R. (1979). Saturation of sensitization of the 110°C TL peak in quartz and its potential application in the pre-dose technique. *European PACT J.*, **3,** 325–335.

[109] Ogundare F. O., Balogun F. A and Hussain L. A. (2005). Heating rate effects on the thermoluminescence of fluorite *Radiat. Meas.*, **40**, 60-64.

[110] Kitis G., Spiropulu, M., Papadopoulos J. and Charalambous S. (1993). Heating rate effects on the TL glow-peaks of three thermoluminescent phosphors. *Nucl. Instrum. Meth.*, **73**, 367-372 .

[111] Betts D. S., Couturier L., Khayrat, A. H., Luff B. J. and Townsend P.D. (1993). Temperature distribution in thermoluminescence experiments. *J. Phys. D: Appl. Phys.,* **26**, 843.

[112] Taylor G. C. and Lilley E. (1982). Rapid readout rate studies of thermoluminescence in LiF (TLD-100) crystals. *J. Phys. D: Appl. Phys.,* **15**, 2053-2065.

[113] Nakajima T. (1976). On the competing trap model for the nonlinear thermoluminescence response. *Japan J. Appl. Phys.,* **15(6)**, 1179-1180.

[114] Jain V. K. (1978). The dependence of TL intensity on heating rate and deep trap in LiF. *J. Appl. Phys.,* **17**, 949-950.

[115] Spooner N. A. and Franklin A. D. (2002). Effect of the heating rate on the red TL of quartz. *Radiat. Meas.*, **35**, 59-66.

[116] Nanjundaswamy R., Lepper K. and McKeever S. W. S. (2002). Thermal quenching of TL in natural quartz. *Radiat.Protect. Dosimetry.*, **100**, 305-308

[117] Barkani-Krachi A., Iacconi P., Bindi R. and Vinceller S. (2002). Analysis with a multilayer model of heating rate effect on TL. *J. Phys. D: Appl. Phys.,* **35**, 1895-1902.

[118] Hornyak W. F., Chen R. and Franklin A. (1992). Thermoluminescence characteristics of the 375 ^{o}C electron trap in quartz. *Physical Review B,* **46**, 8036-8049.

[119] Kıyak N. G. and Buluş E. (2002). Effect of annealing temperature on determining trap depths of quartz by various heating rates method. *Radiat. Meas.*, **33**, 879-882

[120]   9010 Optical Dating System User Manual, Dec. 1993.

[121]   Model 3500 Manual TLD Reader User's Manual, July 30 1994, Publication No 3500-0-U-0793-005.

[122] Hashimato, T., Sakaue, S., Aoki, A., Ichino M. (1994). Dependence of TL-property changes of natural quartzes on aliminium contents accompanied by the thermal annealing treatment Radiat. Meas. **23**, 293–299.

[123] Arik R. (1992). Kubad-Abad Excavations (1980-91), *Anatolica* ,18: 101.

[124] Topaksu M. (2004). Thermoluminescence (TL) dating, reconstructing and interpreting the technologies of Seljuk's ceramics and tiles from Kubad Abad (Konya). PhD Thesis, University of Çukurova.

[125] Chen, R. and Pagonis V. (2004*).* Modelling Thermal Activation Characteristics of the Sensitization of Thermoluminescence in Quartz   *J. Phys. D: Appl. Phys*., **37**, 159.

[126] Kitis, G., Kaldoudi, E. and Charalambous., S. (1990). *Thermoluminescence Dose Response of Quartz as a Function of Irradiation Temperature, J. Phys. D. Appl. Phys.*, **23**, 945-949.

[127] Durani, S. A., Groom, P. J., Khazal, K. A. R. and McKeever S. W. S. (1977). The dependence of the thermoluminescence sensitivity upon the temperature of irradiation in quartz *J. Phys. D. Appl. Phys.*, **10**, 1351.

[127] Chariditis, C., Kitis, G. and Charalambous., S. (1996). Supralinearity of the Synthetic Quartz at Different Irradiation Temperatures *Radiat. Prot. Dosim.*, **65**, 347.

[128] Chariditis, C., Kitis, G., Furetta, C. and Charalambous., S. (2000). Superlinearity of synthetic quartz: Dependence on the firing temperature Nuclear Inst. and Meth. In Phys. **168**, 404.

PERSONAL INFORMATION

Surname, Name: TOKTAMIŞ Hüseyin
Nationality: Turkish (TC)
Date and Place of Birth: 20 July 1976 , Adana
Marital Status: Married
Phone: +90 5354249071
Fax:
email: toktamis@gantep.edu.tr

EDUCATION

Degree	Institution	Year of Graduation
MS	Gaziantep University, Physics Eng.	2002
BS	Gaziantep University, Physics Eng.	2000
High School	Adana Yüreğir Atatürk Lisesi	1993

WORK EXPERIENCE

Year	Place	Enrollment
2000- Present	Gaziantep University	Research Assistance

FOREIGN LANGUAGES

English

PUBLICATIONS

1. Toktamış H. and Gönül B. (2002). Optical Gain of InGaAsP/In(Ga,As)P/InP Multiple Quantum Well Lasers, *BPL10,* **4,** pp.230-235.

2. Toktamış H. and Gönül B. (2003). A Theoretical Calculation of Band-offsets in Semiconductor Quantum Well, *BPL11,* **1,** pp.15-19.

3. Toktamış H., Gönül B. And Oduncuoğlu M. (2004). A Comparative Study of The Band-offset Ratio of Conventionally Semiconductor Quantum Well Strained and Strain-Compensated InGaAs/GaAs QW Lasers. *Physica E*, **24** pp.183-186.

4. Gönül B., Koçak F., Toktamış H. and Oduncuoğlu M. (2004). Theoretical Comparison of the Band Alignment of Conventionally Strained and Strain-Compensated Phosphorus- Aluminum- and Nitrogen-Based 1.3 µm QW Lasers - CHINESE JOURNAL OF PHYSICS VOL. 42, NO. 6 pp.764-775.

5. Yazici A. N. and Toktamış H. (2007). Thermoluminescent Dosimetric Characteristics of Annealed Quartz. *Radiation Effects & Defects in Solids,* **162**, No. 6, 439–448.

6. Toktamış H., Yazici A. N. and Topaksu M. (2007). Investigation of The Stability of The Radiation sensitivity of TL Peaks. *Nuclear Instruments and Methods in Physics Research B,* **262,** 69–74.

7. Öztas M., Bedir M., Yazici A. N., Kafadar E. V. and Toktamıs H. (2007). Characterization of Copper-Doped Sprayed ZnS Thin Films. *Physica B,* **381,** 40–46.

8. Yazici A. N., Kafadar E. V. and Toktamıs H. (2006). Thermoluminescent dosimetric characteristics of b-ray irradiatedRbCl single crystal doped with Eu- and OH-ions. *Nuclear Instruments and Methods in Physics Research B,* **246**, 387–392.

9. Yazici A. N., Dogan M., Kafadar E. V. and Toktamıs H. (2006). Thermoluminescence of Undoped and Ce-doped BaB4O7. *Nuclear Instruments and Methods in Physics Research B*, **246**, 402–408.

10. Yazici A. N., Öztas M., Kafadar E. V., Bedir M., and Toktamıs H. (2007). The analysis of thermoluminescent glow peaks of copper doped ZnS thin films after b-irradiation. *Journal of Luminescence,* **124,** 58–66.

HOBBIES

Music, football, Table tennis, Digital photography, Digital instruments.